DRAFT

EU Programme CADZIE

New concepts in avalanche hazard mapping

20001018-2 16 June 2003

Client: **EU/NFR SIP6**

Contact person: Mohamed Naaim, CEMAGREF

Contract reference: EVG1-CT-1999-0009

For the Norwegian Geotechnical Institute

Project Manager:

Ulrik Domaas

Report prepared by:

Carl B. Harbitz

Reviewed by:

Ulrik Domaas

Postal address:	P.O. Box 3930 Ullevaal Stadion, N-0806 OSLO, NORWAY	Telephone:	(+47) 22 02 30 00	Postal account:	0814 51 60643
Street address:	Sognsveien 72, OSLO	Telefax:	(+47) 22 23 04 48	Bank account:	5096 05 01281
Internet:	http://www.ngi.no	e -mail:	ngi@ngi.no	Business No.	958 254 318 MVA

European Research Framework Programme (PCRD) V (1999-2003)

Contract EVG1-CT-1999-0009

CADZIE

Catastrophic Avalanches: Defence Structures and Zoning in Europe

Work Package 1 deliverable: New concepts in avalanche hazard mapping

Editor: Carl B. Harbitz

Foreword

The present report is a deliverable to Work Package 1 "Integrated system for catastrophic avalanche zoning" of the EU-programme CADZIE (Catastrophic Avalanches: Defence Structures and Zoning in Europe). The practical procedures described will also serve as a contribution to Work Package 5 "Transfer to end-users".

The EU-program CADZIE is partly funded by the European Union under the contract no. **EVG1-CT-1999-0009**. The authors greatly acknowledge the support that has enabled the work.

The following persons (in alphabetical order) have all provided highly acknowledged contributions that made it possible to write the present report:

MB Massimiliano Barbolini (University of Pavia, Italy)
UD Ulrik Domaas (Norwegian Geotechnical Institute, Norway)
UG Urs Gruber (Swiss Federal Institute for Snow and Avalanche Research, Switzerland)
CH Carl B. Harbitz (Norwegian Geotechnical Institute, Norway)
DI Dieter Issler (NaDesCor, previously Swiss Federal Institute for Snow and Avalanche Research, Switzerland)
TJ Tomas Johannesson (Icelandic Meteorological Office, Iceland)
CK Christopher J. Keylock (Dept. of Geography, Univ. of Leeds, UK)
KK Karl Kleemayr (Institute of Forest and Mountain Risk Engineering, University of Agricultural Sciencesm, Vienna (BOKU), Austria)
MM Margherita Maggioni (Swiss Federal Institute for Snow and Avalanche Research, Switzerland)
SM Stefan Margreth (Swiss Federal Institute for Snow and Avalanche Research, Switzerland)
MMe Maurice Meunier (CEMAGREF, France)
MN Mohamed Naaim (CEMAGREF, France)
CW Christian Wilhelm (Swiss Federal Institute for Snow and Avalanche Research, Switzerland).

Summary

The main goal of the CADZIE workpackage 1 is to improve the hazard assessment process by integrating uncertainty and to develop "best-fit" models. This goal can only be achieved if both the stochastic characteristics of the avalanche system as well as the physically describable behaviour are modelled adequately. Although there exist numerous empirical and dynamical models in theory and computational form, till now only few attempts have been carried out to combine these different concepts. The objective of this report is not to develop a new constitutive law for avalanche dynamics or to derive a new statistical function for run-out estimation, but rather to integrate random processes, uncertainty, and also vague knowledge in the system description.

The report must be considered a preliminary stage as it simply presents different ideas and procedures for hazard zoning developed and/or used by the CADZIE participants. No attempt is made of synthesizing the contributions or combining those into a proposed "best practice". However, this latter step is planned as part of forthcoming work.

Section 2 describes various statistical methods to determine avalanche release and avalanche run-out. Two methods are presented to analyse the probability of avalanche release: with and without taking topography into account.

Section 3 concentrates on physical methods. However, it has been tried to include the stochastic character of the input variables (probabilistic mechanical concept for failure estimation, probabilistic dynamical concept for avalanche dynamics). For avalanche release also a model that attempts to bridge the lack of knowledge by integration of expert knowledge is presented.

In Section 4 combined methods are presented. One method proposes the combination of statistical and physical models by statistical determination of physical friction parameters. Another method shows the possibility of using Monte Carlo simulations in combination with a 1D dynamical model.

Section 5 discusses how hazard maps are modified by protective measures in the different countries represented in CADZIE, while Section 6 discusses risk management in avalanche hazard mapping and aerial planning.

Most of the presented methods can achieve a state valuable for practical applications already during the project time. However, it has to be emphasized that several problems still remain: Improved knowledge of initial conditions, modelling of basic physical processes in avalanche dynamics and last but not least comprehensive measurements on real avalanches can be seen as the main points of research in the future.

Contents

Figures

Review and reference document

1 INTRODUCTION

1.1 Motivation and objectives

CH

Increased human activity in mountain regions, deforestation from pollution, forestry and ski resorts, as well as an increased desire to exploit exposed areas combined with a reduced acceptance of risk, have caused a growing need for protection against avalanches in terms of hazard zoning and protective measures.

Both empirical procedures including statistical/topographical and comparative models for run-out distance computations, as well as dynamics models for avalanche motion simulations are now in existence (see Harbitz (1998) for a survey on computational avalanche models). The empirical procedures permit an assessment of run-out distance only, while the more advanced dynamics models give much additional information concerning the nature of the sliding event (flow heights, velocities, impact pressures, etc.). This information is crucial for improved understanding of avalanche dynamics, and for the calculation of impact pressure upon obstacles, run-up heights on protective dams, etc. However, no universal model has so far been developed. The dynamics of avalanches are complex, involving properties similar to those employed in fluid, particle and soil mechanics. The limited amount of data available from real events makes it hard to evaluate or calibrate existing models. Often several models with different physical descriptions of the avalanche movement can be used to replicate the information contained in the available, deficient, recorded observations.

The aim of hazard mapping is to present the spatial variation of hazard on geographical maps. The simplest strategy is to avoid the presence of any human being or constructions in an endangered area. In this case, the only need of the practitioners is the maximum run-out distance of an avalanche. This can be found by statistical methods alone as described in Section 2. However, it is often impossible to keep the infrastructure out of endangered areas. Then the main requirement is the impact pressure of an avalanche event at a given location. For the reliable dimensioning of protective measures also more detailed information about the duration of the impact pressure, the shear forces, the flow height and the run-up height are required. This requires the use of physical methods as described in Section 3. Often a combined use of statistical and physical methods is fruitful, Section 4. Finally, procedures are needed for how to take the protective measures into account on the hazard maps. This topic is discussed in Section 5.

To meet the requirements in the legislation and to perform risk and cost/benefit analyses, the physical quantities must be related to a return period, or given a certain probability. Both statistical and physical computational models give the

avalanche run-out distance, impact pressure, etc. with a certain probability. The probability is a combination of the probability of occurrence and the probability of a certain run-out distance, impact pressure, etc.

The probability of release can, in principle, be calculated using:

- *mechanical/probabilistic models:* The snowpack structure is described by means of physical variables with distribution functions providing the probability of the parameter values; or
- *statistical models:* Based on meteorological data and/or historical avalanche observations. Where a sufficient number of reliable observations do not exist, the meteorological conditions and the exposition of the site relative to the direction of snow-bringing winds are applied to estimate the probability of avalanche occurrence.

Likewise, the probability of a certain run-out distance can be calculated using:

- *dynamic/probabilistic models:* The avalanche dynamics is described by means of physical variables with distribution functions to give probability for parameter values); or
- *statistical/topographical models:* The run-out distance for a given probability is calculated from a basis of recorded known avalanche run-outs.

The probability of a certain run-out distance, impact pressure, etc., is determined by the statistical distribution of the parameters included in the computational model. The statistical distributions also enable quantification of uncertainty in terms of confidence intervals. In the case of two otherwise similar avalanche paths, the probability of long run-out is higher in the path on the leeward snow-accumulating mountain side, than in the windward non-accumulating mountainside. Buildings and vegetation will also influence the run-out distance. However, the maximum conceivable run-out distance, impact pressure, etc. in the two avalanche paths over an infinite period of time will be the same.

To relate avalanche run-out to a certain probability, e.g. an annual probability of 10^{-3}, is a difficult task. However, the computational models are a good remedy to estimate the right order of magnitude for avalanche frequency and avalanche run-out distance, impact pressure, etc.

Even though a house is located beyond a defined avalanche hazard zone, there is still a possibility of being hit by an avalanche. If the hazard zone mirrors an annual probability for an avalanche to reach the area larger than 10^{-3}, an avalanche should reach outside the hazard zone in average once every thousand years. In other words, there is a 1 % chance that the avalanche will reach beyond the hazard zone during a period of ten years. In a municipality with 100 buildings that have this chance of being hit by an avalanche, i.e. are built on the boundary of the hazard zone; in average one of these houses will be hit by an avalanche every ten years.

2 STATISTICAL METHODS

2.1 Introduction

CK

The problem for avalanche engineers is the design and location of settlements to resist an avalanche of a particular recurrence interval (return period), typically in the order of 100 years or so. In this case, one is not concerned with direct prediction in the sense discussed above (a specific event at a particular time). Instead, one considers how often, on average, that an avalanche exceeds a specific run-out distance. As the length of observation (T) tends to infinity, the number of avalanches attaining or exceeding the 100 year return period position will converge upon T / 100. The consideration of return period drives any risk assessment exercise, whether formal or informal. Knowledge of probable degree of damage is a secondary factor. For example, one could envisage a situation where it is estimated that the peak pressures (for the 100 year avalanche) at the 25 year avalanche stopping position and the 50 year avalanche stopping position are similar. The fact that avalanches reach one of the locations twice as often as the other is the more important consideration.

As soon as one begins to discuss return periods, one is operating within a statistical framework. The advantage of statistical methods is that the existence of uncertainty in our measurement and modelling of physical processes is acknowledged and may be quantified. This quantification occurs through a distribution fitting procedure (although this may be implicit within the statistical technique).

Statistical models are based upon real avalanches and consequently provide a very useful validation tool for the mathematical modeller. They subsume the complexities of avalanche flow into a single, important parameter (the stopping position) and then provide an expected distribution of this variable.

An important criticism of statistical models is their inability to examine how return period varies along a given avalanche path – the models are developed for a specific return period. However, there are currently methods emerging that attempt to develop statistical models appropriate for this situation (Keylock *et al.*,1999; McClung, 2000) and this advance will hopefully improve the utility of the statistical methodology, giving error estimates for a range of return periods.

2.2 Statistical methods for determining avalanche release

KK

Since about 30 years statistical methods are used for avalanche release prediction. A summary of most of the methods and applications can be found

in Nairz (1996). Though the statistical models are nearly solely developed for daily avalanche prediction, within limits the results are also valuable for determining avalanche release of catastrophic scenarios with return period of several years.

2.2.1 Statistical methods for daily avalanche prediction

Contr.: KK

According to Colbeck (1982) statistical avalanche prediction can be worked out on weather data, snow cover data or stability data. The data collected for the project consists of a time series of 40 years including avalanche data, weather (daily) and snow cover data (discontinuous) but no direct stability measurements. In the two areas in the central Austrian Alps (Kaprunner Tal, Zillertal) 220 avalanche tracks had been observed with only slightly changing quality over the time. For the corresponding release areas the necessary topographic parameters had been derived in average but also for about 700 sub release zones.

In the first step only the meteorological influences has been taken into account. The linear regression analysis gives the function:

$$P_e = \frac{1}{1 + 45.6e^{-(0{,}086NS + 0{,}17LT + 0{,}014SH01 + 0{,}012ET)}} + 0{,}43$$

with NS: snow precipitation, LT: air temperature, SH: snow depth and ET: penetration depth. The hit ratio (probability that a day is correctly predicted as avalanche day or non avalanche day) for this simple function is 68%. The integrated parameters are the most significant ones form a long list including also wind and cloudiness. Based on data of 40 years the function could not only be used for daily prediction but also for determining the release probability of events with higher return period if the proper values would be used (e.g. precipitation value for 100 years). With the weightings of the parameters also the empirical importance of the influences can be roughly assessed. It is obvious that precipitation has a major effect on release probability (which let us skip further discussions here). The strong influence of the snow depth can be interpreted in two ways: first there is an autocorrelation with the precipitation. Second, with increasing snow cover depth the probability of large areas with smooth surface also increases because more roughness objects of the ground surface are drowned. With this the probability of large weak zones significantly rises.

Air temperature and penetration depth indirectly describe the presence of weak zones and the strength of the upper most layers of the snow cover. Therefore mechanical release models have to be linked in some way with meteorological conditions if an evaluation with empirical data is strived to be done.

Using generalized additive regression models (GAM) these influences can be shown more transparent (although the prediction quality did not rise). GAM's delivers predicted values between 0 and 1. The main difference to the regression models is the transformation of the input parameters. These transformed values show the influence more continuously:

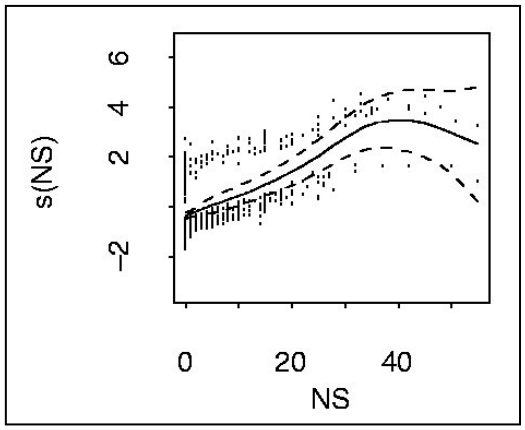

Figure 1.1: Transformed snow precipitation value of the additive model

In Figure 1.1 it can be clearly seen that between 0 and 20 cm precipitation the graph is less steep which indicates lower effect. Between 20 and 40 the importance of precipitation to the avalanche release probability significantly rises. After 40 cm the influence is unrealistically decreasing again. The reason for this is once the low quality of data during conditions of heavy snow fall (a simple but cumbersome problem of many databases) and second the transform function of the used program Splus in relation with the low amount of data sets in this region. It can be assumed that in reality the importance should slightly but permanently increase. Figure 2.2 shows the importance of the air temperature. Snow melting with temperatures above 0° reduces the strength of the snow material and induces avalanche release in very steep terrain.

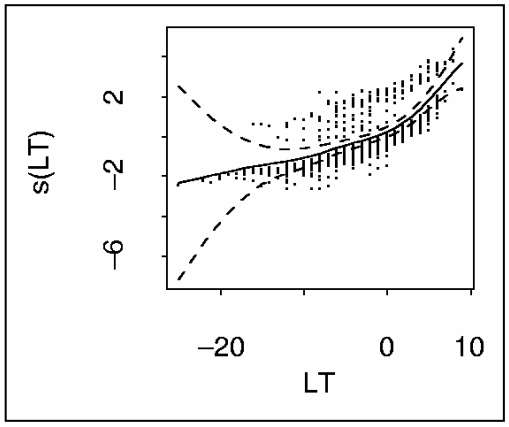

Figure 2.2: Transformed air temperature of the additive model

In the second step the topographic effects on release frequency has been investigated. It could be shown that the distribution of the avalanche frequency with varying aspects is in good congruence with data published from Munter (1998). 53% of the avalanches release on north faced slopes, 33% on east and west and 14% with south aspect. The classification of the release areas with inclination surprisingly did not give a clear trend. Analyses indicate that very steep (average inclination >48°) and small release areas do have significantly higher frequencies. But in most of the cases the events are loose snow avalanches, which are of lower importance for catastrophic avalanche release. For the expected range of inclination between 28° and 48° inclination no statistically significant trend could be shown. Several reasons cause this unpleasant result: a) In the database the avalanche events are connected to a certain track. But with an average size of 4,5 ha the release areas are not homogenous and possess many varying topographic features. The determination of sub release zones with homogenous properties could not used successfully, because no precise information (what sub release zone failed) could be obtained. b) Most of the release areas are surrounded by steep rock slopes, from which loose snow avalanches are breaking. Frequency therefore is artificially triggered. c) During the winter season the size and slope of the release areas is not constant but permanently changed by the snow cover itself. d) Digital terrain models (DTM) still have some quality problems if the terrain surface is steep and rough. The DTM used in the project has been derived from 1:10.000 contour lines (which has been developed by aerial photo interpretation) and breaking lines. It seems to be necessary for future projects implying topographic information to clearly define the necessary topographic properties. Though the terrain model would be absolutely satisfying for dynamic avalanche simulations, it has to be reckoned that applying for release probability analyses some systematic noise is produced. e) Last but not least the various release mechanism types (slab release, loose snow avalanche, gliding avalanche) have different dependence on slope inclination. But there was no direct information on the release type available. The attempt of interpreting the release type by the avalanche type could slightly increase the result, but did not give a break through.

The major constraint of integrating topographic parameters in the statistical analyses is the negative characteristic of the data space. Only 14% of all data are days with avalanches. Although the used data set contained more than 2000 records, the data space is thinning rapidly by classifications. Therefore a semi-physical model (3.2) has been developed which should help to bridge this gap.

2.2.2 Relation between topography and avalanche release area.

MM

Avalanche release area is an important parameter for the assessment of avalanche hazard. Together with fracture depth, the release area determines the possible volume of snow which can release to form the avalanche. While

parameters like run-out distance or deposition height are observable, the release area is not easy to determine. So a good help could be a method enabling the definition of potential avalanche release areas through general rules linked to topographic parameters. Then the idea is to find release area distribution functions for potential release areas with different topographic parameters.

The general rules could be a valuable aid for the avalanche experts in cases where information about historic avalanches is lacking for a particular track. Furthermore, the release area distribution functions can be directly used as input for uncertainty modelling of avalanche run-out distances and impact pressure by Monte Carlo methods.

The three basic steps of this approach are (1) the definition of the potential release areas (PRA) through general rules based on topographic analysis, (2) their characterisation based on significant geomorphologic parameters and (3) a statistical analysis of the past avalanche events, based on the previously extracted geomorphologic parameters. Using Geographical Information System (GIS) technology in combination with Digital Elevation Model (DEM), a topographic analysis is performed based on rough geomorphologic structures.

In the following, the procedure is applied to a testing area in the region of Davos Switzerland (Figure 2.3), where an almost complete database of about 4500 avalanche events over the last 50 years is available on an extent of about 300 km^2. The procedure is general and could be applied in any other different region.

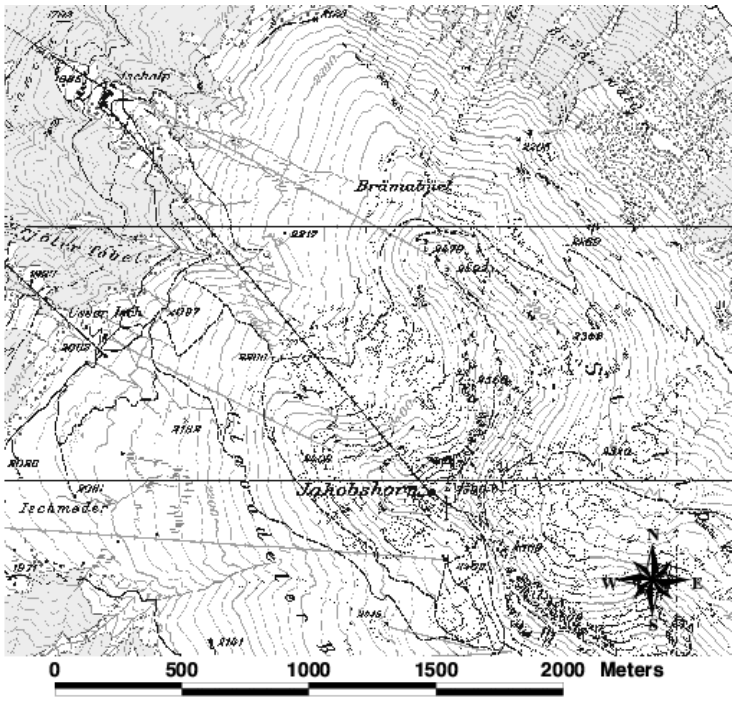

Figure 2.3: A view of a part of the testing area in the region of Davos.

The first important parameter is slope. From the analysis of the terrain of the starting zone of past events, the first selection is done. Slopes with an inclination between 30° and 60° (Figure 2.4) are considered potential avalanche release areas. The reason for this choice is that on slopes with an angle greater than 60°, avalanches are very frequent and of small dimension, since no big deposition without failure is possible on such steep slopes.

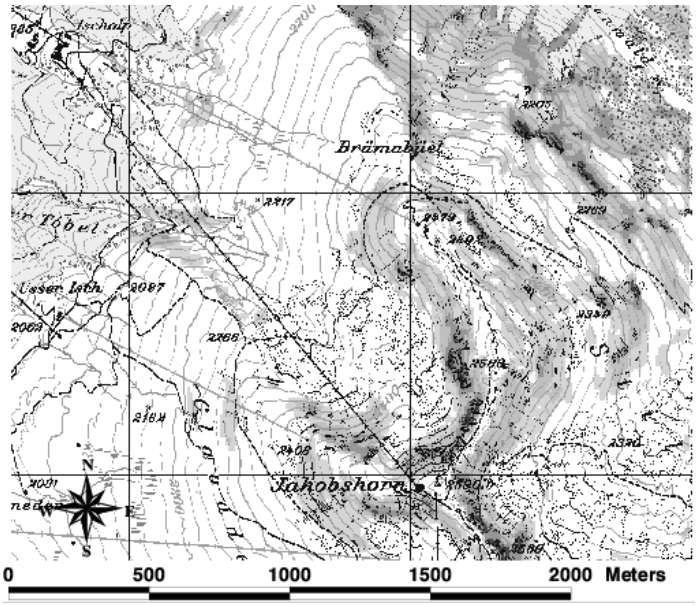

Fig.2.4: First selection of potential avalanche release area based on slope-angle rule.

After this first selection, parameters like curvature and aspect are used to define different release areas. In GIS curvature is computed in a way that it is separated into two orthogonal components where the effects of gravitational process are either maximised (profile curvature) or minimised (plan curvature). In the present method of defining potential release areas the plan curvature is used to separate concave areas from convex ones. A resolution of 50m is used to compute curvature out of the DTM.

Concave areas are differentiated from convex ones (Fig. 2.5) based on the following rule:

concave areas → plan curvature < -0.2
convex areas → plan curvature > +0.2
flat areas → -0.2 < plan curvature < +0.2

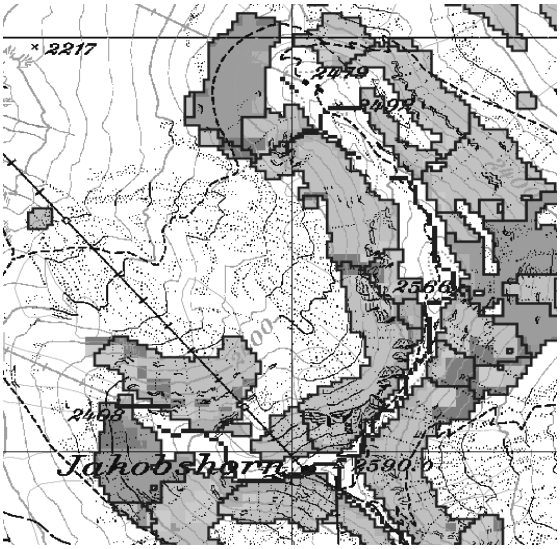

Figure 2.5: Differentiation of concave (light grey) and convex (dark grey) areas.

Areas not well defined by curvature, considered as flat areas, are then separated through different values of the mean aspect, in a way that areas facing to different directions are considered stand-alone. To make this concept clearer, let's think about an area with value of curvature between –0.2 and 0.2. Then it is considered as a unique flat area. But it could be that a part of it is facing SW and another SE, then considering the aspect parameter it will be divided in two different areas.

In Figure 2.6 is shown the result of the complete procedure for the test area in Davos.

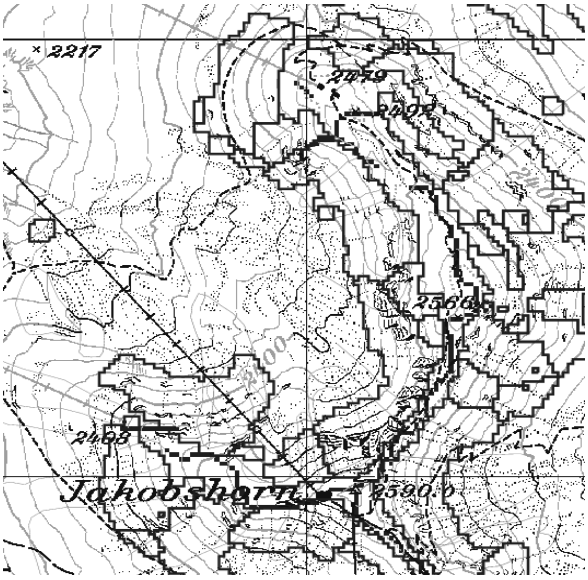

Figure 2.6: Result of the automatic definition or the potential avalanche release areas.

The second step is to perform the more detailed geomorphologic characterisation of the potential release areas resultant from the automatic definition method.

The idea is to find the most representative geomorphologic parameters to give a characterisation of every PRA in order to link these characteristics – in the third step - to different avalanche activities – this is the third step, that is the analysis of the past avalanche events.
In the following we're going to present the second and third step only for 3 PRA in the test area, just to explain clearly the procedure.

The geomorphologic features considered in this work as characterising parameters are:

1. mean slope (in degree)
2. minimum slope (in degree)
3. maximum slope (in degree)
4. curvature
5. mean aspect (in degree clockwise from North)
6. distance to the next ridge (in meter)

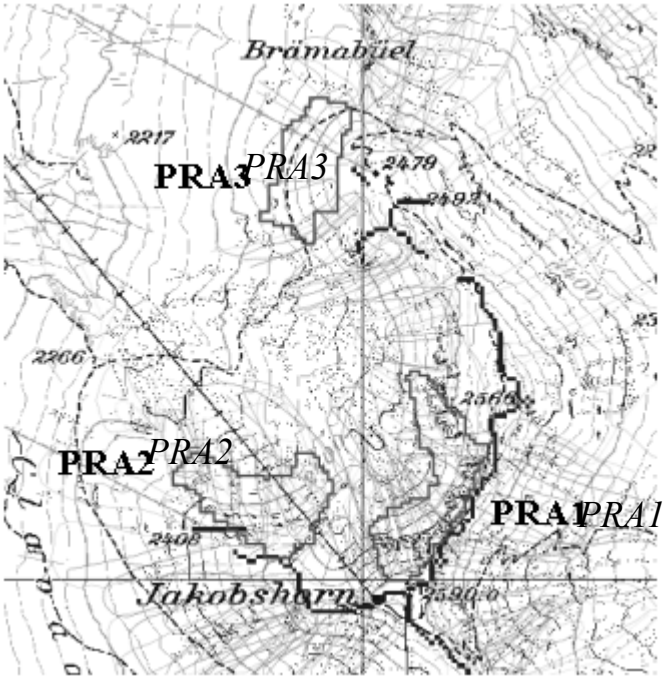

Figure 2.7: The 3 test potential release areas are drawn with thick grey lines. The black lines represent ridges. Past avalanche events are also shown.

Let's consider the three potential release areas in Figures 2.7 and 2.8. Analysing the map it's evident that the first two potential release areas are quite similar and the third one is a bit different, mainly due to curvature. What we expected is that the first two PRA are represented with similar release area distributions and the last with a different one.

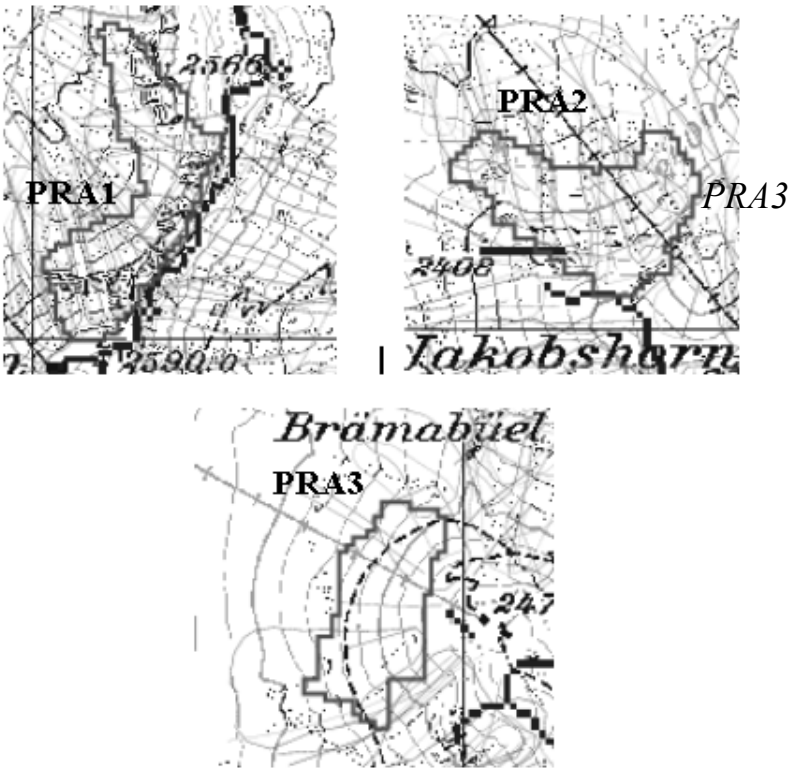

Figure 2.8: Example of release areas with different topographic characteristics and different avalanche activities.

Table 2.1 reports the values of the characterising topographic parameters for the 3 considered PRA.

Table 2.1: Values of characterising topographic parameters for the 3 considered PRA.

	Mean slope	Min slope	Max slope	Mean aspect	Curvature	Distance to ridges (m)
PRA1	38.6	30	49	302 (W/NW)	concave	0
PRA2	36	30	47	346 (N/NW)	concave	0
PRA3	34	30	40	276 (W)	convex	30

The third step is the analysis of past avalanche data and the derivation of the release area distribution functions. Every potential release area is considered and in it's done the analysis of the release area of past avalanches. Fig. 2.9 shows the distribution of the release area's extent in the 3 test PRA.

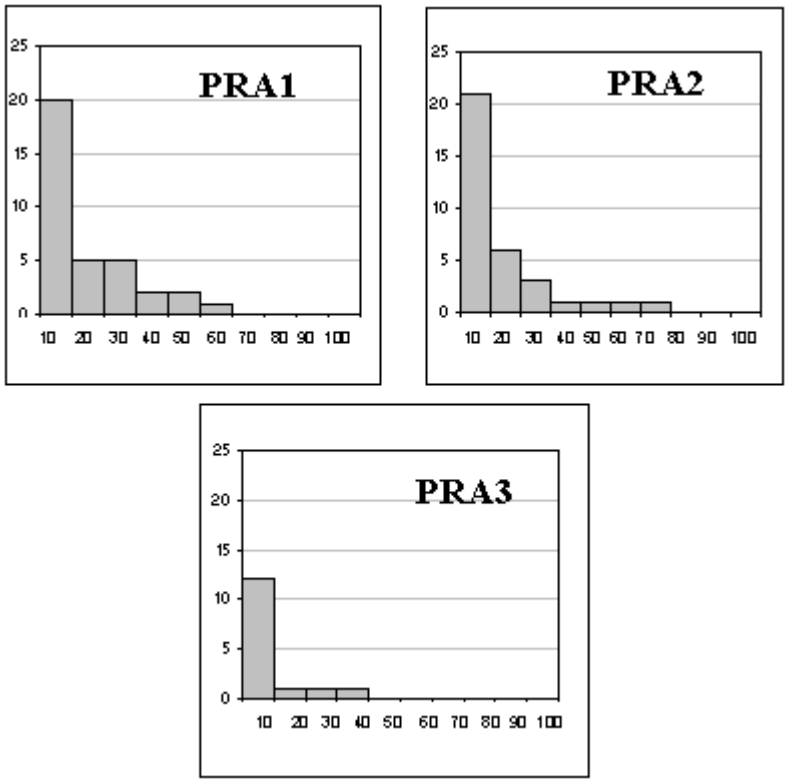

Figure 2.9: Release area distribution: on the x-axis there's the share of the potential release area.

What we can see in this result is that pra1 and pra2 has similar distribution of historical avalanches and that instead pra3 has a slightly different avalanche activity (only 15 avalanches versus 35 and 34 of pra1 and pra2 respectively).

The idea is to find release area distribution functions for every different potential release areas. As we already said, what we expected is that release areas with different geomorphologic characteristics have different avalanche activities and then different release area distribution functions. In fact what results from this analysis is that potential release areas with similar or different topographic features have respectively similar and different distributions of historical avalanches.

The automatic procedure for the definition of potential avalanche release areas could be a valuable help for an avalanche expert in cases where information about historic avalanches is lacking for a particular track. He is helped by a good and objective tool for the definition of the avalanche release area and then, as an expert, he can combine the results of this procedure with the analysis of the few available avalanche data and the evaluation in loco of the starting zone.

Another interesting result is the definition of release area distribution functions linked in a way to different topographic parameters. So that we can say that certain avalanche activities are related to specific topographic features.
Furthermore, the distribution function for the release area can be directly used as input for uncertainty modelling of avalanche run-out distances and impact pressures by Monte Carlo methods.

This study is a part of a more complete study concerning release mass of avalanches. Nothing has been done yet, but the next step will be the derivation of a mass distribution function. This will be done analysing snowfall data and combine the release area distribution function with a distribution related to the fracture depth.

2.3 Statistical methods for determining avalanche run-out

CH and CJ

Empirical models for snow avalanches are based on statistical/topographical models or comparative models for estimation of avalanche run-out distance. In statistical/topographical models the run-out distance relations are normally found by regression analysis of data from observed events. Comparative models are based on methods for evaluating the similarity between path profiles. An alternative approach is to present pure limiting criteria for flow behaviour, as from considerations of subaerial debris flow behaviour.

Empirical procedures are normally applied to dense snow avalanches. However, in principle, there is no reason why they could not be applied to slush flows and powder snow avalanches if a sufficient number of precise observations are available.

Statistical run-out computations based on the transfer of avalanches between paths using a physical run-out model are an integrated part of the Icelandic hazard zoning procedure that is described in Appendix A. In addition, an alpha/beta-model has been calibrated based on a data-set of Icelandic avalanches (Jóhannesson, 1998).

3 PHYSICAL METHODS

3.1 Introduction

KK

In contrary to statistical methods physical models give not only description but also explanation of real world phenomena. From a practical point of view, physical models facilitate the work out of numerous variants, which can describe the danger on a given location more accurate than with only statistical methods.

With the physical modelling concept, two sources of uncertainty are associated:

a) System uncertainty: System uncertainty subsummizes uncertain knowledge as well as vague knowledge. Many of the parameters affecting avalanche release and run-out are random variables and have strong interdependency to other processes or influence parameters. This leads to the situation that most of the parameters are hard to measure and the delineation of general valid models is hardly to achieve.

b) Model uncertainty: As long as physical models cannot explain the whole system taken into consideration, physical modelling has a conceptual character and uncertainty therefore is an intrinsic quality of the developed model. This uncertainty can only be reduced by validation and verification based on laboratory tests and real world observations.

The methods presented – from release estimation to run-out determination – try to solve the problem in different ways. But all concepts are guided by the idea to include uncertainty already in the modelling process.

3.2 Snow mechanical methods for determining avalanche release

3.2.1 Mechanical model for avalanche release

CH

Harbitz et al. (2001) apply models based on the mechanics of slab avalanches and structural reliability methods or Monte Carlo simulations as a basis for calculation of the annual probability of avalanche release.

3.2.2 Semi-physical model for avalanche release

KK

By statistical methods alone it is hardly possible to determine the probability of an avalanche release for a given area (See chap. 2.2). This aim should be easier reached with mechanical or physical models. But like for all other complex systems with stochastic character “pure” physical modeling is exacerbated if chaotic and scaling issues are taken into account. Not arbitrarily hybrid modeling is a booming keyword in simulation technique, which tries to combine discrete and continuous modeling (Breitenecker, 2001). But with the advantage to link system states that cannot be described by one set of functions alone, also some disadvantages are coming up. The analytical force of a rigorous mathematical-physical model is reduced, because the coupling of system states is usually done by stochastic models or control systems.

Harbitz (2002) introduced a very promising probabilistic – mechanical method to calculate the probability of slab release. Till now the probability distributions of the variables (thickness, slope angle, material strength, shear strength, width, length, density and external load) based on the assumptions of Lackinger (1989) are quite vague and have to be derived from empirical data if the model is applied for "real" cases and practical purposes. But trying to obtain the probability of shear strength in weak zones with a return period for e.g. 100 or 300 years depicts the problem in a strikingly way. If adequate measurements would be available the derivation could be performed by statistical methods. But except for single Rutschblock tests there is no direct information available. The other possibility would be to define the shear resistance by physical laws. Including energy balance, mass movement processes and meteorological boundary conditions this could be possible. Unfortunately the problem again cannot be solved directly because many of the meteorological driving parameters are stochastic.

The modeling concept presented in the following tries to find a modeling position in between. The selection of the included parameters is once driven by the statistical analyses pointed out before and second by a basic mechanical – physical concept. Except for the external load, all physical parameters of the Harbitz model are integrated. Opposed to this model, the variables in the ARIS model (Avalanche Risk Information System) are not defined by theoretical probability distributions. They are determined by statistical functions, expert knowledge and simple physical laws. The model is already in use for daily avalanche prediction on the spatial level of single release slopes (Kleemayr, 2002). It has to be emphasized, that this modeling approach is absolutely preliminary, because the "final state" of a release model has to be much more physical. But the results obtained give rise to the hope that the empirical distribution of the variables can be define more precisely via this intermediate concept.

Focus definition

In 1939, the Swiss snow researcher Haefeli presented the first systematic work concerning snow mechanics. Since then, the understanding of mechanical behavior has continuously increased. But for all of these efforts, it has to be stated that "…the properties of snow are not yet well enough known for use with a high degree of confidence. …Its properties have been determined for only a few cases" (Brown 1989). Though Bartelt (1998) for the first time tries to develop a coupled thermodynamic-mechanical model, we are far away from a "global model", a model which would be able to describe the system behavior for all interesting influence parameters and time scales. But as long as a full description of the system by observations is still missing, a mathematical model has to focus on subsystems. As Casti (1992) states, there is no algorithm to determine these fractions of the whole system. One possibility is to fix a set of observations which enable mathematical modeling by first being measurable, and second describable due to some rough ideas of causality

(perhaps this sounds like a platitude, but it is not easy to achieve for many natural processes). In the case of snow mechanics, two classes of properties could be used for system reduction: a) stress-strain behavior or b) failure mechanism.

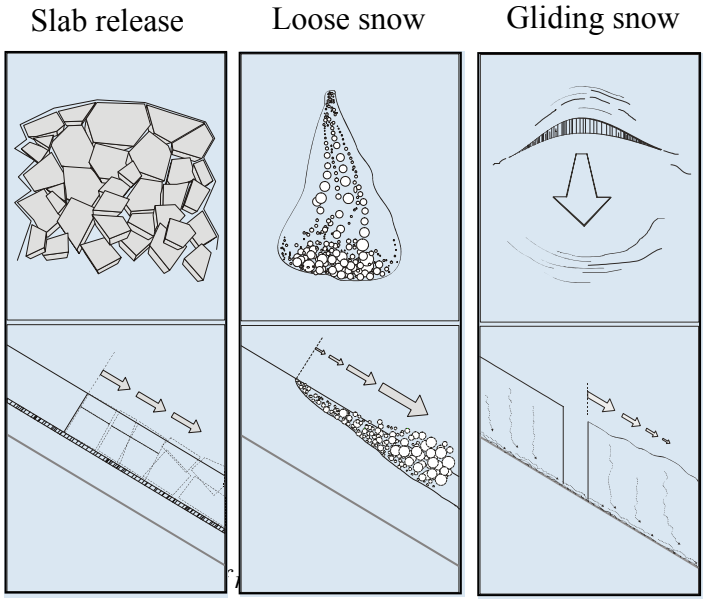

Figure 3.1 shows three types of an avalanche release mechanism. This classification is not a pure phenomenological classification, but tries to group the different mechanical processes. Loose snow avalanche release is dependent only on the local loss of connection between the crystals or ice grains. It is highly sensitive to temperature and the change of temperature of the snow grains near the snow cover surface. The depth of the snow cover, strength within the snow cover, or the slipping conditions on the ground, do not affect this mechanism at all. In contrast to loose snow release slab avalanches are strongly connected with the presence of a weak layer with a certain thickness or simply a weak connection between two layers. Experience gives rise to the assumption that so called super weak zones (very weak zones within the weak layers) are able to cause an initial failure with high failure velocity and following elastic brittle failure of the whole slab lying above the weak layer. This kind of avalanche release is of high practical importance because of the scarcely predictable release area and the tendency of instantaneous mobilization of a vast amount of snow mass. Slab avalanche release is mainly dependent on the strength of the weak layer and all influence factors, which increase or decrease the stability of it. Till now there have only been few attempts to measure important quantities like shear strength, and there are only ideas of the spatial distribution of these weak layers. Furthermore, the strength of the weak layer undergoes a permanent change affected by meteorological conditions and the isolation capacity of the layer above. High modeling efforts have been put into it recently, but a concise mathematical-physical description is still missing.

The third mechanism is avalanche release caused by snow gliding. In contrary to the previously mentioned failure mechanisms, fracture by snow gliding is not sensitive to the strength of the upper most layers in the snow cover. This is important because daily changes of temperature near the snow cover surface and the subsequent intensive variations of strength have minor importance. Observations show that snow gliding mainly depends on a) the roughness of

the ground b) the free water content in the lower most snow layers and c) the viscosity near the ground. The practical importance of snow gliding and avalanche release by snow gliding also differs from the release types mentioned above. Snow gliding causes high loads on control measures. In average the related avalanche types are much smaller compared to slab release avalanches. Snow gliding release has not been realized in ARIS, because both experience and statistical analysis show, that only a simulation of the whole snow cover can deliver reasonable results.

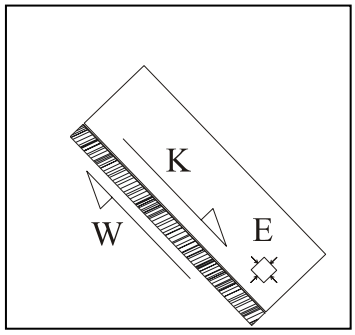

Figure 3.2: Snow cover properties influencing the probability of avalanche release. K: Driving forces, W: Resistance forces, E: Material properties

Mechanical concept

The probability of avalanche release can be seen as consequence of the probability of strength of the snow cover (Figure 3.2: E), the probability of accelerating forces (Figure 3.2: K) and the probability of resistance forces (Figure 3.2: W). At least one of the factors has to be in a critical range in order to trigger a failure. New snow does not lead to an instantaneous increase in failure probability. The hazard of slab release strongly depends on the adhesion condition to the snow cover surface (resistance force). But continuous snowfall up to a critical snow height significantly rises the failure probability with relative lower influence of the snow cover surface properties. Loose snow release probability in contrary is nearly independent of the surface conditions. It is mainly effected by the material properties.

To enable the calculation of avalanche release for a given release zone it is necessary to determine the snow depth for each release unit. Although the release area in reality is not constant from a practical point of view it has been a priori defined in this project. Based on field investigations and topographical analysis, areas with more or less topographically homogenous characteristics have been determined as release units. With this approach the above-mentioned scaling effect clearly is lost. But it was the hope, that in case of proper hazard calculation neighboring units with similar hazard levels can be grouped at the end of the calculation algorithm.
The computation of “local” snow depth has to take into account radiation, snow redistribution and the history of the snow cover. Here only the integration of the last two parameters is shortly described. For further details please see Kleemayr et al. (2002).

Snow depth model

The snow depth model in ARIS tries to integrate the experience, that with increasing sow depth the asperities of the terrain surface are smoothened and therefore probability of homogenous weak zones rises (the roughness of every

release zone has been classified in the field). The snow depth for the release areas than was supposed to be the summary of the old snow cover depth and the additional amount of new snow and redistributed snow.
The redistributed snow amount is calculated by the relation of Meister (1989), which defines the transported mass with:

$$\Delta m = \left(\frac{M_2}{M_{th}}\right)^3 \left(\frac{p_r + 2 mmw.e.h^{-1}}{200}\right)\Delta t \qquad \text{[kg/m²] or [mm w.e.]}$$

Δm: transported mass
M_2: average wind speed for the period Δt, [m/s]
Mth: wind speed threshold for beginning transport [m/s]
Pr: rate of precipitation [mm w.e. /h]
Δt: time discretisation [h]
w.e.: waterequivalent.

For the continuous change of snow cover depth two processes can be made responsible. Metamorphosis processes cause a strongly time dependent settlement rate, which can be described by the function (Rohrer, 1992):

$$H_{sn} = H_{s0}(n+1)^{-k}$$

H_{sn}: Depth of the snow cover on the n-the day, [cm]
H_{s0}: precipitation, [cm]
k: rate of settlement depend on winter season.

For the temperature dependent depth reduction Kuhn (1983) proposes:

$$S_{sn} = Temp_n * a$$

S_{sn}: Settlement of the snowcover on the n-the day [cm]
$Temp_n$: average positive daily air temperature [°C]
a: rate of settlement depend on winter season [cm/°C].

Based on the methods described by Rohrer (1992), a fuzzy set has been developed to apply these simple functions to varying aspects and winter seasons.

Determination of the release probability

For the two failure mechanism under consideration the probability is determined separately. The possibility of a slab release *p_slab* is determined by

$$p\_slab = e^{\left(0{,}25 * \ln\left(p\_surface * p\_hcrit^2 * p\_extend\right)\right)} + 2{,}302585093\,.$$

The component probability p_surface describes the adherence of the new snow to the snow cover surface. Because of lack of information, it has been tried to get the information by an expert inquiry including the Tyrolean avalanche information center. The information given by the experts was satisfyingly congruent so that a "heuristic" function could be determined. Figure 3.3 depicts the assumed relation between air temperature, intensity of surface hoar and the probability of "shear strength".

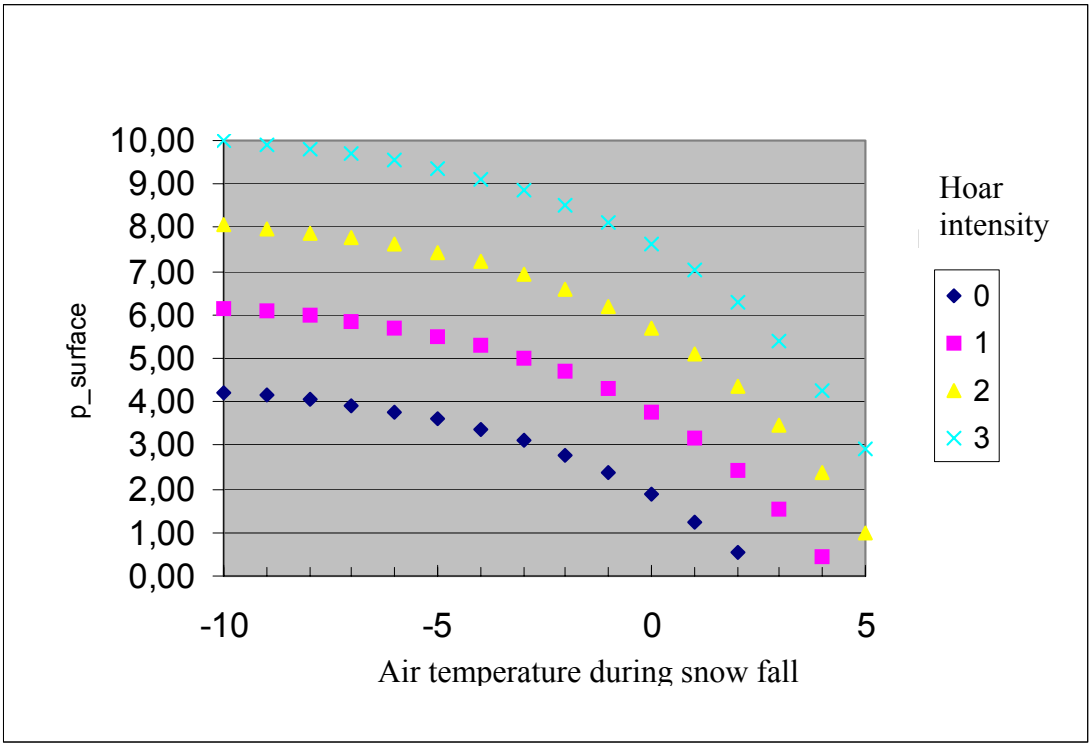

Figure 3.3: Heuristic function of p_surface depending on air temperature during snow fall and surface hoar intensity. The relation is based only on expert knowledge.

It has to be emphasized again, that – if available – a more scientific definition should be used. But also with this strongly simplifying approach the qualitative evaluation is positive and the results are in most of the cases plausible. For daily prediction the results can be easily verified every day. But for events with higher return periods again the question rises: what is the probability of e.g. surface hoar or sun crust?

To answer this question the daily avalanche bulletins of the Tyrolean avalanche center has been analyzed. Figures 3.4 and 3.5 show the empirical probability of weak adherence, surface hoar and sun crust for altitude ranges between 500 – 1000 m and 2500-3000 m.

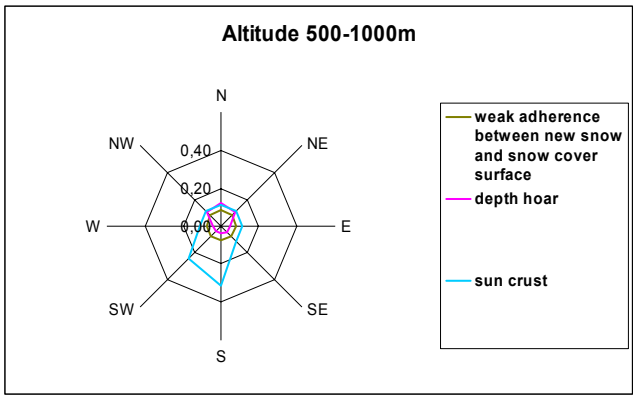

Figure 3.4: Probability of weak adherence conditions for an altitude range of 500-1000 m and varying aspects.

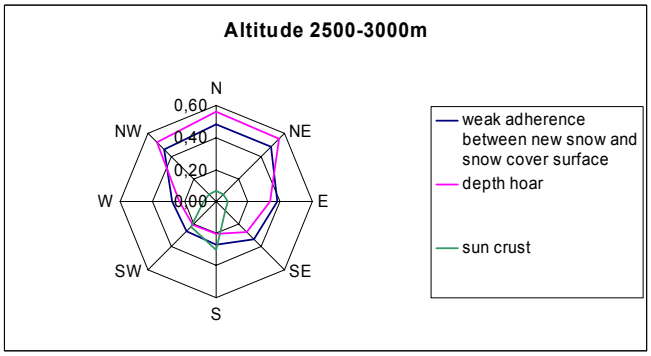

Figure 3.5: Probability of weak adherence conditions for an altitude range of 2500 - 3000 m and varying aspects.

The component probability *p_hcrit* describes the probability of a failure caused by increasing depth of new snow based on the basic snow mechanical function:

$d_{krit} = k/(\rho g(\sin\psi - tg\delta\cos\psi)$
with: k =250 (Pa)
ρ = density (kg/m³)
δ = angle of repose (°)
g = 9,81 (m/s²).

The last component probability *p_extend* describes the relation between the snow depth and the terrain roughness.
P_loose, the probability of loose snow release, is given by

p_loose = (*p_strength* * *p_hcrit*)^0,5 * 10.

In contrary to the purely empirical determination of the shear resistance forces mentioned above, the probability of strength has been derived with statistical methods by using the penetration depth of the database.

Results

The model has been implemented in risk information system which allows imaging the release probability for every release unit (Figure 3.6).

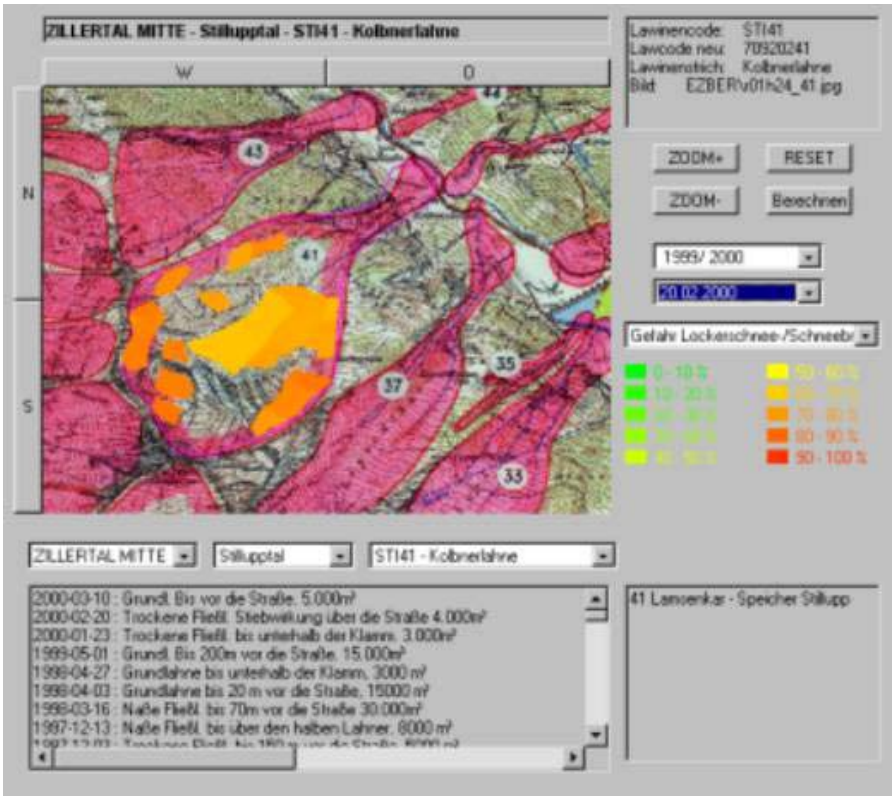

Figure 3.6: Graphical user interface of the avalanche risk information system. Picture shows the release danger of one day for several release units.

The prediction of loose snow probability is satisfying, because nearly 90% of the avalanche days could be predicted correct. Figure 3.7 shows the “release graph” for the winter 2001/2002 for the Bärrinne Lawine.

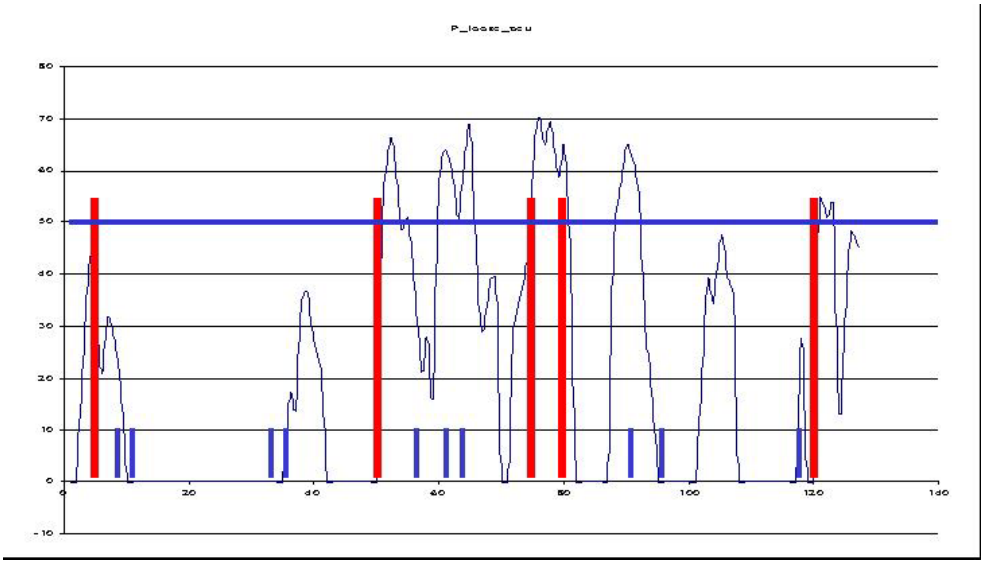

Figure 3.7: Graph of the predicted avalanche probability. X-axis: days. Y-axis: probability between 0 and 100 %(50% means medium danger). Thick red columns: avalanche events in the track. Short blue columns: avalanche events in the neighboring tracks.

The statistical evaluation of the slab model is still running, because winter 2002/2003 has been the first in which all necessary data are collected by the practitioners. But the qualitative evaluation during the winter was very positive.

Yet some basic problems came up in the winter 2002/2003. If the release probability is triggered by snowfall events the model delivers quite reasonable results. But in winter 2002/2003 the snow cover development was strongly influenced by nearly two months of could but sunny weather. Snow depth calculation as well as surface conditions differed from reality at the end of the period. Although the release hazard of the following snowfall period has been predicted quite well, the mechanical parameters in the model have not been estimated correctly (which is not satisfying in the same way for a distinct physical model as well as for a simplified model).

3.3 Dynamical methods for determining avalanche run-out

CH, CK, and TJ

While empirical procedures may permit an assessment of run-out distance, the more advanced dynamics models give much additional information concerning the nature of the sliding event (flow heights, velocities, etc.). This information is crucial for improved understanding of avalanche dynamics, and for the calculation of (amongst others) the impact pressure upon obstacles.

Previous examinations of the existing models shows that: (1) there is not - and probably never will be - a single model that adequately describes all avalanche types; (2) in order to account for the extraordinary variability of avalanche motion in response to initial and boundary conditions, flow-regime transitions and the snow mass balance should be properly described in future models; (3) calibration and validation of these models will require a comprehensive measurement programme; (4) determination of realistic initial conditions is a serious problem. We suggest that using simple models to scan the relevant parameter space with more advanced models for detailed simulations of selected scenarios could improve this situation, cf. Section 3.5.

Some of the most commonly used avalanche run-out models in Europe have been tested and compared in the EU program SAME by Barbolini et al. (1998). Four models have been integrated in a common user interface that allows a direct comparison between those models. The common user interface is described by Naaim and Gruber (1998).

An experienced modeller working with a complex mathematical model of avalanche flow will have to select appropriate ranges of values for various model parameters that act as initial and boundary conditions. The selected set of parameter ranges for an extreme avalanche (e.g. 100 year return period) will, when implemented in the model, yield a range of predicted run-out distances. The diligent modeller should compare the distribution of run-out distances obtained from a number of simulations using various parameter combinations to the error range of the statistical models. It is the error distribution rather than the simple first moment prediction (i.e. the mean value) that should be the focus of attention for the mathematical modeller who wishes to compare numerical results to a statistical model. Ideally, the two distributions should have similar moments (again, one should examine more than the first moment). Where this is not the case, there are two possibilities: either the statistical model performs poorly (likely to occur if the topography of the particular path is different to that of events in the database); or particular parameter values or parameter combinations are inappropriate. If the latter is the case, the modeller will have to re-inspect and re-think the appropriate parameter ranges. To eliminate the first possibility it would seem to make sense to first apply the mathematical model to a path where an extreme avalanche has been recorded and used in the development of the statistical model and which was not an outlier in this event database.

The statistical models provide an estimate of error based upon a sample of real events. By tuning the numerical model to this error range, the modeller can then go beyond the information contained in the statistical models and give predictions for velocities, impact pressures and related phenomena. It is important to note that of the two statistical models, the run-out ratio model (ref…) gives a positively skewed distribution of run-out distances, while the α/β model (ref…) is symmetrical. Thus, certain parameter combinations may be tolerated by one model and not the other.

The concept of a run-out index that is used in the Icelandic hazard zoning procedure (see Appendix A) facilitates the transfer of avalanches between paths and makes it possible to employ a dynamical model in a statistical manner, similar as is traditionally done with statistical models based on geometrical properties of the avalanche path, such as the alfa/beta-model.

3.3.1 Brief overview of dense snow avalanche dynamics models

CH and CK

Depth-averaged models for an avalanche in a three-dimensional terrain exist, but most models in common use are either one-dimensional rigid body models (lumped mass or sliding block on a linear slope or in two-dimensional terrain) or two-dimensional depth-averaged deformable body models (two-dimensional continuum in a two-dimensional terrain).

Rigid body models describe the slide initiation well. Due to their simplicity they are also widely applied to the rest of the avalanche motion. Deformable body models describe the dense snow avalanche as a continuum. Difficulties arise in choosing convenient constitutive equations, boundary conditions, initial conditions and in solving the equations.

The sliding block (also called lumped mass or rigid body) model describes the avalanche as a rigid body on a linear slope or as a flexible body (“blanket”) following the terrain. Alternatively, the motion can be described by a centre-of-mass consideration, incorporating the sum of external forces acting on the body. These models describe the slide initiation well. Due to their simplicity they are also widely applied to the rest of the avalanche motion. Back-calculated friction coefficients tend to be low compared with measured values.

Most dense snow avalanche dynamics models are rooted in hydraulic theory, although granular flow models utilising various geotechnical methods from soil mechanics have also been developed. Hydraulic deformable body models are distinguished by the use of depth-averaged equations of motion similar to those used for calculating unsteady flood waves (from an analogy with open-channel hydraulics). Both wet snow and dry snow avalanches involve a high internal deformation and are more or less in a liquid state.

There may be some confusion in the terminology concerning the dimensionality of models. The basic dimensionality of the deformable body models is the number of space dimensions in the dynamics equations. The term "quasi two-dimensional model" means one-dimensional equations with depth or width averaging. "Quasi three-dimensional model" is ambiguous since it could mean a one-dimensional model with height and width averaging, or a two-dimensional model with height averaging. A depth-averaged deformable body model that uses a profile plus transects is said to have dimension 2.5,2.5

(the flow is described down and across the slope, but the height of the flow isn't all there, while the terrain is not quite fully three-dimensional).

The main problems of dense snow avalanche dynamics models are related to the choice of initial conditions and the understanding and description of material properties that in the first place differ considerably during the flow and after deposition.

The main weakness of the models appears to be related to:

- the form adopted for the bed resistance (in particular it does not appear to be possible to properly reproduce a certain event from release to run-out using constant values for the drag coefficients μ and *n);*
- the omission of an erosion term;
- the assumption of incompressibility.

Special attention is currently directed towards overcoming this weakness, but results will be achieved only when more experimental information about the mechanical behaviour of the material and quantitative data related to the exchange of mass is available.

3.3.2 Model input parameters

3.3.2.1 Initial conditions

See previous sections 2.2 and 3.2 on release conditions.

3.3.2.2 Flow parameters

3.3.2.2.1 Introduction

MB

One of the main problem associated to the use of avalanche dynamic model in practical mapping application is represented by the relevant uncertainties that underlay the definition of the model input-data, given the strong sensitivity of the models to their input parameters (Barbolini et al., 2000a). In particular, it appears that there is an urgent need for new procedures for evaluating the appropriate values of the friction parameters, especially for the new generation of hydraulic-continuum models (Harbitz, 1998). To date, the only reference table for friction coefficients that provides well-defined ranges in relation to the avalanche features (snow conditions, avalanche frequency) and path features (degree of channelling, vegetation) is that contained in the *Swiss Guidelines* (Salm et al., 1990). However, as shown by Barbolini et al. (2000a), these reference values, which result from the calibration of the classical

Voellmy-Salm model (Voellmy, 1955; Salm et al., 1990), cannot be applied to other types of model, even if they use similar expressions for the flow resistance. Furthermore, these ranges have been demonstrated to be too wide to allow a reasonable precision in the model results, given the sensitivity of the models (Barbolini et al., 2000a). The alternative procedure is to perform a direct "on-site" calibration of the model on the basis of suitably recorded historical events. Apart from the common lack of data on avalanche events appropriate for model calibration, it should also be noted that the release of a given snow volume can produce different run-out distances depending on the released snow characteristics and on the snow cover properties along the track.

Recently Barbolini and Savi (2001) and Meunier and Ancey (2003) suggested that this inherent variability, which results from either physical processes that are oversimplified (e.g. energy dissipations) or not explicitly modelled (e.g. erosion-deposition), could be captured by expressing the friction coefficients in terms of site-specific probability distributions, (assumed to be dependent on the avalanche frequency). In particular, Meunier and Ancey (2003) proposed a method to derive such probability distribution on the base of at-site data alone (see Section 3.3.2.2.2); this approach is feasible in the case of well-documented avalanche path. However, to overcome the usual lack of site-specific avalanche data needed to infer these probability distributions, Barbolini and Savi (2001) proposed a different method that allow to evaluate their parameters at a "regional scale", i.e. by using friction coefficient values calibrated on different avalanche sites (see Section 3.3.2.2.3).

It should be noticed that expressing the friction parameters in terms of probability distribution has a twofold advantage: (i) allows a systematic best-guess estimate of the friction parameters of the design avalanches (e.g. using the mean value), within a "classic" hazard mapping scheme; (ii) allows to explicitly take into account for the uncertainties in the friction coefficients estimate, when approaching the mapping problem by way of a Monte Carlo simulation procedure, as discussed in Section 3.3.6. The method proposed originally by Barbolini and Savi (2001) is presented in the following Section, where also some successive improvements are briefly discussed.

3.3.2.2.2 Site-specific estimate of friction coefficients based on at-site data

MMe

Calibrate a dynamic model on a specific event is a well known operation that every avalanche scientist is able to practice. The differences in doing such operation come from its objective and from the information one has on the event. We will explain now two opposite cases:

a) the estimation of the avalanche friction coefficient in order to simulate one event only, but in the most complete way, using

all the available information. Generally, this is done for a catastrophic event where some information may appear contradictory, and this creates some difficulties. This is called the scenario method in France.

b) The estimation of the friction coefficient on many events in order to make them comparable. In that case, we have to use the same quantity of information for all the events. Consequently, we have less information than in the precedent case.

When there are not enough results for each avalanche path of a region and if the avalanche paths have the same behaviour, it is then possible to solve the problem in a regional way: this will be seen in the following Section 3.3.2.2.3. Here, we will examine the treatment of the events of a single avalanche path, in order to get a sample of the friction coefficient, then to fit a statistical distribution on it.

a) The scenario method will be described later

b) Obtaining a statistical distribution of site-specific friction coefficients

There is a great variety of dynamic models which can be used in order to reproduce the propagation of an avalanche event and each of them has its own friction parameter, even when the friction law introduced in the model is the same from one model to another. So, up to now, none dynamic parameter can be used in an universal way for any type of model, as it has been shown by Barbolini and al, 2000. It means also that the dynamic model is used here as a conceptual model and not as a deterministic one, even if it seems to have a physical basis. We will explain the method using the well known one-dimensional sliding block model explained briefly in 3.3.1.1. It has 2 friction parameters μ and ξ. The equation of the model is the following:

$\frac{du}{dt} = g\cos\theta(\tan\theta - \mu) - \frac{g}{\xi H}u^2$, where u is the velocity, H is the height of the avalanche and stays constant, θ is the local slope angle (we suppose that the path profile is known).

The <u>first step</u> of the method consists in gathering all the data of the single path and to examine if there are enough information to carry on the simulations. As input parameter, we need the height H; this means that we have to deduce the heights of each event from the available information we have on the initial conditions of the event. These information may be the avalanche height itself, but, in the general case, it can be the snow mantle height, or the avalanche release volume, or the avalanche release deposit, or anything else. Sometimes, it is possible to get a combination of values of these different data, and we have to examine their complementarity's. So, for this step, there is no general

method; each case is specific and we have to solve it according to the available input data. In the following, we will consider that we have obtained a set of avalanche heights for each event for which we have the output data. We will present a specific case in Section 3.5.1.

As input parameter, we need also the starting altitudes or the starting distances of the event. Generally, people think that this variable has little effect on the result and it would be correct to adopt a high plausible value for the starting altitude of all the avalanche events. In fact, we saw on a specific case (see Meunier and Ancey, 2003) that this variable is important when the friction parameter ξ is higher than 1000. So, it is better to use the right starting altitudes when they are available.

The second step of the method consists in examining the available output data. As the dynamic model has 2 friction parameters, the number of available output data should be equal to 2 also, if we want to fit exactly the friction parameters. It is generally not the case, and in the better case we have to fit the model on one output data only, the stopping distance or stopping altitude. Of course, when we have no output data, the method is not usable and we are obliged to act as the practitioners (using for instance the Swiss guidelines). Later on, we will adopt the hypothesis that we have one piece of information for each event, the run-out distance. So, we have an infinity of couples (μ,ξ) that give the right run-out distance of one event, as it is shown in Figure 3.8, for four events of the Favrands path.

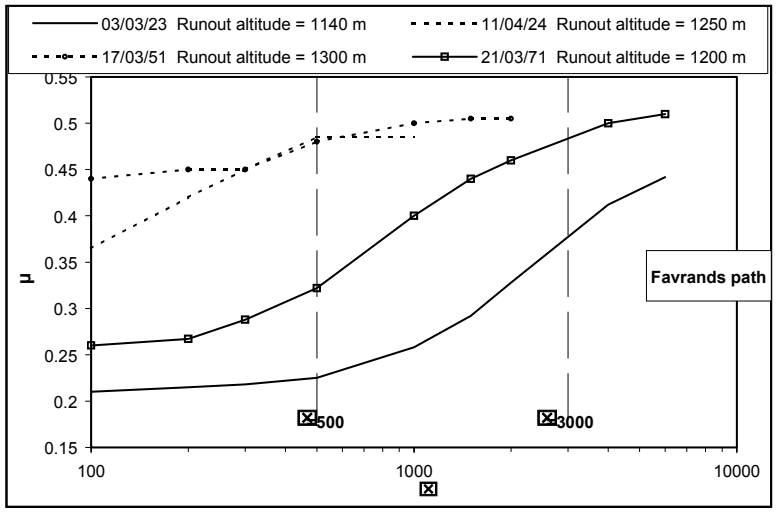

Figure 3.8: Couples of (μ,ξ) that give the right run-out distance of for four events of the Favrands path.

So, in the third step we have to decide which parameter we will fit on the output data, as we have the possibility to fit only one of the two friction parameters of the model. We are obliged to fix the other one and to keep it constant for all the events. According to the practitioner habits, ξ should be kept constant for all the events of the same path. The only problem is then to

determine its value. This hypothesis is accepted for instance here for the regional estimate of friction coefficients (3.3.2.2.3).
But, when we use the rigid block model as a conceptual model, the two parameters have no peculiar a priori physical meaning and we are allowed to fix anyone for all the events and fit the second one on each event. We compared the two approaches on the example proposed in Section 3.5.1 and saw that both are acceptable (Meunier and Ancey, 2003).

So, at the end of the third step, we should have decided which friction parameter is kept constant and with how many successive values. For instance if we decide to keep ξ constant, the figure shows that ξ may vary from 300-400 to 5000-6000. Of course, we may decide to keep μ constant, and have ξ different for one event to the other one. According to the figure μ can vary from 0.2 to 0.55.

In the fourth step, for each event, the input variables (height and starting distances) are known and one friction parameter is fixed and known (but possibly, we can give many different values to this parameter in order to compare the results); so, the problem is now simply to fit the second friction parameter in order to obtain a calculated stopping distance equal to the measured run-out distance. This is relatively simple to do, but one important previous condition is that the slope profile should be smoothed enough. The DTM obtained from the different points of a grid is too irregular and not usable; it should be strongly smoothed. Of course, this corresponds physically to the smoothing of the real summer profile by the snow mantle.

So, at the end of this step, for one value of the fixed friction parameter, we have a sample of values of the other friction parameters corresponding to each avalanche events. If we give many different values to the fixed parameter, we obtain the same number of samples of the fitted parameter.

In the fifth step, the last one, we have to find the statistical distributions which can be fitted on the samples of friction parameters. This is not a trivial work as it seems that the histograms of the friction parameters have not only one mode. And we have to decide how many types of avalanches can exist on the path.

In Figure 3.9, we show the example of Entremere path for which we thought that there are two groups of events and that each group should be represented by one statistical distribution. We used two Beta distributions for the values of $\mu|\xi$, and two gamma distributions for $\xi|\mu$. But it is obvious that other statistical distributions may fit the samples as well, as one can see for this example which will be more developed in Section 3.5.1, where we will use normal distribution for $\mu|\xi$ and lognormal distributions for $\xi|\mu$.

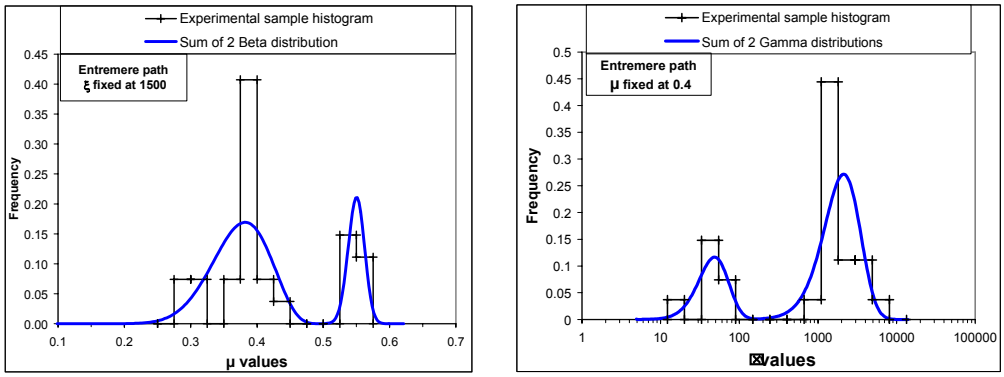

Figure 3.9: Avalanche frequency for the Entremere path. Two Beta distributions are used for the values of $\mu|\xi$ (left) and two gamma distributions are used for $\xi|\mu$ (right).

3.3.2.2.3 Site-specific estimate of friction coefficients based on regional data

Contr.: MB

Method

When calibrating a dynamic model on a given site, usually very limited information on the dynamical features of historical events is available — typically run-out distances only. It is then possible and advantageous to set the "turbulent" friction coefficient (usually indicated with ξ) to a constant value and to reproduce different avalanche events by varying the Coulomb friction coefficient only (usually indicated with μ). This is due to the strong sensitivity of run-out distance to this latter coefficient, with ξ influencing this variable much less (Barbolini et al., 2000a). Therefore, within the current calibration procedure, it appears reasonable to restrict the variability and the related analysis of uncertainties to μ, and to use for ξ a constant (average) value related to the site features only - typically the degree of channelling and vegetation of the avalanche path (see Section 3.6.2.1); this assumption is in agreement with the indication of Salm et al. (1990) and with the results obtained by Barbolini and Savi (2001) in various Italian Alpine ranges. Therefore, in the following we will focus our attention on methods for estimating the probability distribution of the friction coefficient μ only.

According to the proposal of Barbolini and Savi (2001), the evaluation of the friction coefficient μ could be made using weighted moments. A total of M paths in the same region to the path under consideration are plotted in a multivariate space defined by the path topography. For each of these i calibration paths one (or more) values for μ has previously been determined by model calibration (μ_i). The path to be examined (path j) can also be plotted in

this space and the distances to all the calibration locations can be found. On the assumption that paths with similar characteristics will have similar μ values, the μ values for the nearest neighbours can be given a high weighting and those further away a low weighting. These weights (w_{ij}) can then be used to derive moments for the distribution of μ_j , in particular the first and second moments of μ_j (average value and standard deviation, respectively):

$$\overline{\mu}_j = \frac{\sum_{i=1}^{M} \mu_i w_{ij}}{\sum_{i=1}^{M} w_{ij}} \tag{3.1}$$

$$\sigma(\mu)_j = \left[\frac{\sum_{i=1}^{M} (\mu_i - \overline{\mu}_j)^2 w_{ij}}{\sum_{i=1}^{M} w_{ij}} \right]^{0.5} \tag{3.2}$$

Given the moments, once a suitable probability distribution has been chosen, its parameters can be estimated straightforwardly.

The multivariate space formulated by Barbolini and Savi (2001) used nine topographic parameters (Table 3.1), with values standardised by subtracting the mean and dividing by the standard deviation. An Euclidean metric was used to determine the distance (d_{ij}) between the i'th and j'th paths in the space based upon the K=9 topographic parameters x_k (Equation 3.3) and these distances were then rescaled to a range between zero and one. The weights w_{ij} were derived from the rescaled distances d^*_{ij} by a simple inversion procedure (Equation 3.4).

$$d_{ij} = \sqrt{\sum_{k=1}^{K} (x_{ki} - x_{kj})^2} \tag{3.3}$$

$$w_{ij} = (1 - d^*_{ij}) \tag{3.4}$$

Both parametric and non-parametric tests showed that (Barbolini and Savi, 2001), if the calibration avalanche events are tentatively classified in two general frequency classes - say relatively frequent and extremely rare events -, the resulting sub-samples of calibration values ($\mu_{i/RF}$ *and* $\mu_{i/ER}$ respectively) belong to different populations (see also Section 3.6.2.1). Therefore, it is assumed that for each avalanche site events from the two mentioned frequency classes (i.e. with different return periods) need separate probability distributions, whose moments are determined by running equations 3.1 and 3.2 over the two separate calibration sub-samples, $\mu_{i/RF}$ *and* $\mu_{i/ER}$. This implicitly

represents a way of correlate the probability distribution of the friction coefficients with the avalanche return period that is with the probability distribution of the release variable.

The multivariate space outlined by Barbolini and Savi (2001) is a useful *a priori* formulation. All the terrain variables included are physically reasonable, all are given equal weighting and a minimum degree of manipulation of the space is required. Furthermore, measuring distances in this space has proven effective in capturing topographical similarities between avalanche sites that result in close values of calibration for the friction coefficient μ (Barbolini, 1999; Barbolini and Savi, 2001).

Table 3.1. Parameters used to measure topographical similarities between avalanche paths. The reference inclination of the β-point has been set to 14° to include in the analysis as many sites as possible. The aspect is measured in degrees from North; in order to account for the fact that the most relevant differences between snow conditions are related to North and South aspects, equal values for the aspect in the East and West quadrants are used, i.e. E is measured in the following way: N=0°; NE/NW=45°; E/W=90°; SE/SW=135°; S=180°.

	Symbol for parameter (x_k)	Parameter description
1	β (°)	Average inclination of avalanche track, measured between the starting point and a point of 14° inclination along terrain profile.
2	δ (°)	Average inclination of the run-out zone, measured from the point of 14° inclination along terrain profile.
3	ψ (°)	Average inclination of the whole avalanche track, given by the ratio between total vertical drop and length of path.
4	H (m)	Total vertical drop of the path.
5	y'' (m^{-1})	Curvature of the best-fit parabola.
6	R^2 (-)	Squared coefficient of correlation of the best-fit parabola with the real path profile.
7	Z_R (m a.s.l.)	Average altitude of the release zone.
8	Z_D (m a.s.l.)	Average altitude of the run-out zone.
9	E (°)	Path aspect (in the case of path with bends the aspect of the release zone should be considered).

Space distortion

Recently an alternate ways in which the multivariate topographical space might be defined to give more effective site-specific definition of μ has been suggested (Barbolini et al, in press). In fact, the nine topographic parameters presented in Table 3.1 are unlikely to contribute equally to the prediction of the friction parameter μ and thus, the multivariate parameter space should be distorted in some way to reflect this. Furthermore, some of the variables are likely to be more or less similar to one another and thus, sampling from a space that does not account for this and considers all variables to be independent will

introduce a bias into the distance measure (Equation 3.3). Eight methods for weighting the dimensions of the multivariate space were formulated and tested (Barbolini et al, in press). These were classified into three groups based upon the general method used.

(A) The *k*'th dimension of the multivariate space was weighted by the partial correlation between μ and x_k. Thus, variables will contribute to the space in a manner proportional to their correlation with the parameter of concern (μ). Three separate methods were selected:

(i) Weight the dimensions of the multivariate space by multiplying each axis by a factor equal to the magnitude of the partial correlation coefficient;
(ii) Weight the dimensions of the multivariate space by multiplying each axis by a factor equal to the square of the partial correlation coefficient, a parameter similar to the coefficient of determination ;
(iii) Change the dimensionality of the multivariate space to only include variables that show a significant relationship with μ.

(B) Step-wise linear regression (Mendenhall and Sincich, 1996) was used to predict μ from the terrain parameters. Again, three different ways of manipulating the multivariate space suggests themselves:

(i) Specify a threshold value for the *F* statistic from the regression Analysis of Variance and only include terrain parameters that exceed this threshold;
(ii) As for B(i) but then weight the selected terms according to their contribution to the degree of variance explained by the regression model;
(iii) Include *K*-1 terrain parameters in the regression model, but then weight them as in B(ii).

(C) A different approach for reformulating the *K*-dimensional terrain space is to ignore the relationship of particular parameters with μ and to focus upon the way that the *i* avalanche paths are distributed within this space. Principal Components Analysis (PCA) (Johnson, 1998; Koel, 2001) was the technique used to reduce the dimensionality of the space. Two methods for redefining the *K*-dimensional space using PCA are:

(i) Use the more important components to collapse the space into a lower dimensional space, and perform the weighted moments analysis upon this reduced space;
(ii) Weight the space derived in C(i) by the proportion of the variance explained by that component.

The testing procedure of the performances of the different methods of space distortion was based on a set of calibration values for the friction coefficient μ; the calibration sample was obtained by calibrating a one-dimensional hydraulic-continuum avalanche dynamics model (Natale et al., 1994; Barbolini et al., 2000a) - using a classical two-parameter Voellmy-like resistance law (Bartelt et al., 1999) - over a group of well documented avalanche paths from an Italian Alpine region, the Veneto region (Barbolini et al, in press; see also Section 3.6.2). The methods C(i) and C(ii) showed relatively small differences from the original Barbolini and Savi (2001) formulation. Very small differences in the μ-moments estimations were found also between B(ii) and B(iii); this suggest that little error is introduced by neglecting the less significant terms. However, from a theoretical perspective, the approaches based upon stepwise regression (B) are less robust than those that use partial correlation (A). This is because stepwise regression does not account for second or higher order effects. As the fundamental concern is to predict moments for μ, it makes sense to determine the space with this end in mind. Consequently, approach A would seem to be preferable. For practical purposes, the useful aspect of space A(i) is that it includes all variables. Hence, this space can be derived automatically without having to make decisions about which variables to include. Thus, it is suggested that A(i) is the most useful method for deriving site-specific moments for μ.

A possible way to look at the precision of the different methods of estimation is to jack-knife the results: Table 3.2 shows the mean and standard deviation of μ estimated for each of the 22 considered sites (from the Veneto region, see also Section 3.5.2) when its value for μ is assumed unknown and its predicted from the remaining 21 sites by two different methods - the original Barbolini and Savi (2001) method and the method based on the new space formulation A(i).

The RMS (Root Mean Square Error) for the new space formulation is 0.0456, about 13% less than for the original space formulation (RMS=0.0522), demonstrating that the new formulation is not just a better one from theoretical considerations. It gives the mean value more freedom to adjust and therefore permits a less biased site-specific estimate of μ. It is also interesting to observe that for the new formulation the average value of SD(μ) is 0.046, 6% reduced with respect to the Barbolini and Savi (2001) formulation (0.050), showing also an overall increased accuracy in the estimate of μ. Therefore, it is suggested that, when measuring distances between avalanche paths - equation 3.3 - weighting the dimensions of the topographical space according to the partial correlation coefficient between the terrain parameters (of Table 3.1) and μ is a theoretically justified and practically advantageous approach.

Table 3.2. Mean and standard deviation of μ for different avalanche sites from an Italian Alpine region (Veneto) predicted for each of the 22 sites from the remaining 21 sites by the original Barbolini and Savi (2001) method and by the method based on the new formulation A(i).

Site Name	Observed μ	μ estimated with the original Barbolini and Savi (2001) method		μ estimated with formulation A(i).	
		Mean	St.Dev.	Mean	St.dev.
2	0.32	0.313	0.049	0.323	0.045
8	0.39	0.315	0.044	0.334	0.047
14	0.28	0.310	0.047	0.304	0.048
15	0.32	0.310	0.048	0.314	0.046
38	0.29	0.317	0.053	0.316	0.046
36	0.41	0.310	0.046	0.320	0.042
61	0.40	0.313	0.049	0.334	0.048
65	0.32	0.309	0.055	0.306	0.048
69	0.40	0.313	0.055	0.328	0.048
70	0.30	0.307	0.050	0.303	0.049
73	0.33	0.309	0.051	0.310	0.046
80	0.32	0.308	0.059	0.312	0.048
83	0.21	0.309	0.046	0.304	0.043
91	0.31	0.311	0.048	0.306	0.047
105	0.30	0.316	0.047	0.301	0.049
106	0.30	0.318	0.049	0.301	0.049
107	0.32	0.319	0.048	0.318	0.045
108	0.37	0.321	0.048	0.326	0.048
120	0.35	0.316	0.050	0.339	0.050
21	0.22	0.305	0.051	0.307	0.044
87	0.28	0.307	0.052	0.305	0.048
Voltago	0.24	0.309	0.046	0.302	0.046

Introducing a threshold for distances

The preceding analysis has used all the available calibration data to determine the moments of the distribution for μ in a given path. An alternative approach is to only consider those sites within a threshold distance $\hat{d}$ (e.g. the mean or the median distance). In this way the site-specific moments (Eqs. 3.1 and 3.2) are derived using only the topographically more similar paths (namely those that lie within the hypersphere of radius $\hat{d}$ in the multidimensional topographical space, i.e. for which d_{ij} from equation 3.3 is equal or lower than $\hat{d}$), and excluding from the analysis the paths that show a relevant (topographical) dissimilarity from the site under analysis.

Figure 3.10 shows the RMS error between the predicted and known μ when trying to predict μ at one of the 22 sites (of Table 3.2) based on some or all of

the other 21 sites. The x-axis shows the number of sites used in the prediction, so 1 just uses the nearest neighbour, while 21 uses all the data available.

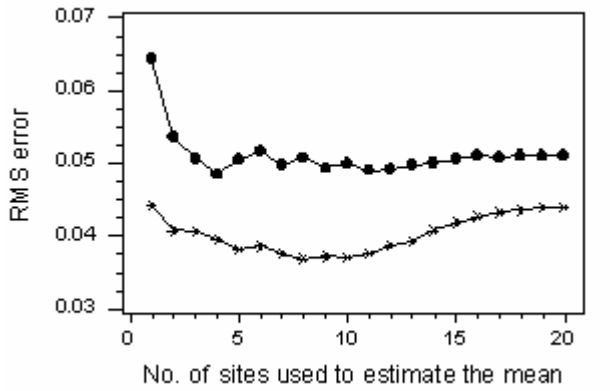

Figure 3.10: RMS error when trying to predict μ at a site, based on the values from the closest N locations (x-axes) in the Veneto dataset. The circles are for the original model of Barbolini and Savi (2001) and the asterisks for the new model, A(i).

The new version of the space formulation gives a lower value for RMS, independently from the number of sites used to estimate the moments of μ, which once again confirms that this method provides more precise estimates. However, it also appears that using 10 predictors (i.e. a threshold distance set at the median distance when $n = 20$) gives the best results (RMS = 0.0376). This pattern is clearer for the new multivariate space, but is also partly evident for the original formulation. Therefore, we can tentatively justify the usefulness of introducing a threshold distance (in particular a threshold at the median distance).

3.3.3 Uncertainty estimates

MB

3.3.3.1 Introduction

As widely known, the degree of precision required in hazard mapping applications is far beyond that presently achievable by dynamic models, as dramatically shown in many parts of the Alps by the avalanche occurrences of the winter 1999 (Barbolini et al., 2000b; Gruber, 2000; Holler, 2000; Rapin, 2000). In fact, substantial uncertainties characterise the definition of the avalanche starting conditions (namely release area and release depth as a function of a given return period) and of the model parameters (namely friction coefficients as a function of the avalanche and path features). It is also the case that all dynamic models in common use turn out to be remarkably sensitive to both these types of input data. A detailed analysis on a group of dynamic models of hydraulic type, performed within the EU 4th Framework project SAME (Barbolini et al., 1998; 2000a) has clearly shown that even relatively small variations of the friction coefficients (within 15%), can produce

remarkable variations of the model output, either in terms of run-out distance (up to the order of 10^2 m) or impact pressure (up to the order of 10^1 kPa at a fixed location). The sensitivity to release conditions was found to be lower, but sufficiently strong to obtain different mapping scenarios as a consequence of realistic variations of the release variables.

The uncertainties inherent to the dynamic model's input-data specification, although well acknowledged, are usually not explicitly incorporated into the analysis and considered in the mapping results. These sources of error are normally addressed through conservative estimates of the parameters or, in some cases, by sensitivity analysis. However, each of these approaches ha**ve** limitations for assessing the statistical implications of uncertainties. In the present Section some preliminary ideas - originally proposed by Barbolini (1999) - are put forward for working in this direction in order to allow more appropriate risk assessment in avalanche-prone areas.

3.3.3.2 Monte Carlo approach: basic concepts

The new idea is to introduce a Monte Carlo approach to avalanche hazard mapping (Barbolini, 1999; Barbolini and Savi, 2001; Barbolini et al., in press). This method combines statistically-based criteria for the evaluation of the input data of the dynamic models and deterministic avalanche modelling techniques (see Figure 3.11).

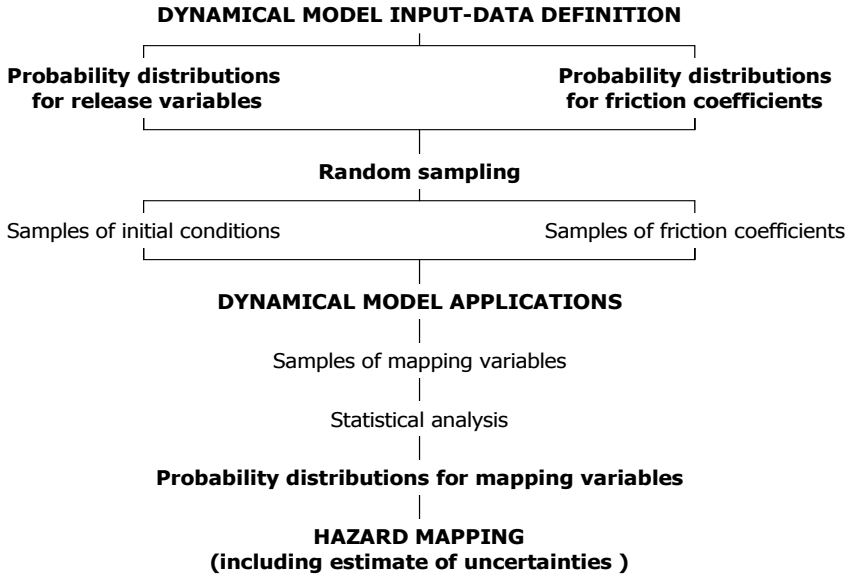

Figure 3.11: Schema of Monte Carlo approach to avalanche hazard mapping

The uncertainties inherent in the use of dynamic models for mapping applications are explicitly accounted for by expressing the release variables and the friction coefficients in terms of "site-specific" probability distributions.

These are then used to randomly generate samples of values for each model input, which are transformed into samples of mapping output by successive applications of the dynamic model. Thus, the mapping variables — essentially run-out distance and impact pressure — are given in a form suitable for statistical analysis, and the effects of uncertainties can be formally considered in the hazard maps (by way of confidence intervals on the mapping variables). The specific methods introduced in order to estimate the "site-specific" probability distributions for the release variables and for the friction coefficients (as well as to eventually correlate them) have been discussed extensively in the previous Sections (see Sections 3.3.2.2.2 and 3.3.2.2.3), whereas an example of implementation of the Monte Carlo methodology to a real world mapping problem will be presented in Section 3.6.3).

3.3.3.3 Monte Carlo simulations

Mme

In 3.3.2.2.2, we studied how to use avalanche events and the sliding block model in order to fit its friction parameter on the output data (the run out distance). It was necessary to have the corresponding input data (avalanche height and starting distances) and to fix the other friction parameter. Generally, this parameter is fixed by the researcher, using for instance the Swiss guidelines, or its own knowledge. It may be fixed also through a regional analysis. In 3.3.2.2.2, we explored the possibility to obtain the friction parameter samples for the whole range of variation of the fixed friction parameter; so, we obtained the samples of $\mu|\xi$ and of $\xi|\mu$. Then, we studied the corresponding statistical distributions. We saw that, in order to keep a good coherence to the distributions, we had to narrow the range of variation for each parameter and for each group of avalanches (see Figure 3.19 and Table 3.5).

We will here use all these results with Monte Carlo method and the sliding block model for determining a large return period run-out distance estimate. As we will obtain as many estimates as we got statistical distributions, we will be able to compare them.

The first step is to obtain a set of statistical distributions for all the variables which will be used later on as random variables. We already have the results for $\mu|\xi$ and $\xi|\mu$. So, it is necessary to fit theoretical distributions for the avalanche heights and for the starting distances. For the first one, we may choose the best fit between many possibilities as Gumbel, renewal model, lognormal, etc. For the starting distances, it seems that the beta distribution is appropriate, as we can see for the Entremere site, Figure 3.12.

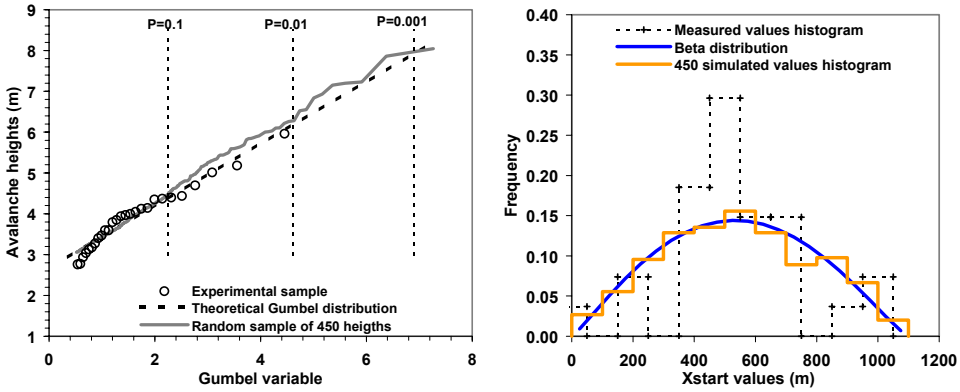

Figure 3.12: Theoretical Gumbel distribution for avalanche heights (left) and Beta distribution for starting distance (right) for the Entremere site.

The second step consists in using the complete set of the statistical distributions to generate random samples the size of which is as large as we wish. For the Entremere site, as we have 27 events for 60 years, we calculated at first 1000 years which correspond to 450 events. We can see the corresponding sample on the preceding figures. But, according to the study of the uncertainty of the 500 years run out distance we made for this site, it seems necessary to adopt a size as large as 10 or 20 times the return period we wish to calculate.

The third step consists in computing the *Xstop* values with the model from the samples of the simulated random variables, as it is explained in Figure 3.13:

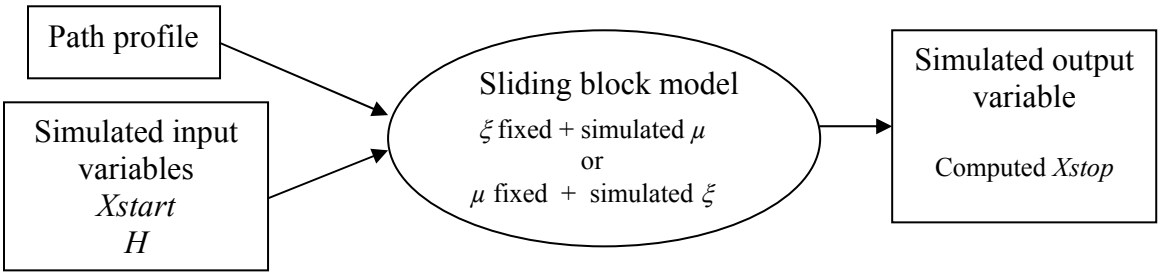

Figure 3.13: Principle sketch of procedure for computation of Xstop value

We do that repetitively and we obtain as many samples of *Xstop* values as we have different sets of samples of the three variables (*Xstart*, *H* and one friction parameter).

In the fourth step, we can use the *Xstop* samples to fit a statistical distribution, then deduce the values of the quantiles we are looking for. Generally, it is not necessary to fit a theoretical distribution on the experimental samples of *Xstop* values as it is not allowed to extrapolate this distribution. So, a simple figure where we draw the experimental points (*Xstop*, T) is enough (T is the return period in years). We then have only to compare these different estimates of this quantile and decide the right value we will adopt.

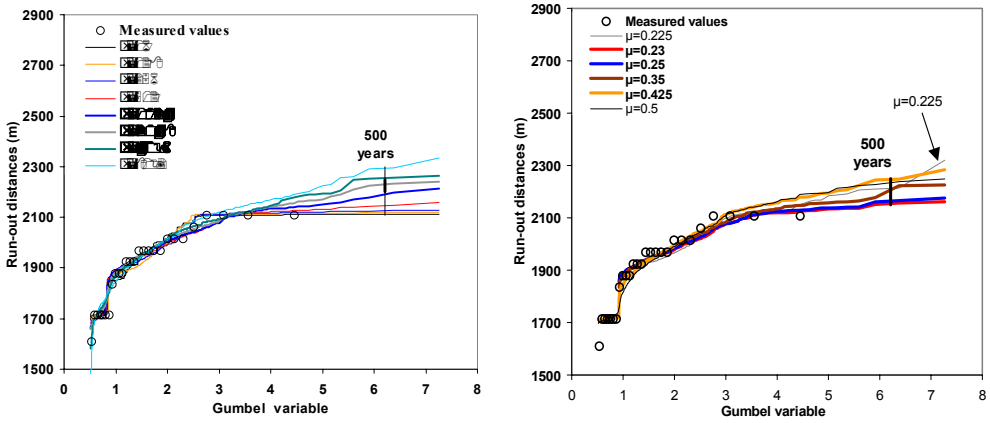

Figure 3.14: The results for Entremere site for a 1000 years simulation period and the two cases $\mu|\xi$ and $\xi|\mu$.

Figure 3.14 show the results for Entremere site for a 1000 years simulation period and the two cases μ|ξ and ξ|μ. We see that the scatter is rather wide if we consider the whole field of variation of the fixed friction parameter. But if we select the results corresponding only to the practical field of variation of the friction parameters we obtain at the end of the Section 3.6.1, we get a more narrow range for the results, as we can see in Table 3.3.

Table 3.3: Range of results based on practical variation of friction parameters.

Practical range for μ (1st group of avalanches) 0.23–0.46		Practical range for ξ (1st group of avalanches) 900–5000 m/s²		Difference between the means
Mean	Standard deviation	Mean	Standard deviation	
2206 m	42 m	2228 m	29 m	22 m

The difference between the two approaches (μ|ξ or ξ|μ) is rather thin and compatible with the uncertainties. It means that when we consider the sliding block model as a conceptual model and not a deterministic one, we don't find any reason to fix one friction parameter rather than the other one, contrarily to the habit of practitioners.

With the same example, we studied a fictitious profile which stays inclined in the final part. It gave analogous results but the mean run out distance is greater: the difference with the flat profile goes from 150 to 190 m. On this profile we studied also the uncertainty of the approach in considering the confidence limits of the 500 years return period run-out distance obtained with the 1000 years simulation samples. The result is depicted in Figure 3.15.

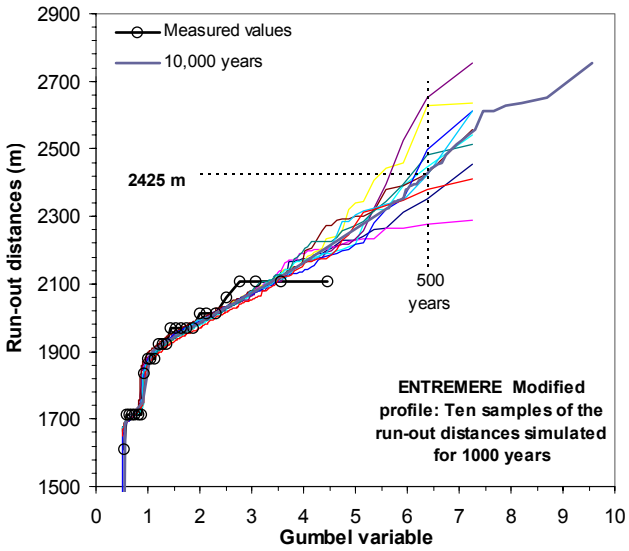

Figure 3.15: 500 years return period run-out distance obtained with the 1000 years simulation samples for a modified Entremere path.

The scatter of the 500 years return period run-out distances is great. It is possible to deduce the histogram of the quantile as it is proposed in the Section 3.6.3.3. We can also mix the run-out distances samples and obtain a larger size for the resulting sample. We can also increase its size up to 20 times the return period we want to compute. Figure 3.16 shows the results for 20000 years samples which give a good estimate of the 500 years return period quantile. The two approaches give regular curves up to 500 years and the 500 years quantiles are different from only 30 m.

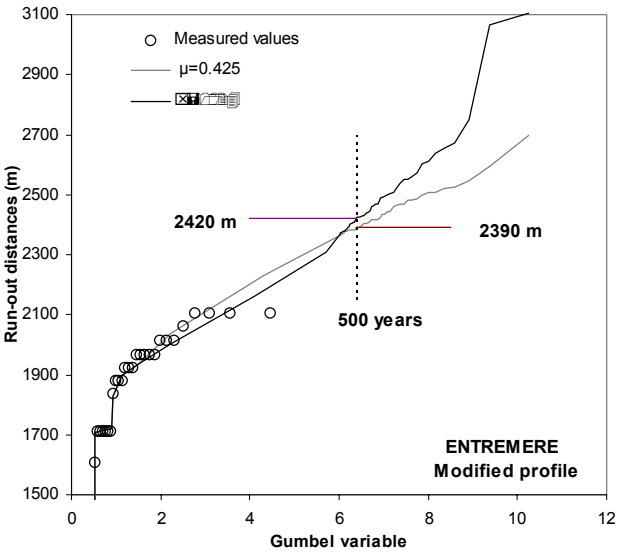

Figure 3.16: 500 years return period run-out distance obtained with the 20000 years simulation samples.

3.4 Thoughts on integrated use of simple and sophisticated avalanche run-out models in mapping applications

CH, CJ, and DI

To meet the practical needs in hazard mapping and the theoretical needs for better understanding of the underlying physics in avalanche dynamics, a substantial effort in computational model development is desirable. The cruder the knowledge of initial and boundary conditions, the more one should favour relatively simple and robust models at the expense of detail in the predictions. Nevertheless, very often great detail is required and thus rather sophisticated models are needed, too.

Determination of realistic initial conditions is a serious problem in practical applications that has not received sufficient attention in the past. Typically, both the initial avalanche mass (fracture area and depth) and the flow behaviour (friction coefficients, snow entrainment and deposition rates, fraction of suspended snow) are non-linearly dependent upon the return period. On the one hand, very simple models do not adequately reflect this non-linearity and may give strongly distorted results; on the other hand, determination of the effect of uncertainties in the initial conditions on the results requires a large number of simulations that are not presently possible with the more demanding advanced models. We suggest that combining simple models allowing rapid scanning of the relevant parameter space with more advanced models for detailed simulations of selected scenarios could help bridge this gap. The simple models will not disappear but acquire new meaning when combined with the more sophisticated ones.

For such combined analyses to yield meaningful results, the simple and advanced models must be properly matched. The following are among the relevant criteria:

- The input and output parameters of the simple model must be among those of the advanced model.
- The physical processes described by the simple model should also be contained in the matching advanced model so that parameter dependencies found with the simple model will also be reflected by the advanced one. E.g., a one-dimensional model with a simple snow entrainment mechanism explores dimensions of the parameter space that are inaccessible to two- or three-dimensional models without snow entrainment.
- Before practical applications are considered, the two models should be compared in situations that can reasonably be described with the simple model. In this way, a set of parameter values for one model can be approximately related to a set of values for the other model (e.g., friction or entrainment coefficients).

3.5 Examples

3.5.1 Estimation of site specific estimate of friction coefficients

The Entremere site is situated in the Chamonix valley (France) on the right side of the Arve river, just downward the town of Chamonix. The path is very regular on its main sloppy part and ends on the flat alluvial Arve valley.

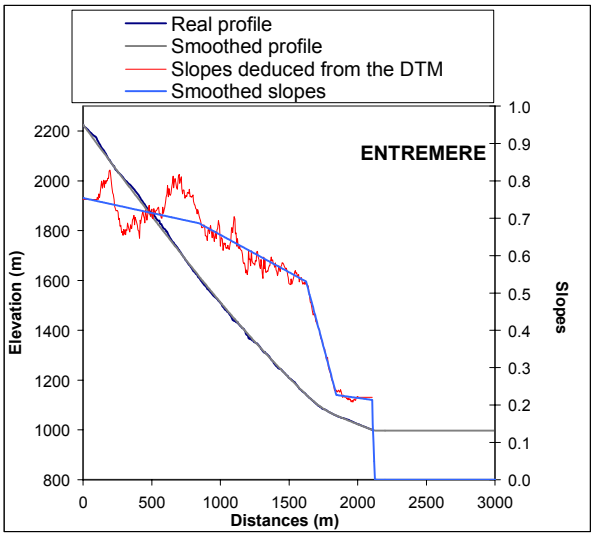

Figure 3.17: Real and smoothed profiles and slopes.

The figure shows the real profile deduced from a DTM with a 5 m grid and the very irregular corresponding slopes. We choose to smooth the profile in equalizing the slopes. We strongly smoothed these slopes in the upper part but this gave a maximum elevation difference of 20 m only, while the elevation difference in the stopping area between the real and the smoothed profile is less than 1 m.

The data on Entremere site are collected since 1907. Among these data, we are mainly concerned by the date of the event, the starting and stopping elevations, and the dimensions of the deposit. Unfortunately, the deposit dimensions were not gathered after 1970. Taking into account the lack of data for some events (see table), we finally had 27 events for 60 years which were completely documented.

As explained in 3.3.2.2.2 b), one problem is to deduce the avalanche heights from the available data. Here we transformed first the three dimensions of the deposit into a volume of the deposit. We obtained the following data (see Table 3.4):

Table 3.4: Avalanche volumes

date	Zstart (m)	Zstop (m)	volume (m^3)
19/03/05	2200	1050	3000
14/01/09	2100	1050	11520
20/01/10	1850	1010	478800
18/11/10	1800	1100	67200
08/01/12	1800	1030	32400
23/01/13	1850	1060	24000
26-27/03/14	2100	1020	72960
19/02/16	1950	1020	252000
28/03/19	1900	1040	82500
24-25/12/19	1850	1020	288000
09/01/22	1900	1040	136800
02/03/23	1850	1040	140000
23/12/23	1900	1030	150000
27/12/25	1850	1030	86400
14/02/28	1750	1100	192500
31/01/29	1950	1100	15750
/04/35	1600	1100	18000
12/01/38	1850	1100	37500
30/01/38	1750	1100	
09/03/39	1700	1050	7500
02/01/43	1700	1050	
08/12/44	1700	1030	144000
11-12/01/1947	1800	1100	105000
09-10/02/50	1800	1030	96000
20/01/51	1850	1000	90000
28/02/52	1850	1000	2700
24/02/57	1500	1150	48000
14/03/58	1500	1000	48000
29/03/62	1500	1100	
03/02/70	1700	1000	108000

We can see in the table that four events end in the flat part of the valley; for these events we only know a minimum value of the run-out distance.

Then, we asked the practitioners who knew the site very well to propose minimum and maximum values of the height of the avalanche. We did the hypothesis of relationships between on one side width and length of the avalanches and on the other side their height. We obtained finally an empirical relationship between the deposit volume and the avalanche height, that we used to generate the heights of all the avalanche events of the table.

The following step is to fit a friction parameter with the sliding block model, while the other one is fixed. We tried to explore the whole range of variation for the two friction parameters, $[1 - \infty]$ for ξ and $[0 - 1]$ for μ. The values of ξ that we used in the research were 1, 2, 4, 8, etc., and for μ, we adopted 0.1, 0.125, 0.15, etc. For some values of μ, it was not possible to fit the measured values of the run-out distances. These results are presented in Figure 3.18 first for $\xi|\mu$, then for $\mu|\xi$:

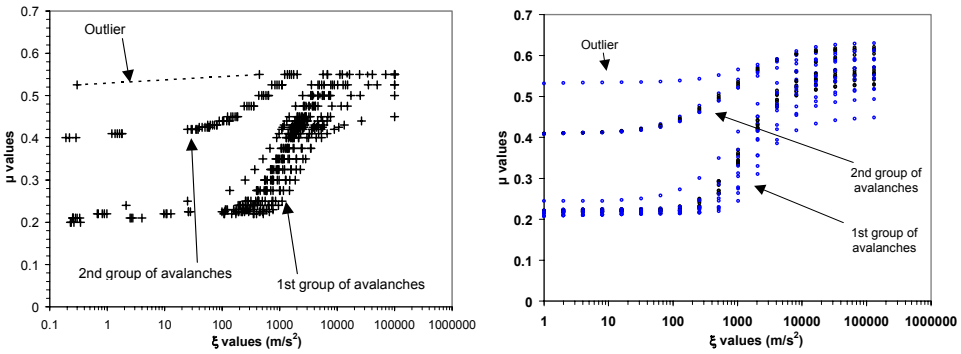

Figure 3.18: Friction parameter values for ξ|μ (left) and for μ|ξ (right).

The two panels of Figure 3.18 are very similar and show:

- that there is an outlier that we didn't consider later on
- that it exists two groups of avalanches, the first one having low values of μ, giving so higher run-out distances than the 2nd group
- that, for each avalanche, there is an asymptotic behaviour of the value of μ when ξ is either low or high. So, there is a practical field of variation for ξ that, by visual fitting according to the figure, we may propose between 100-500 and 6000-8000. A more precise field will be determined later on.

It is now possible to fit statistical distributions on the samples of μ|ξ and ξ|μ. In the text (Section 3.3.2.2.2 b)), we showed that a sum of two beta distribution fits well the μ|ξ samples and that a sum of two gamma distributions fits well the ξ|μ samples. As the aim is finally to practice Monte-Carlo simulations from these distributions, it is easier to use a sum of two normal laws for the μ|ξ samples and a sum of two lognormal distributions for the ξ|μ samples. Figure 3.19 shows the results: as we have many curves on each figure, we use the probability for the ordinate and not the frequency.

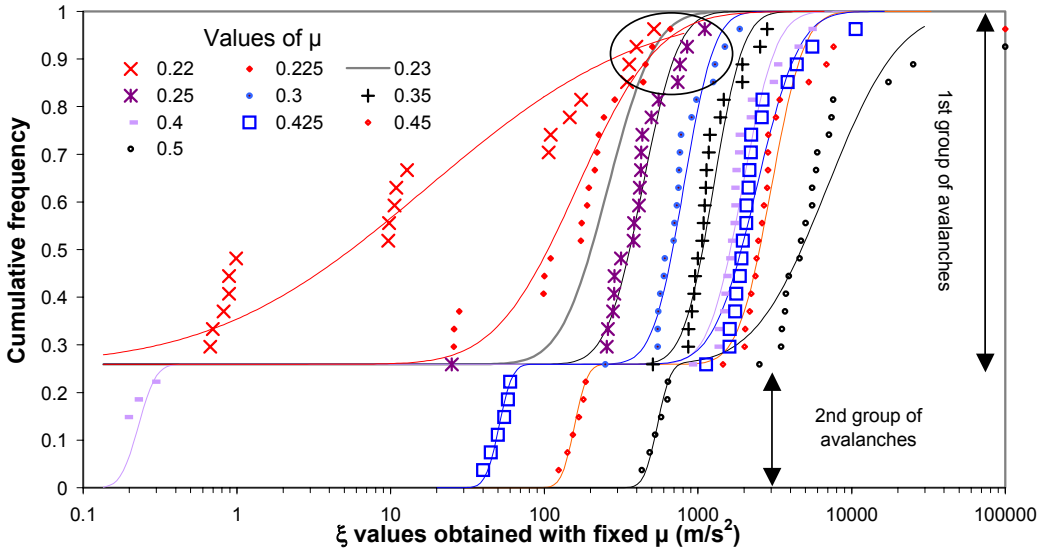

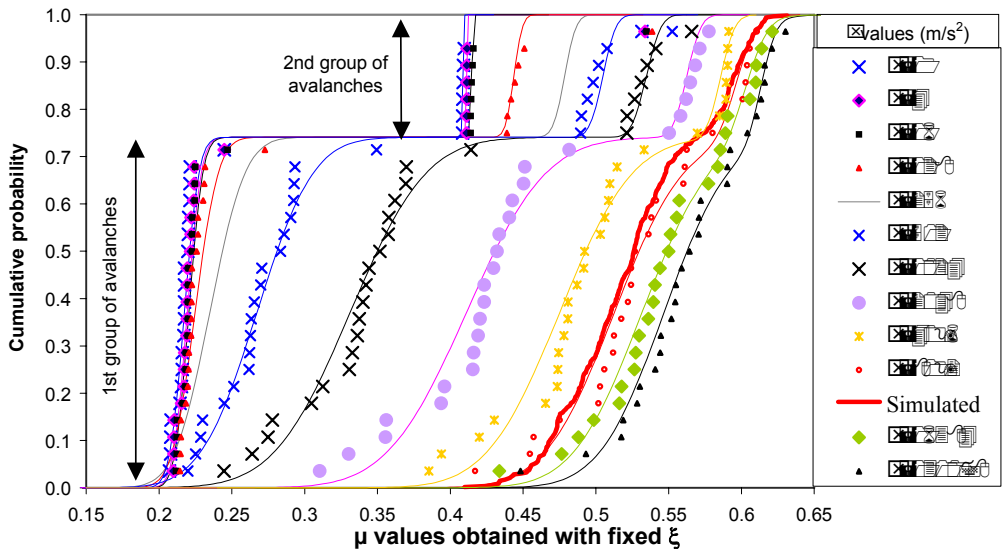

Figure 3.19: Cumulative probability for $\xi|\mu$ (upper) and for $\mu|\xi$ (lower).

The two figures show that the statistical distributions fit quite well the experimental samples. We see that, if they are parallel in the middle of the field, they are not for the low and the high values of the fixed parameter. In these parts of the figures, the representative curves are either nearer or more spaced than in the middle part. In the first figure, we see also that the curves cut one another for the low values of μ and the large values of the probability. In order to select the middle field of variation of the fixed parameter, we choose a criterion using the variation of the means ($\bar{\xi}$ and $\bar{\mu}$) and of the standard deviations (σ_ξ and σ_μ) of the experimental samples: $F(\mu) = \left|\frac{d\bar{\xi}}{d\mu} + \frac{d\sigma_\xi}{d\mu}\right| \le k$ for the case μ fixed, $G(\xi) = \frac{d\bar{\mu}}{d\ln\xi} - 6\left|\frac{d\sigma_\mu}{d\ln\xi}\right| \le k'$ for the case ξ fixed. Suitable values of k and k' allow us to obtain the practical fields of variation for ξ and μ (Table 3.5).

Table 3.5: Practical fields of variation for ξ and μ.

	Practical range for μ in order to have ξ as a random variable	Practical field for ξ in order to have μ as a random variable
1st group of avalanches	0.23–0.46	900–5000 m/s²
2nd group of avalanches	0.43–0.55	165–2800 m/s²

3.5.2 Estimation of site-specific friction coefficients at regional scale

3.5.2.1 The data set

The VARA1D model (a one-dimensional hydraulic-continuum avalanche dynamics model using a classical two-parameter Voellmy-like resistance law, developed in recent years at the University of Pavia, Natale et al., 1994; Barbolini et al., 2000a) has been calibrated against adequately documented historical events (with known release conditions and run-out positions) from the Veneto region, a mountain range located in the Eastern Italian Alps. The avalanche events were representative of occurrences with different return periods and were tentatively classified in two general frequency classes: (a) relatively frequent events; (b) extremely rare events. A synthesis of the calibration of VARA1D model over this dataset is given in Table 3.6; more details can be found in Barbolini (1999).

Both parametric and non-parametric tests demonstrate, at a significance level of 5%, that for the friction coefficient μ the calibration samples for relatively frequent events and extremely rare events belong to different populations; this confirms the need of using for this variable different probability distributions depending from the event frequency (see Section 3.3.2.2.3); in particular, according to the work of Salm et al. (1990), the rare events have a lower mean value of μ (0.24), compared to that for the more frequent events (0.32), see Table 3.6. Conversely, a statistical analysis of the available calibration values shows that a separation of the general calibration sample of Table 3.6 made on the basis of the avalanche **frequency does not produce a significant** difference in the mean value of the coefficient ξ. However, significant differences (at the 5% level) arise when the degree of channelling of the path is used as the discriminating variable, as proved by a one-way ANOVA test (with ξ=3500 sm^{-2} for open slopes, ξ=2800 sm^{-2} for partly channelled slopes and ξ=2300 sm^{-2} for fully channelled slopes).

3.5.2.2 Estimate of friction coefficient μ for the Voltago site

The Voltago avalanche path is a SE-facing channelled-slope site located within the Veneto range, characterised by a quite intensive avalanche activity and with a village at its foot. It has a length of approximately 3.5km, and a total vertical drop of about 1200m. The average inclination of the release area is about 32°, and that of the whole path approximately 21°. The main topographical parameters of this path are listed in Table 3.6; the longitudinal path profile is presented in Figure 3.20.

In Figure 3.21 are presented the result of the "proximity" analysis (i.e. equation 3.3) for the site Voltago over the relatively frequent avalanche event of the data sample of Table 3.6. The distances between sites are measured with equation

(3.3), applying a weight to the different topographical variables according to method A(i) of Section 3.3.2.2.3. The result of Figure 3.21 shows the ability of the proximity algorithm to capture those topographical similarity between path that results in close calibration value for the friction coefficient μ, with calibration μ values progressively diverging to that of the Voltago site (0.24) going from the nearest neighbour sites (number 91, 87, 73, 15, 70, 83) to those further away (number 69, 108, 61, 36, 106, 105).

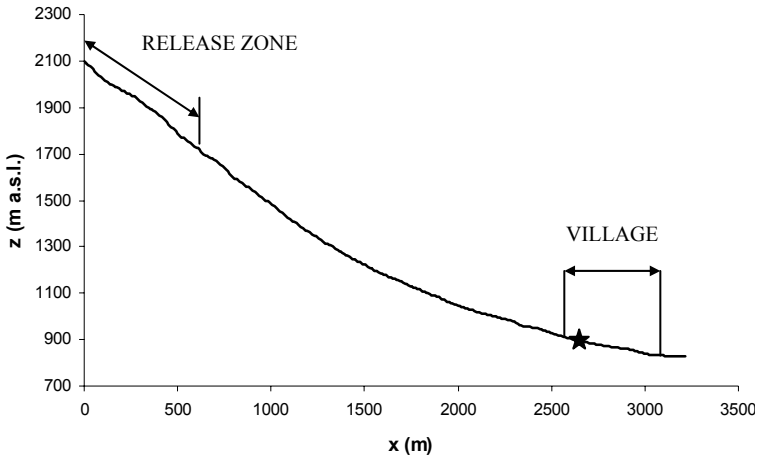

Figure 3.20: Voltago site: longitudinal path profile with an indication of the release zone, of the urbanised area and of the maximum known avalanche run-out (indicated with the star)

Figure 3.22 is an alternate way of looking at the effect of the proximity analysis. In this figure:

- the solid diamond represent the "regional" expected value and standard deviation of μ (calculated over the data of Table 3.6), E(μ) and σ(μ), respectively;
- the solid line indicate the known calibration value of μ at Voltago (0.24);
- "+" indicates E(μ) and σ(μ) at Voltago obtained with method A(i) with no at-site calibration value assumed available;
- "□" is similar to "+" but introducing knowledge of the site-specific calibration value (0.24);
- "☝" is similar to "+" but with a threshold distance set to the median distance;
- "○" is similar to "☝" but with the on-site calibration value included in analysis.

The proximity analysis improves the accuracy and precision of the parameter estimates relative to a simple estimate based on regional values, and the efficiency of the proximity algorithm increases with the use of a threshold distance criterion. The introduction of site-specific knowledge seems to reduce the bias of the estimate.

Figure 3.21. Proximity analysis for the site Voltago over the relatively frequent avalanche of the Veneto data sample. The distance between sites are rescaled to a 0-1 range (d); μ are the calibration values listed in Table 3.6 for relatively frequent avalanches.*

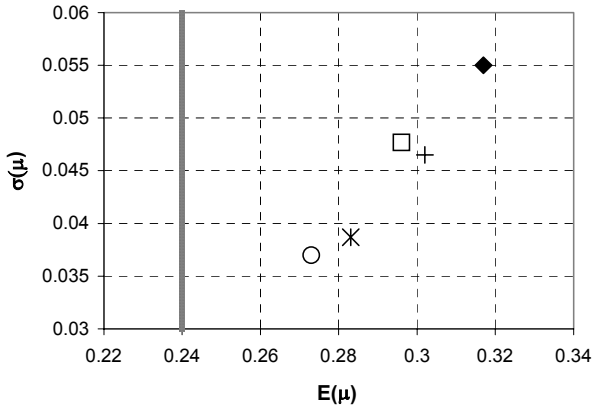

Figure 3.22. E(μ) and σ(μ) at the site Voltago for relatively frequent events, based on different methods of moments estimation (see text for details).

Site name	Calibration values		Topographical parameters								
	μ (–)	ξ (s m^{-2})	β (°)	δ (°)	ψ (°)	y'' (m^{-1})	R^2 (–)	H (m)	Zr (m a.s.l.)	Zd (m a.s.l.)	E (°)
Relatively frequent events											
Voltago	0.24	2300	24.1	6.2	21.5	0.0002	0.999	1200	2000	800	135
2	0.32	4500	23	18	21.9	0.0001	0.9995	400	1900	1500	180
8	0.39	4000	33.5	24.5	31.3	0.0004	0.9994	500	2000	1500	135
14	0.28	3000	23.4	11.8	18.7	0.0006	0.995	200	1400	1200	135
15	0.32	10000	30.7	15.9	24.2	0.0004	0.9978	500	1700	1200	135
38	0.29	6000	26.4	16	25.4	0.0002	0.9997	600	2700	2100	45
36	0.41	4500	31	18.4	28.1	0.0006	0.9992	400	2800	2400	45
61	0.40	5000	42.1	25.9	38	0.0001	0.9945	1200	2000	800	0
65	0.32	2500	38	13.2	36.2	0.00012	0.9968	1600	2350	750	90
69	0.40	2000	46.3	20.6	43.1	0.0006	0.989	1100	1900	800	90
70	0.30	2000	37.3	11.4	32.2	0.0004	0.997	800	1600	800	90
73	0.33	2500	33.7	14.9	30.2	0.0004	0.9994	850	2000	1150	90
80	0.32	2500	35.1	15.2	33.2	0.0004	0.9956	1000	2400	1400	45
83	0.21	2500	34.2	7.9	30.9	0.0004	0.9958	1050	2400	1350	45
91	0.31	3500	27.7	13.5	25.2	0.00014	0.9974	650	2000	1350	180
105	0.30	2500	39.2	9.5	36.5	0.00012	0.9973	300	2000	1700	180
106	0.30	2500	37.3	9.8	34.8	0.001	0.9967	300	2000	1700	180
107	0.32	2500	37.2	15.9	35	0.0004	0.9982	400	2150	1750	180
108	0.37	2500	39.7	18.4	38	0.0012	0.9973	350	2100	1750	180
120	0.35	3000	30.5	26.2	29.3	0.00018	0.9964	950	2200	1250	135
21	0.22	3500	30.9	11.8	26.6	0.0004	0.9927	1100	2000	900	0
87	0.28	2000	30.1	13.2	27.3	0.00012	0.9966	1100	2000	900	0
Extremely rare events											
Voltago	0.20	2300	24.1	6.2	21.5	0.0002	0.999	1200	2000	800	135
7	0.22	3000	29.5	9.5	28.2	0.0006	0.9978	500	2000	1500	135
40	0.25	1500	30.1	9.5	26.2	0.0006	0.9961	300	2050	1750	90
63	0.28	2000	38.6	17.4	37	0.0002	0.9958	1200	1900	700	0
64	0.27	1500	34	10	31	0.0006	0.9981	550	1250	700	0
76	0.15	3000	32.5	7.5	28.6	0.0004	0.9969	1050	2300	1250	45
82	0.20	2500	32.6	6.7	29	0.0004	0.9958	1050	2400	1350	45
95	0.26	3500	28.5	17.9	26.7	0.00002	0.9974	450	2100	1650	45
89	0.29	3000	31.9	15.5	28.1	0.0012	0.9991	350	1900	1550	135

Table 3.6. Calibration of the model VARA1D within the Veneto mountain range: synthesis of results, including the main topographical parameters of the involved sites (for the meaning of the parameters see Table 3.1). Apart from the case of the site Voltago, the remaining sites are indicated using the cadastre number)

3.5.3 Application of Monte Carlo procedure

3.5.3.1 The Solco case stydy

The *Solco* avalanche site is located in the Rhetian Alps, in the inner part of Valmalenco, a tributary valley of Valtellina situated in the central Alps, within the Lombardia region (Figure 3.23). It is a SE-facing open-slope site, affecting a road and some isolated houses in the valley bottom (Figure 3.24) and characterised by a quite intensive avalanche activity (on average one or two avalanche events every year). The path length is approximately 1600m, with a total vertical drop of about 800m. The average inclination of the release area is about 40-45°, that of the whole path approximately 30°. The release zone is characterised by two rather distinct basins, the eastern one being at present largely ineffective due to the construction of snow bridges (Figure 3.24).

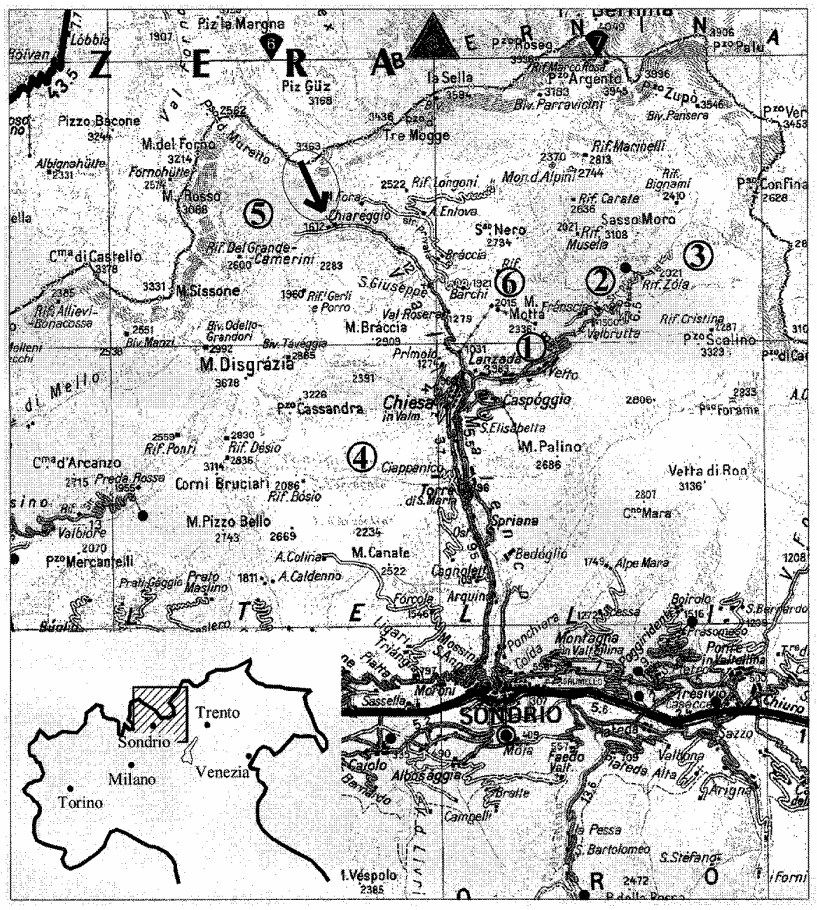

Figure 3.23. Overview of the Valmalenco Valley. The location of the Solco avalanche site is indicated with an arrow; the numbers indicate the location of the different meteorological stations used for analysing the snowfall regime at this site.

3.5.3.2 Application of the Monte Carlo procedure to the Solco avalanche path

The methods previously outlined (see Section 3.3.2.2.3) were used to derive site-specific moments of μ for the Solco case study; the mean value of μ was found to be 0.260 and 0.215 for relatively frequent and extremely rare event respectively, while the standard deviation of μ was found to be 0.025 and 0.040 for the two event types. A log-normal probability distributions was chosen to describe the variability of μ; its parameters were estimated by the method of ordinary moments (details can be found in Barbolini, 1999, and Barbolini and Savi, 2001). The method adopted to obtain the probability distribution of the release variables (release depth H_r, and release lenght L_r) for this case study are explained in detail in Barbolini et al. (2002). In accordance with the Monte Carlo approach (see Section 3.3.3.2) 1000 values for each release variable (namely H_r and L_r) and 1000 values for the friction coefficient μ were randomly (and independently) generated from the related probability distributions, for both relatively-frequent events (say T=30 years) and extremely-rare events (say T=300 years); 1000 dynamical simulations were subsequently performed with the VARA1D dynamic model (Natale et al., 1994); Barbolini et al., 2000a) for each of the two cases. The friction coefficient ξ was set to a value 3500 sm^{-2}, kept constant for all the simulations. The reference profile used for calculations is indicated in Figure 3.24 by the dash-dot line. In addition, two cycles of simulations considering the individual effects of uncertainties on the release condition and on the friction coefficient μ were carried out. Alternately, the friction parameter μ and the release variables (H_r and L_r) were held constant at their mean value while the other parameter was free to vary.

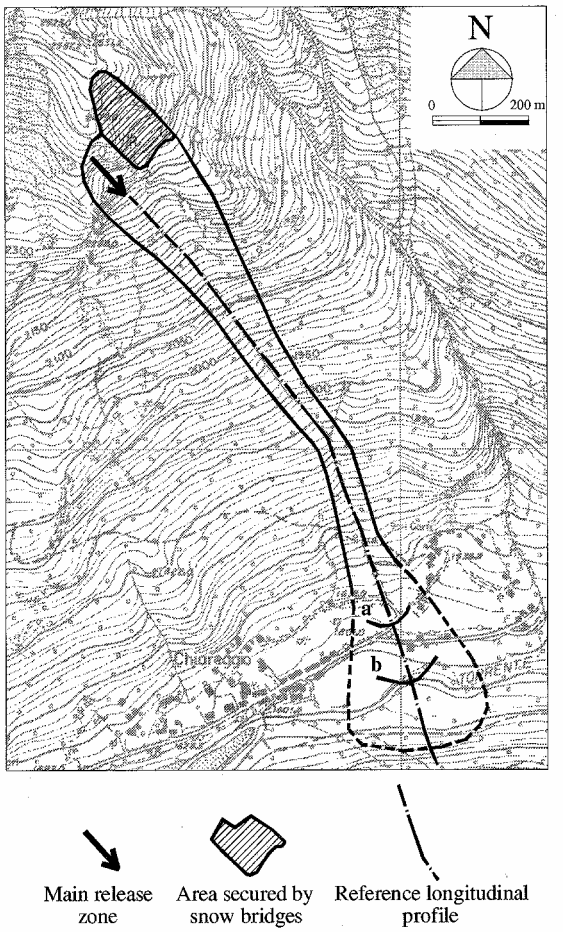

Figure 3.24: Overview of the Solco avalanche site. The run-out positions of more frequent events (a) and of the biggest known event for the site (b) are marked; the former refers to a well documented avalanche event occurred in January 1994, that was used for "direct" model calibration on this site.

3.5.3.3 Results

Figures 3.25a-b display the results of simulations where the uncertainties underlying the definition of both the friction coefficient μ and the release conditions are simultaneously accounted for. The obtained run-out distances vary very strongly, both for the case of relatively frequent events (up to 65m) and extremely rare events (up to 180m). The variability of impact pressures, even if smaller, is still significant: the location of the 30 kPa impact pressure limit varies up to 40m for relatively frequent events, and up to 120m for extremely rare events. The degree of uncertainty of the results is strongly related to the considered return period: the confidence intervals for the case T=300 years, either for run-out distance or impact pressure, are considerably wider (about three times) than those for the case T=30 years. However, it is important to note that for this latter case the difference between the average run-out distance and the downslope limits for the 95% confidence intervals

would lead to the inclusion of both the main road and a group of houses in the zone endangered by the more frequent avalanches (Figure 3.25a), with relevant consequences in terms of risk assessment for the considered area. It should also be highlighted that the mean values obtained for the run-out distances, both for T=30 years and T=300 years (Figure 3.25a), are very close to the known extensions of relatively frequent and extreme historical events, respectively (Figure 3.24). This appears to be an important confirmation of the effectiveness of the method introduced to define suitable friction coefficients for avalanche sites where the calibration data are limited or even completely lacking.

It is also interesting to observe the effects of the run-out zone topography on the distributions of the run-out distances. The lower part of the avalanche site Solco is characterised by a rather gentle alluvial fan located between the altitudes 1620 and 1605 masl, which steepens again between 1605 and 1590 masl, and terminates on the valley bottom, represented by the almost flat river bed. Many simulated long-running extreme events, mostly associated to the higher T, are able to reach the valley bottom, and therefore undergo the slope changes; this results in a "bimodal" distribution for the run-out distances (Figure 3.26a). This is not the case for the more frequent event, that for the most terminate on the alluvial fan, giving rise to a distribution of run-out distances that better conforms to a Gaussian-like behaviour (Figure 3.26b).

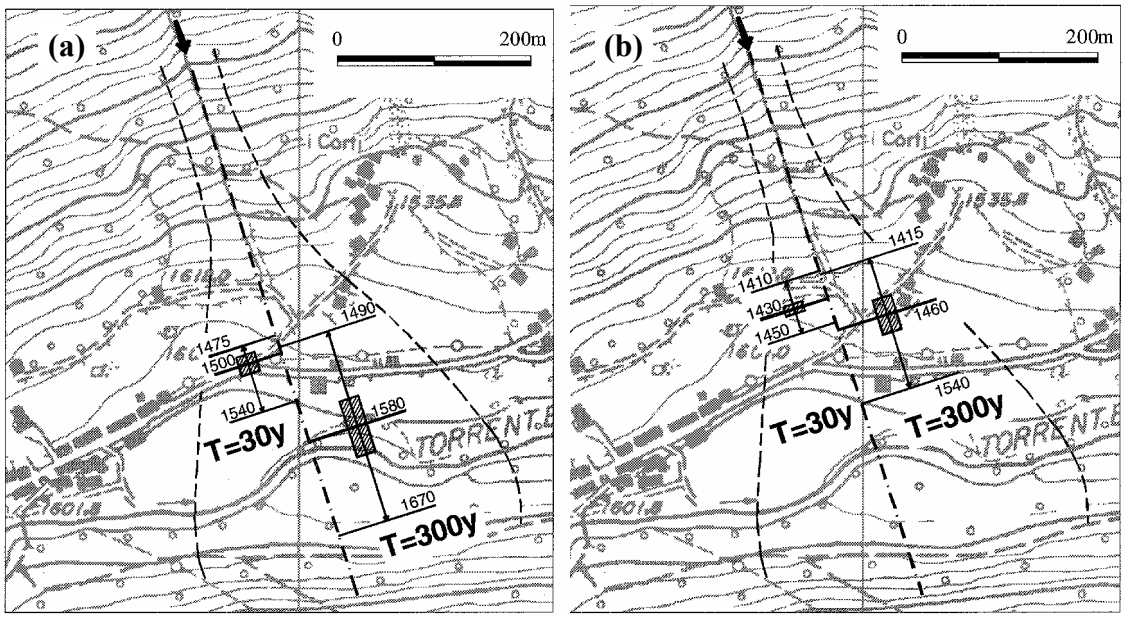

Figure 3.25a-b. Overview of the run-out zone of the Solco site. For the cases T=30 years and T=300 years average values and 95% confidence intervals for the run-out distances (a) and for the final locations with 30kPa impact pressure (b) are indicated along the reference profile (and expressed in meters measured along the path from the upper release point). The hatched rectangles have a length equal to one standard deviation. The dashed outline indicates the possible extension of the avalanche deposit, and has been determined from field surveys.

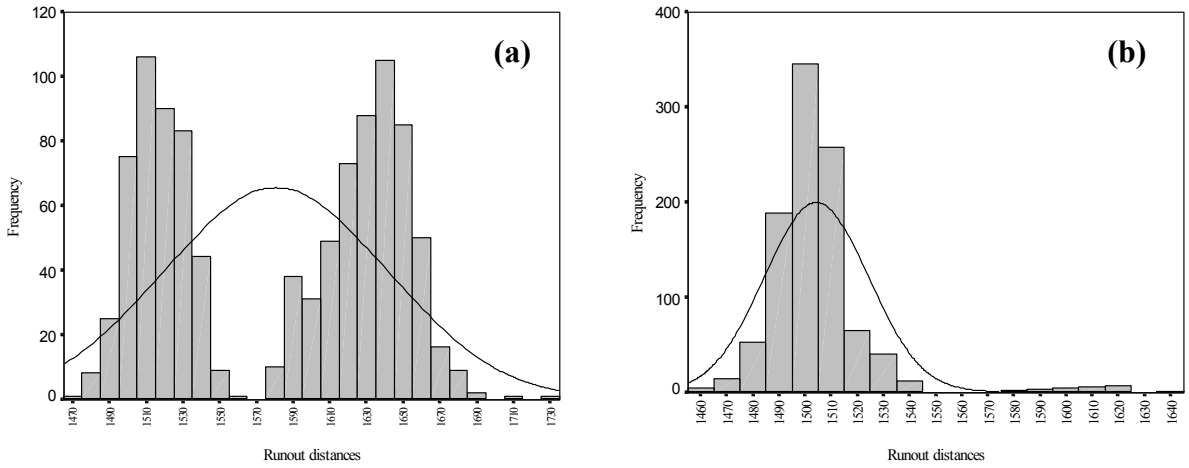

Figure 3.26a-b. Run-out distance histograms for the case T=300 (a) and T=30 (b).

With respect to run-out distance calculation, Figures 3.27a-b provide a comparison between the individual effects of the uncertainties in the release conditions and in the friction coefficient μ.

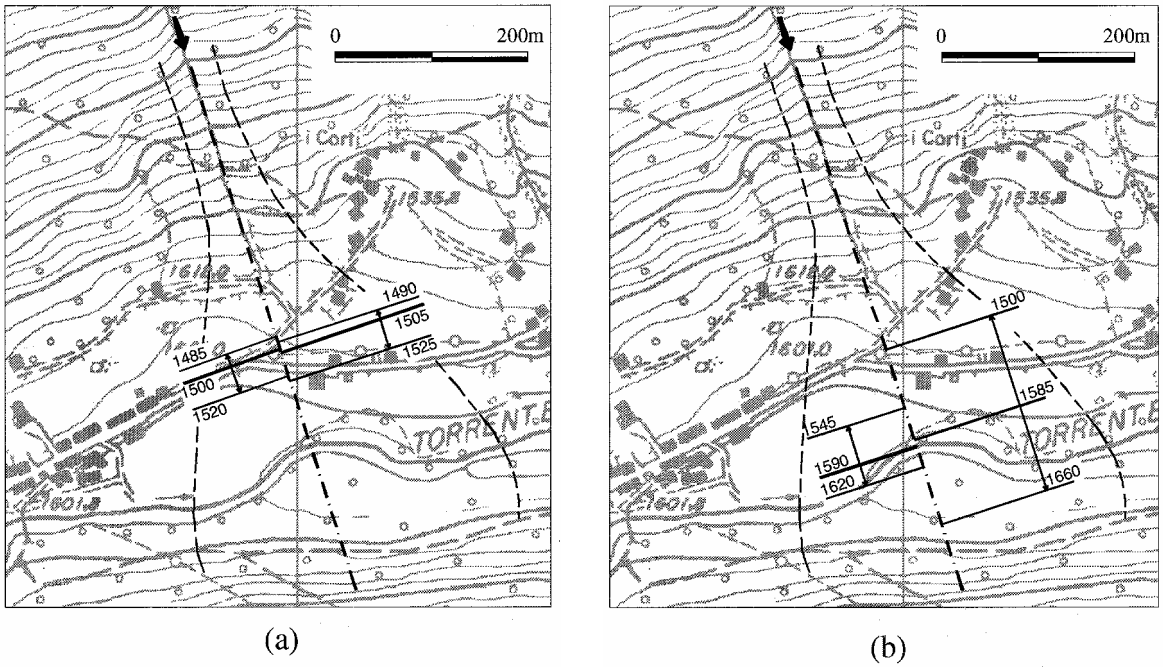

Figure 3.27a-b. Individual effects of the uncertainties of release conditions (left hand side) and friction parameter μ (right hand side) on run-out distance calculations. Average values and 95% confidence intervals are displayed along the reference profile. (a) T=30 years; (b) T=300 years.

For the case of relatively frequent events (Figure 3.27a) the uncertainties in the friction coefficient μ and those in the release conditions have comparable

effects on run-out distance calculations. The respective 95% confidence intervals are very close, both in terms of location and width (about 35m in both cases). The results for the case where both types of uncertainty are simultaneously accounted for (left hand side of Figure 3.25a) seems to combine the two separate effects, with the width of the 95% confidence intervals for run-out distance (65m) about twice that of the two previous cases. Conversely, for the case of extremely-rare events (Figure 3.27b) the uncertainties in the friction coefficient μ produce estimation errors of the run-out distance that are considerably higher than those generated by the uncertainties in the initial conditions. The extension of the 95% confidence interval for the first case (160m) is about twice that for the latter (75m), and when combined (right hand side of Figure 3.25a) only a small increase of the 95% confidence interval extension occurs with respect to that for the case of the friction coefficient μ only (right hand side of Figure 3.27b). This result could have important consequences in practical terms, if confirmed by further analysis made on other avalanche sites and using an enhanced module for the definition of the release variables (able to also account for uncertainties in the estimate of snowdrift overloads, for effects of release area width variation, etc.). Provided the uncertainties in the release conditions for extreme avalanche events have negligible effects on run-out distances relative to those for friction parameters, it would be possible to calibrate the model on the known extension of the deposits even for the cases where only a rough estimate of the release conditions is available. It must be highlighted that this is a common situation for records of historical avalanches.

3.5.3.4 Concluding remarks

The first practical implementation of the proposed method, without any claim for findings of general validity, supports its usefulness for reducing the overall degree of subjectivity in avalanche hazard assessments. Within the framework of a Monte Carlo approach there is no need to perform an arbitrary “a-priori” definition of design conditions that can be thought to produce “safe-enough” results. In fact, once the probability distributions for the various model outputs have been obtained, one can directly derive hazard maps with any desired level of reliability, simply by adopting the value with the appropriate non-exceedance probability P for each mapping variable (Figure 3.28a-b).

One important advantage of the proposed procedure is connected to its modular nature; the various simplifications currently introduced in each module do not in principle affect the validity of the overall approach, and might be removed once specific investigations and data collection have been carried out.

From a practical point of view, an immediate follow-up to the present work could reconsider the existing hazard maps by way of the proposed procedure, evaluating to what level of non-exξceedance probability the current hazard

limits actually conform. This analysis would present a valuable opportunity for standardising the existing hazard cartography.

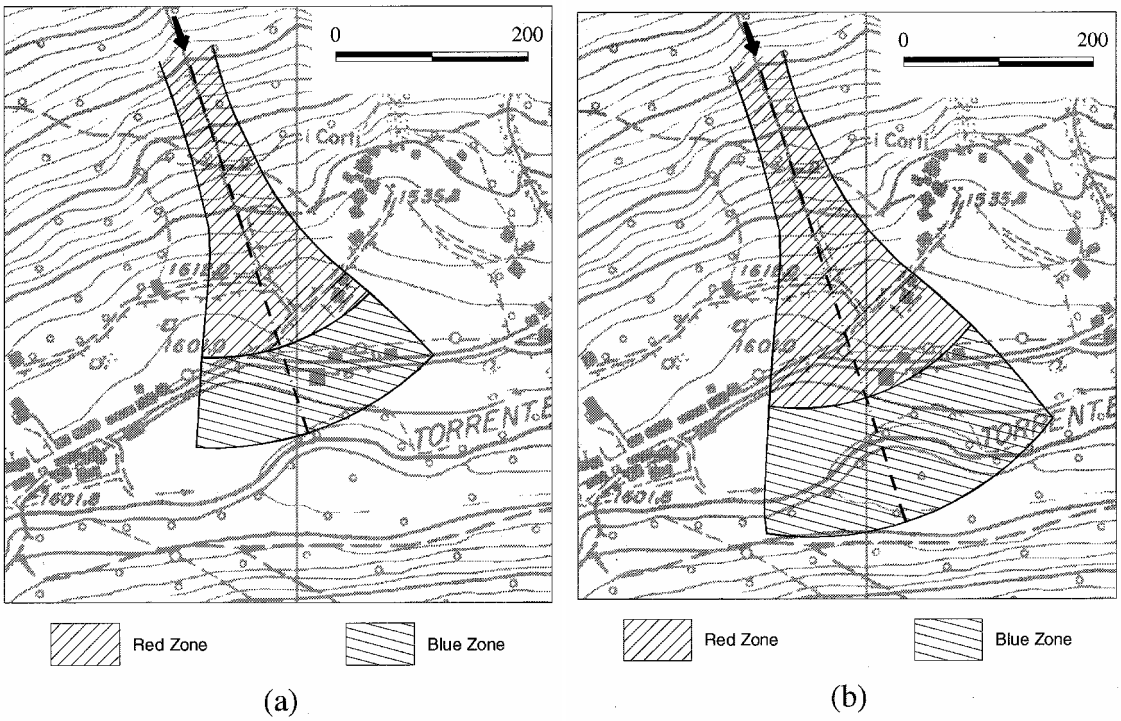

Figure 3.28a-b. "Red/Blue" Swiss type hazard maps for given non-exceedance probabilities. (a) P=0.5; (b) P=0.975. The lower outlines of the hazard zones have been defined by circles drawn from the apex of the alluvial fan with radius given by the run-out position (and/or by the 30kPa impact pressure location) calculated along the main flow line.

4 COMBINED METHODS

4.1 Introduction

MB

In the previous sections have been presented either statistical (Chapt. 2) or physical (Chapt. 3) modelling approach to the problem of avalanche run-out calculation and hazard mapping. Both approaches have their own advantages and drawbacks. The main advantage of statistical methods is their simplicity and relative objectivity in practical use; furthermore they are grounded on real avalanche data. However, a relevant limitation of these models is that they give no information concerning avalanche velocities, impact pressures, flow and deposition heights – i.e. on the potential damages of the design avalanches; the estimate of such physical parameters related to the avalanche intensity is required in a way or another by all the current alpine legislation concerning avalanche hazard mapping. Nevertheless, the approaches based on the use of avalanche dynamics model, despite the greater amount of information they can

provide, are strongly conditioned in practice by the relevant degree of uncertainty usually affecting the model input-parameter definition: (a) estimating the avalanche release volume/mass for a given return period is subject to error, particularly for sites with short snowfall records and complex release zone topographies; (b) if historical avalanche run-out information is sparse, as it usually is, model calibration will be problematic and embody error.

In the present section some new ideas are put forward in order to overcome the above mentioned problems. To this aim a new method for avalanche hazard mapping that uses a combination of statistical and deterministic modelling tools is proposed: the two approaches are combined in a way to reduce their respective drawbacks and use at best their respective advantages. The methodology basically uses an avalanche dynamics model embedded within a statistical framework. A statistical model is used to obtain avalanche encounter probability as a function of avalanche size and location along the path, as well as to obtain the frequency distribution of avalanche sizes, ultimately the unconditional encounter probability as a function of location. An avalanche dynamics model perhaps Bartelt et al. 1999 is better as Journal of Glaciology is a more prestigious journal. The full reference is Bartelt, P., Salm, B. and Gruber, U. 1999. 'Calculating dense-snow avalanche run-out using a Voellmy-fluid model with active/passive longitudinal straining,' Journal of Glaciology, 45, 150, 242-254.which is tuned to the run-out distances provided by the statistical model, and is used to derive impact pressure estimates; the impact pressure are then weighted using the estimated avalanche frequency at a location as appropriate weights. The outlined procedure could provide a useful way for avalanche experts to produce hazard maps for the typical case of avalanche sites where historical records are either poorly documented or even completely lacking, as well as to derive confidence limits on the proposed zoning.

Whitin the same "perspective" also an approach to hazard mapping based on the integrated use of simple and sophisticated avalanche run-out models could be considered, as discussed in Section 3.4.

4.2 Combination of statistical and physical methods for avalanche hazard mapping

MB

4.2.1 Introduction

According to the usual (and sometimes legally required) avalanche hazard mapping procedure for settlements in the mountainous regions of Europe (BFF/SLF, 1984; Hopf, 1998; Pasqualotto, 1998) areas of land are allocated to zones with a different degree of danger based upon return period and impact pressure information; within this general mapping scheme differences arise from country to country only with respect to the return periods and impact

pressures chosen as design values. The most important boundary in these systems is usually that between the *high danger* and *moderate danger* zones, due to its implication in terms of land use restrictions (new buildings are generally not allowed in the high danger zones, whereas they are allowed, even if with proper restrictions, in the moderate danger zones). This boundary is placed at the position where the expected avalanche return period T is T_1 years unless avalanches with return periods between T_1 and T_2 years (with $T_1 < T_2$) exert impact pressures I of greater than $\bar{I}$ kPa at this position. In which case, the boundary between the high and moderate hazard zones is moved downslope until the expected value for the impact pressure for avalanches where $T_1 \leq T \leq T_2$ years is less than $\bar{I}$ kPa.

In practice, this evaluation is usually performed by estimating the $T = T_1$ and $T = T_2$ year snow volume in the starting zone (from meteorological data analysis and release zone morphology), and then using this volume as input to an appropriately calibrated avalanche dynamics model to determine the run-out distances $x(T=T_1\ yrs)$ and $x(T=T_2\ yrs)$ for these two events. Because the dynamics model gives I as a function of position, $x(T= T_1\ yrs)$ may be compared to $x(I = \bar{I}$ kPa) for the $T = T_2$ years event, and whichever is further downslope locates the boundary between the *high danger* and *moderate danger* zones (in the following indicated as $x_{H/M}$). The downslope boundary of the *moderate danger* zone, x_M, is simply represented by the run-out distance of the T_2 years event, $x(T= T_2\ yrs)$. The reference value for T_1, T_2 and $\bar{I}$ adopted by different European mapping guidelines are summarised in table 4.1

Table 4.1: Reference values of avalanche return periods and impact pressure according to the hazard mapping criteria of different European countries.

Country	T1 (years)	T2 (years)	$\bar{I}$ (kPa)
Austria	10	150	10
Italy	30	100	15
Swiss	30	300	30

There are a number of uncertainties that are inherent in this type of analysis, but which are not explicitly incorporated into current avalanche hazard maps:

(1) estimating the avalanche release volume for a given return period is subject to error, particularly for sites with a short snowfall record;
(2) if historical avalanche run-out information is sparse, as it usually is, model calibration will be problematic and embody error;
(3) the simulated run-out distance could differ from the true value, even if the release volume estimate is exact, due to the inherent variability of the dynamics of otherwise similar avalanche events (a given volume of snow can give a range of expected run-out distances, depending on the propertiesy of the released snow and ofthe snow cover along the track; or similarly tthat is, for a given run-out distance, there is a distribution of avalanche sizes).

In this section it will be shown how different modelling techniques – say statistical and physical avalanche models - can be properly combined to estimate the hazard limits for poorly documented (or even undocumented) avalanche paths, and how Monte-Carlo techniques can be used to evaluate the expected error in the estimation of these limits, in particular of $x_{H/M}$.

4.2.1.1 Method

The "combined-method" here proposed for hazard mapping uses an avalanche dynamics model embedded within a statistical framework and is essentially based on frequency-weighted impact pressure. A brief description of the procedure is given in the following points; for more detail see the work Keylock and Barbolini (2001) and Barbolini and Keylock (2002).

(1) A statistical model for avalanche run-out distance is used to obtain avalanche encounter probability as a function of avalanche size and location along the path, as well as to obtain the frequency distribution of avalanche sizes. This model can be derived on the base of avalanche data from a number of paths in a certain mountainous region and ultimately gives an represent the "average (unconditional) encounter probability versus run-out distance" relation for that a region, such as the one shown in Figure 4.1. Such kind of statistical model has been recently derived by Keylock et al. (1999) for Icelandic avalanche; for details concerning the statistical modelling procedure refer to that work. The curve of Figure 4.1 gives the percentage of avalanche (P) reaching a given position along the path, expressed in terms of the runout ratio, RR (McClung and Lied, 1987). If F indicates the average number of avalanche per year on the considered path, Equation 4.1 relates the actual avalanche return periods T and the probability $P/100$ of an avalanche attaining a given run-out ratio.

$$F \cdot \left(\frac{P}{100} \right) = \frac{1}{T} \qquad [4.1]$$

Figure 4.1 gives RR as a function of P, which allows ultimately the run-out positions related to any given return period to be determined, in particular x(T= T_1 yrs) and x(T= T_2 yrs).

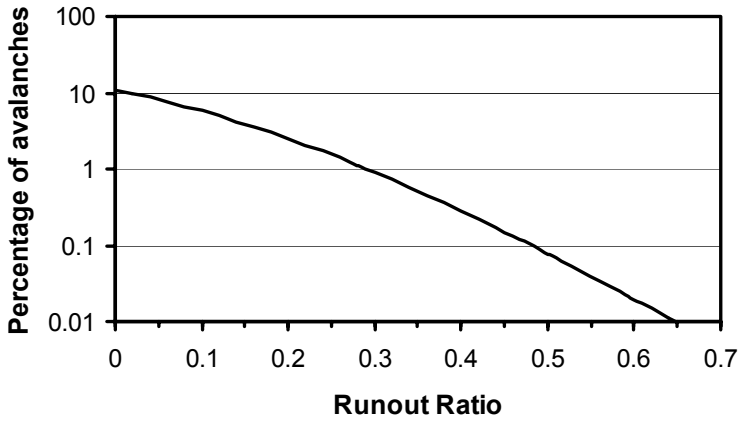

Figure 4.1. Avalanche exceedance P (expressed as a percentage) as a function of runout distance (in terms of the runout ratio RR), using the model derived by Keylock et al. (1999) for Icelandic paths.

(2) An avalanche dynamics model is then tuned to the run-out distances provided by the statistical model, and is used to derive impact pressure estimates along the path. Impact pressure can be calculated as the product of snow density and velocity squared, according to the proposal of Salm et al. (1990) - or even using any other suitable relation - and are weighted using the estimated avalanche frequency at given location as appropriate weights. In particular, within the statistical model of Keylock et al. (1999), different sized avalanches (according to the Canadian size classification, McClung and Schaerer, 1993) can have the same stopping position, but a different probability of stopping at this position. Therefore, for each avalanche size the impact pressure at $x(T=T_1\ yrs)$ is calculated by simulating the dynamics of the different sized avalanche stopping at the location $x(T=T_2\ yrs)$. If the impact pressure for the size i avalanche is larger than $\bar{I}$ kPa at the $x(T=T_1\ yrs)$ location, the location x_i where the impact pressure is equal to $\bar{I}$ kPa is found (see Figure 4.2), and then the relative frequencies of each size (w_i) are used as weights to give the frequency-weighted average position of the high/moderate hazard zone boundary, $\bar{x}_{H/M}$:

$$\bar{x}_{H/M} = \frac{\sum w_i x_i}{\sum w_i} \qquad [4.2]$$

(3) In addition, the uncertainty in the statistical model estimate of $x(T=T_1\ yrs)$ and $x(T=T_2\ yrs)$ can be incorporated by concentrating the statistical model error onto the estimate of F. If we assume that the error on F conforms to a symmetric triangular distribution, by Equation 4.1 and Figure 4.1 the position of $x(T=T_1\ yrs)$ and $x(T=T_2\ yrs)$ can be given in terms of (skewed) triangular distributions. Given that, it is possible to obtain the complete Probability Distribution Function (PDF) for $x_{H/M}$ by

the following steps: (i) randomly sampling a value for $x(T=T_1\ yrs)$ and $x(T=T_2\ yrs)$ from their respective probability distributions; (ii) taking the probability distribution of avalanche sizes at each random estimate for $x(T=T_2\ yrs)$; (iii) selecting one of these sizes at random according to this distribution, and calculating the respective position for $x_{H/M}$, by comparing $x(I=\bar{I}\ kpPa)$ for the selected size with the randomly estimated location of $x(T=T_1\ yrs)$; (iiii) repeating this many times by Monte Carlo simulation, the properties of the PDF of $x_{H/M}$ can be inferred.

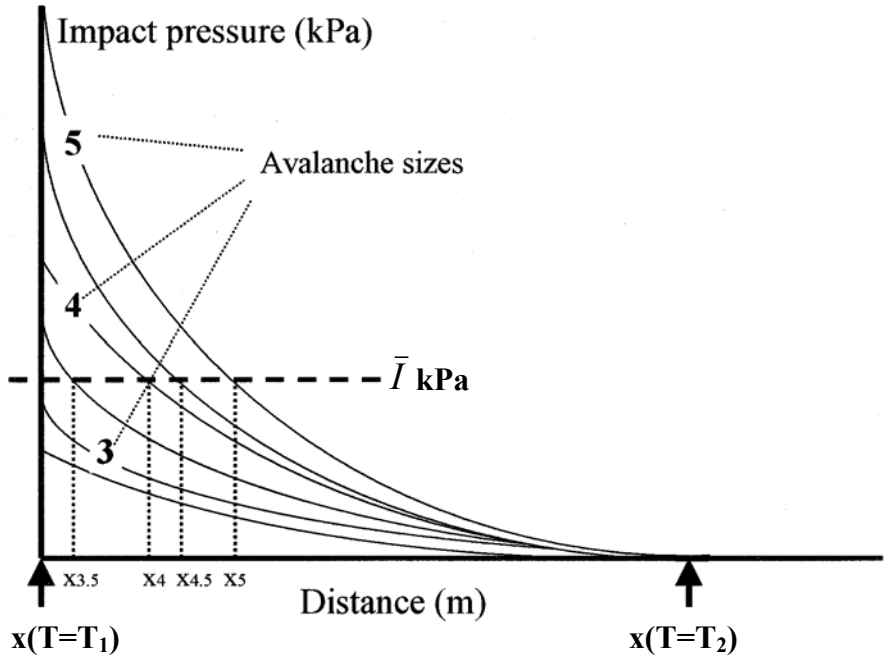

Figure 4.2: Impact pressure as a function of distance for different size avalanches stopping at x(T=T2yrs). The positions xi show where the pressure for different sizes (i) reaches $\bar{I}$ kPa. If an avalanche size j does not reach $\bar{I}$ kPa by x(T= T1yrs) (in the figure this is true for sizes 2.5 and 3), then in Equation 4.2 xj is set to x(T= T1yrs).

4.3 Examples

MB and CK

4.3.1 The Súðavík avalanche path, Iceland

In this Section it is shown an implementation of the methodology presented at Section 4.2.2 to a practical mapping problem. Without lost of generality, this is done using the Swiss mapping criteria; this means that T_1, T_2 and $\bar{I}$ are set to 30 years 300 years and 30kPa respectively, and that the high hazard/moderate hazard boundary became the red/blue zone boundary ($x_{R/B}$) according the colours used in the Swiss hazard maps. On Monday, January 16th, 1995 an

avalanche damaged or destroyed 22 houses from a total of seventy in the village of Súðavík in the North-West of Iceland, killing 14 people. The location of this village in Iceland can be seen in Figure 4.3; in figure 4.4 is given a view of the avalanche site. This avalanche path is used to illustrate the proposed approach. A hydraulic-continuum avalanche dynamics model (Natale et al., 1994; Barbolini et al., 2000), using a classical two-parameter Voellmy-like resistance law (Bartelt et al., 1999), is used to perform the impact pressure calculations. The calibration procedure for the dynamics model at this site as well as details concerning the combined modelling procedure is explained in more detail in Keylock and Barbolini (2001).

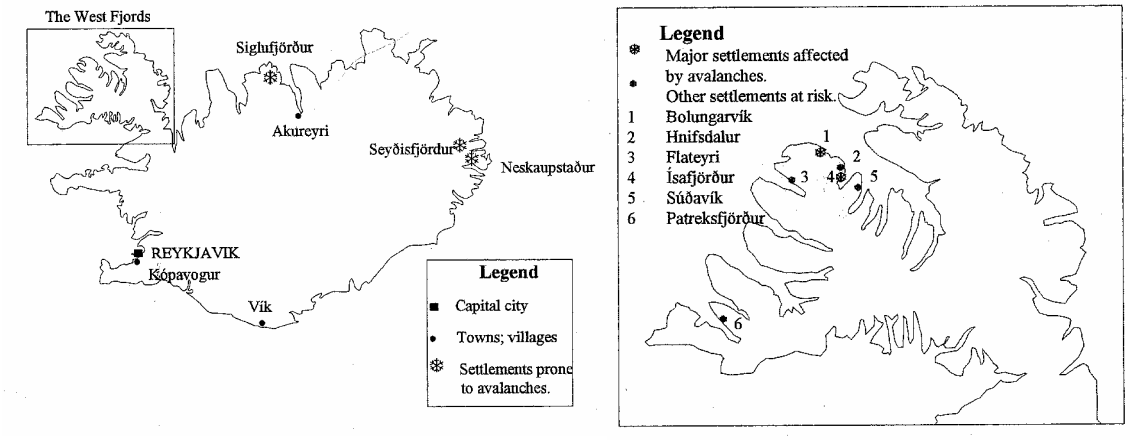

Figure 4.3: Location of the Súðavík village

Figure 4.4: View of the avalanche path affecting the Súðavík village

According to the statistical model, the most probable locations for *x(T=30yrs)* and *x(T=300yrs)* upon this path are 1173 m and 1346 m, respectively (see

Figure 4.5). That is, at elevations above sea level of 12.5m and 0.0m and run-out ratios of 0.29 and 0.48. The major limitation of our approach to run-out distance estimation is the value for *F*. Our best-guess value for *F* was 3.26 (approximately 3) avalanches per year based upon historical avalanche information for this path, with an estimated error of approximately 2 avalanches per year. Hence, the lower and upper limits for the triangular distributions for the error in the estimation of *F* were given by the locations *x(T=10yrs)* and *x(T=50yrs)* for *x(T=30yrs)* and *x(T=100yrs)* and *x(T=500yrs)* for *x(T=300yrs),* see Figure 4.6. These positions equated to values for *F* of 1.08 and 5.45 avalanches per year for the lower and upper limits respectively.

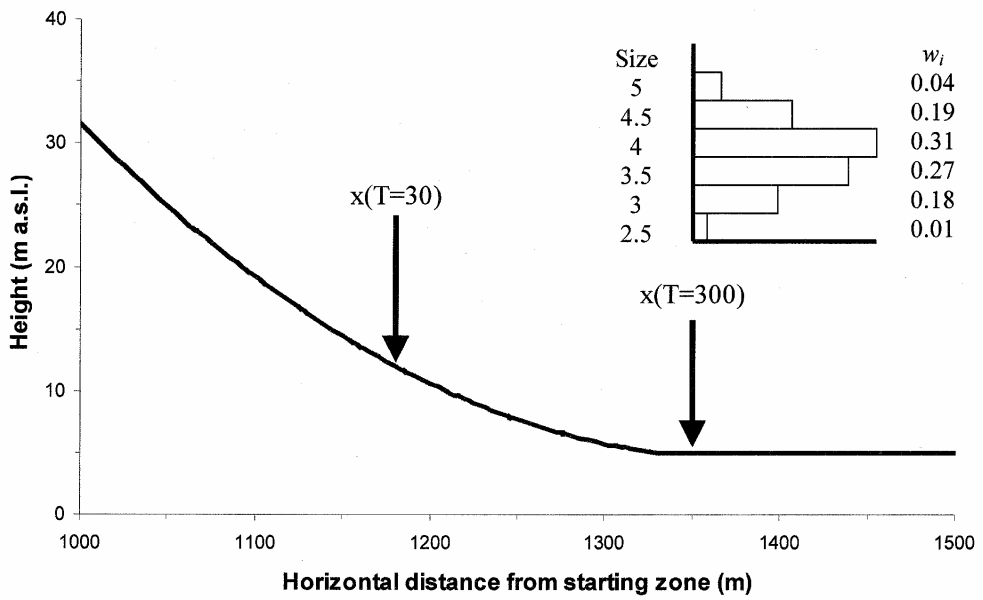

Figure 4.5: Along the longitudinal profile of the Súðavík avalanche path (only the run-out zone is presented) are indicated the estimated run-out position for the T=30 years and T=300 years avalanche, and the relative frequency (w_i) of avalanches with different sizes stopping at x(T=300yrs). The Canadian classification uses five sizes (1 to 5), although it is common for avalanche observers to use half sizes; in this work we have followed this approach. In the figure sizes 1, 1.5 and 2 are not included (i.e. $w_1=w_{1.5}=w_2=0$) because they do not reach x(T=300yrs), i.e. for these sizes the probability of reaching the target location is below a threshold value (fixed at 0.005).

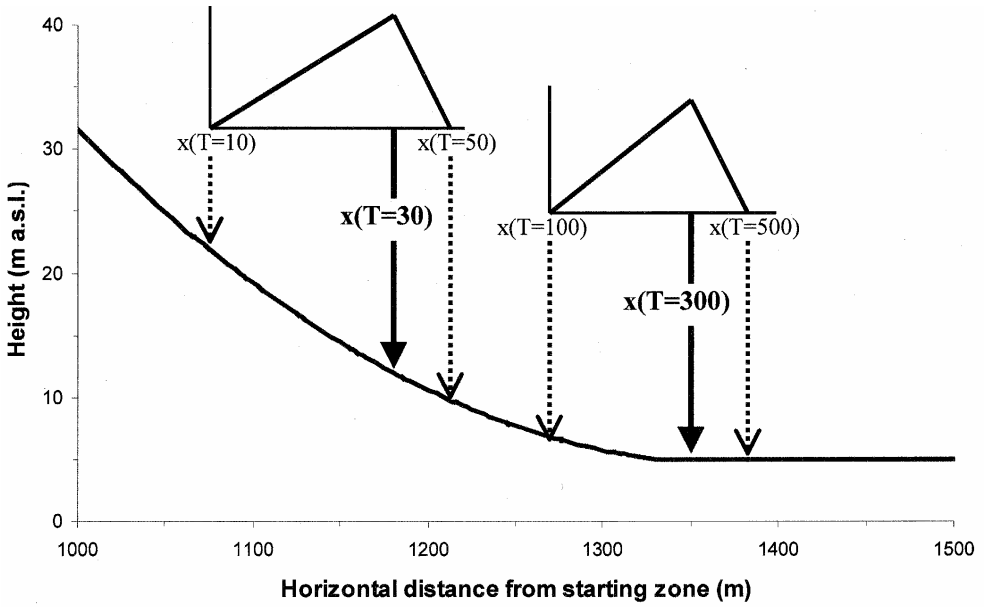

Figure4.6: Triangular distributions for the position of x(T=30yrs) and x(T=300yrs) due to uncertainty in F. In this study, we assume that the value for F is sufficiently constrained that the limits for these distributions lie between x(T=10yrs) and x(T=50yrs) in the former case, and x(T=100yrs) and x(T=500yrs) for the latter.

Figure 4.7 shows the values for $\bar{x}_{R/B}$, calculated with equation 4.2 (step 2 of the procedure presented in Section 4.2.2) and the full PDF for $\bar{x}_{R/B}$, including the mean value and the 5% and 95% confidence limits, obtained when the uncertainty in the statistical model estimate of *x(T=30 yrs)* and *x(T=300 yrs)* is incorporated (step 3 of the procedure presented in Section 4.2.2). It is interesting to note that the value for $\bar{x}_{R/B}$ (1243m) obtained using the best estimate for *x(T=30yrs)* and *x(T=300yrs)* appears to be quite close to the median of the PDF of $x_{R/B}$ obtained by Monte Carlo Simulation (1237m). This suggests that the best-guess estimate provides a useful indicator of the central tendency for $x_{R/B}$ even if the value for *F* is not well known.

The lack of sensitivity of the median to the assumed distribution for *F* is shown in Table 4.2 where the properties of the PDF given in Figure 4.7 are compared to a PDF where the estimates for *x(T=30yrs)* and *x(T=300yrs)* are believed to occur between *x(T=3yrs)* and *x(T=300yrs),* and *x(T=30yrs)* and *x(T=3000yrs)*, respectively. Note that some of the statistical properties of the PDF of $x_{R/B}$ listed in Table 4.2 (e.g. mean, median, standard deviation) as well as the value previously indicated for the best guess estimate of *x(T=30yrs)* and *x(T=300yrs)* are given to an accuracy (of the order of the meter) that is actually unreasonable. This is done for the purposes of analysis only and does not imply that these variables can be calculated with such accuracy.

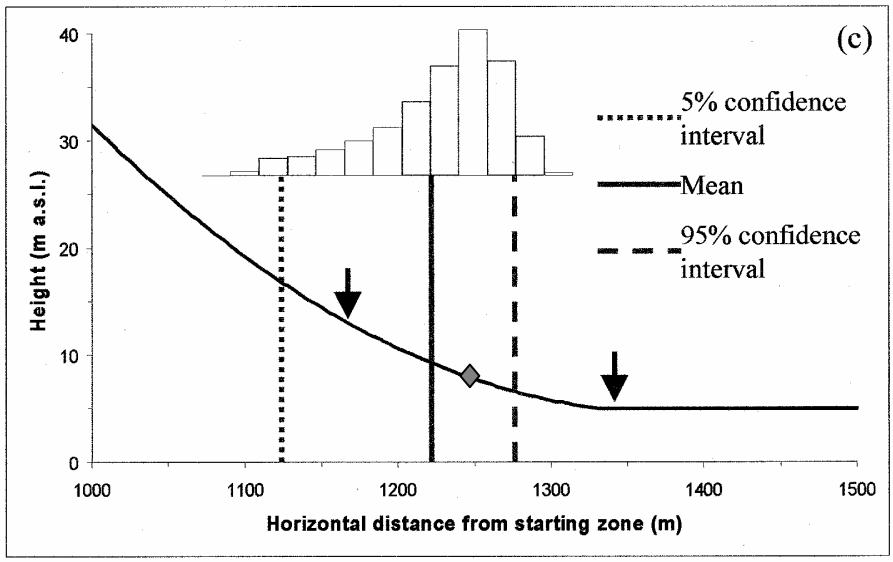

Figures 4.7: Are indicated the value for $\bar{x}_{R/B}$ calculated with equation 4.2 using the best guess estimate (arrows) for x(T=30 yrs) and x(T=300 yrs) (solid diamond), and the full PDF for $\bar{x}_{R/B}$, including the mean value and the 5% and 95% confidence limits, obtained when the uncertainty in the statistical model estimate of x(T=30 yrs) and x(T=300 yrs) is incorporated.

Table 4.2: Properties of the PDF of $x_{R/B}$ given in Figure 4.7 (PDF_1) compared to a PDF where the estimates for x(T=30yrs) and x(T=300yrs) are believed to occur between x(T=3yrs) and x(T=300yrs), and x(T=30yrs) and x(T=3000yrs), respectively (PDF_2).

	PDF_1	PDF_2
Mean (m)	1226	1224
Median (m)	1237	1237
Standard deviation (m)	46	82
Skewness	-0.92	-0.79
Kurtosis	0.28	0.64
5% confidence bound (m)	1130	1064
95% confidence bound (m)	1283	1334

Figure 4.8 shows a map of Súðavík with the largest known historic avalanche events, the results of an alpha-beta model analysis (Lied and Bakkehøi, 1980) using the relation derived by Jóhannessson (1998), and of a risk analysis performed by the Icelandic Meteorological Office (Jónasson et al., 1999) and the results from this study. The results presented are those taken from Figure 4.7 The best-guess estimate for *x(T=300yrs)* is marked with a black solid line and occurs at a similar position to α - 2 standard deviations. The three grey lines indicate $x_{R/B}(0.05)$, $E(x_{R/B})$ and $x_{R/B}(0.95)$ and are labelled '0.05', 'Mean', and '0.95', respectively. Our value for $E(x_{R/B})$ lies close to α - 1 standard deviation and the 90% confidence bands seem to correspond to 1 standard

deviation of α. It would be interesting to determine if such relations are true in general, because this would open for the possibility of a practical interpretation of the alpha-beta model results within the Swiss zoning scheme. However, the fact that the alpha-beta model seems to perform relatively poorly upon this path would suggest that this may not be the case.

The optimum location for the red/blue zone boundary should be conservatively located downslope of $E(x_{R/B})$, but within the 90% confidence intervals. Table 4.1 shows that the median is a robust estimator of central tendency and, due to the negatively skewed distribution that results when return periods are translated into run-out distances (see Figure 4.7), it will always lie between $E(x_{R/B})$ and $x_{R/B}(0.95)$. Thus, for this path, a location 1237m downslope is perhaps the optimum location for the red/blue zone boundary from our analysis. This appears to be close to the 2×10^{-3} risk contour line shown in Figure 4.8, which equates to a return period of about 150 years (Jónasson et al., 1999), a recurrence interval that is sensible for the location of the red/blue hazard zones boundary.

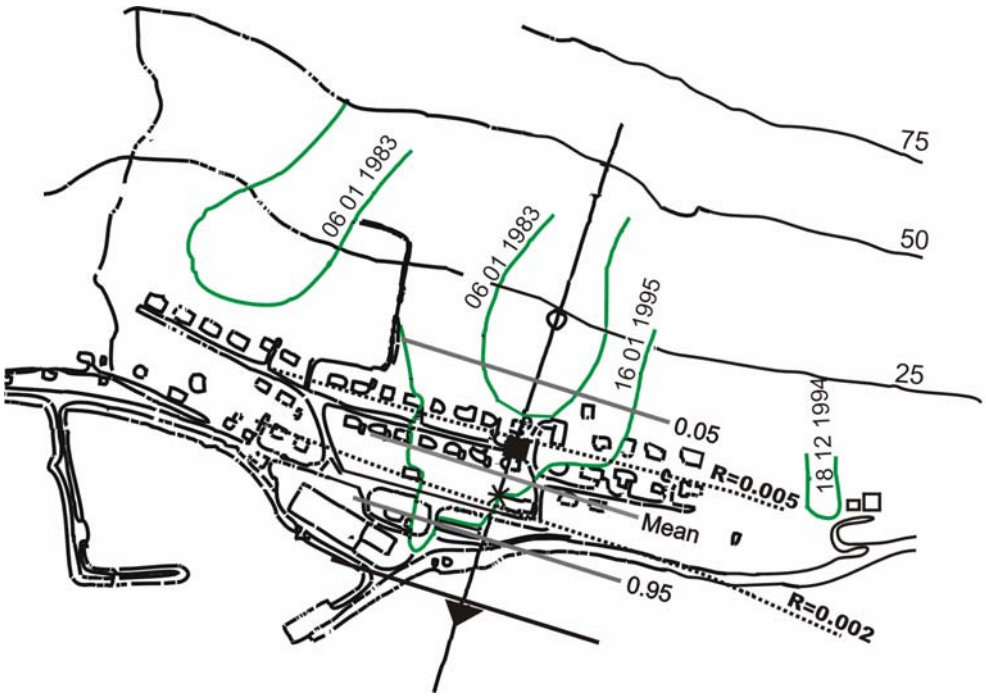

Figure 4.8. A map of the Súðavík avalanche path showing the largest historical avalanches, the results of an alpha-beta model and of a risk analysis, and the positions for $x_{R/B}$ obtained in this study from Figure 4.7. The three grey lines are described in the text. The asterisk indicates the location of the median of $x_{R/B}$. The black solid line is the best-guess estimate for x(T=300yrs). The open circle is the predicted alpha point and the solid square and solid triangle are alpha minus one standard deviation and alpha minus two standard deviations, respectively. The alpha-beta model simulations and the risk analysis were performed at Icelandic Meteorological Office and are provided for comparative purposes.

The results that we have presented are only from one avalanche path. In order to investigate the usefulness of the approach outlined in this paper, testing upon many more paths is required. However, it is to be expected that for paths where the avalanche run-out is adequately described by the statistical model and where the run-out zone is of a smooth, continuous, approximately parabolic shape, the general conclusions from this study should hold true. Therefore, it should be possible to place confidence limits on the location for $x_{R/B}$ using our method. In future, it may be possible to extend this approach to two dimensions using a more sophisticated dynamics model and a more complex statistical approach (Keylock et al., 1999). However, as run-out distance is more commonly known to a higher accuracy than the width, uncertainties in the width data underlying the statistical model and the greater difficulty in validating the dynamics model might make this problematic at present.

4.3.2 Icelandic example

TJ

An example of hazard zoning from Iceland is given in the "Case studies" section of Appendix A, where hazard zones for the village of Neskaupstaður in eastern Iceland are described.

4.3.3 Austrian example

KK

In winter 1999 more than 200 avalanches occurred in Paznaun valley and the neighboring Pitz valley. By surveying all deposition areas and as far as possible the appending release areas, an interesting base for sound analyses of avalanche models has been created. In contrary to the two chapters above the aim of this work is less to establish a new combining method. Based on the data, various models should be evaluated which could give interesting information for further development of combined methods.

In the first part of the work the models are derived or calibrated. In the second part, these calibrated models are applied to the catastrophic avalanche track of Galtür.

4.3.3.1 Topographic regression model

Every event of the year 1999 was compared to the chronicle data. The run-out of the maximum event has been chosen for the regression analysis

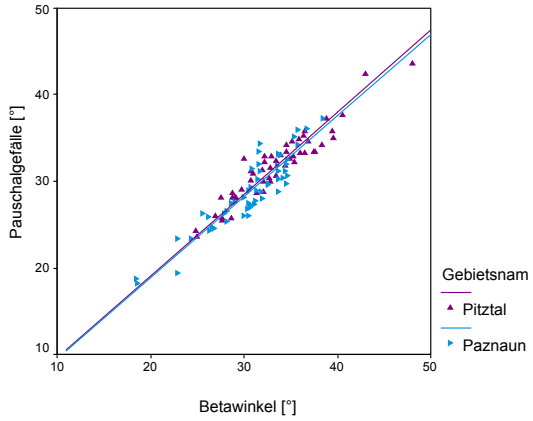

Figure 4.9: Correlation of run-out (Pauschalgefälle) and track slope (Beta-angle).

The correlation functions found are:

Paznaun:	$\alpha = 0.91 * \beta + 0.81°$	$R = 0.91$	$S = 1.7°$
Pitztal:	$\alpha = 0.83 * \beta + 4.07°$	$R = 0.95$	$S = 1.3°$
Gemeinsam:	$\alpha = 0.89 * \beta + 1.77°$	$R = 0.94$	$S = 1.5°$

4.3.3.2 1-D dynamical models

For all avalanche tracks the PCM model has been applied and for 30 % of the tracks also the analytical Voellmy and the AVAL1D model. Till now only the application of the "standard" values proposed by the SLF is tested. But analyses are still going on, so no statistical information can be given. Qualitatively the AVAL1D model seems to be the "best" model in this group, which means that in most of the cases the calculated run-out corresponds satisfactorily to the maximum observed run-out. But there is the hope that with this data the combined methods described above could be additionally to the original data calibrated.

4.3.3.3 2-D ELBA model

The model ELBA is the attempt to enhance the capabilities of the Voellmy model by a 2D application.

The acceleration of a mass unit for the 1D case is calculated with

$$\frac{\mathbf{dv}}{\mathbf{dt}} = \mathbf{g} * (\sin\beta + \sin\omega - \mathbf{sign}(\mathbf{v}) * (\mu.\cos\beta + \frac{\mathbf{v^2}}{\xi * \mathbf{h}}))$$

with β: slope of the track, ω: slope of the hydrostatic flow height, μ: dry friction parameter, ξ: turbulence friction parameter and h: flow height.

The model is realised on a regular grid. For each grid cell the linear momentum determined. According to the Courandt condition, the fastest mass particle must not further then the next grid cell. The distribution of the masses over the 2D-slope of the DTM is calculated by vector addition considering the conservation law of momentum. A detailed description of the model is in preparation.

Although there are recently many discussions about the entrainment process and how it is influencing the whole process of the gravity current for ELBA a very simple approach has been chosen. If the shear stress exceeds on a certain point the threshold value a predefined amount of snow is added to the avalanche body. It has to be emphasised that the whole modelling process from Voellmy to Elba can be characterised as a "macroscopic" view. The aim of the erosion implementation was not a better understanding of the erosion process itself (this has to be done necessarily) but to improve the "mass balance" according to reality. shows the clear positive effect of this rough modelling concept. The additional mass by snow erosion has been implanted in the following way:

The linear momentum is given by I=m*v. By vector addition the linear momentum and the corresponding masses of the next grid can be easily achieved so that the new velocity V_n is given by

$V_n=I_{summary} / m_{summary}$. Before calculating the velocity v_n the entrainment mass m_e is added so that the velocity is given by $v_n=I_{summary} / (m_{summary} + m_e)$. Increasing amount of additional snow in proportion the original mass leads to decreasing velocity. It is clear that no forces for mobilising the eroded snow mass can be taken into account with this concept.

The ELBA model has been calibrated in two ways. In tracks where the flowing boundary of the 1999 events could be surveyed by aerial photo interpretation, a closer look to the flowing behavior has been made. It could be seen that ELBA tends to have higher velocities then real avalanches. It can be also observed that in some cases (e.g. contour slopes) the flowing behavior with low speed is not realistic. ELBA tends to "flow out" like water. But in most of the cases the simulations match the observed avalanches very good.
In a next step the friction and entrainment parameters has been calibrated by recalculating all events of 1999 in the both valleys. Figure 4.10 shows that with release areas determined by aerial photo interpretation (left, green columns) the simulations tend to slightly underestimate the runout, but the error distribution is almost bell shaped.

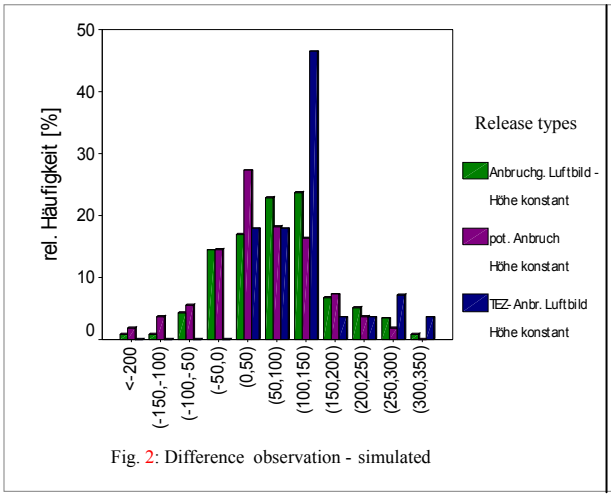

Figure 4.10: Comparison between ELBA run-out calculation and observed runouts of the 1999 events. The three release types strongly influence the quality of the simulations.

Based on this calibration the ELBA model has been used to recalculate the Galtür event February 1999. Figure 4.11 shows the run-out without entrainment. The run-out length is almost identical compared to the AVAL1D simulation.

Figure 4.12 shows the run-out with varying snow entrainment. The release height is kept constant to 1 m. The avalanche is stopping in the flat area in the middle of the slope. But assuming 0.2 and 0.4 m the run-out more and more corresponds to the observed (outermost blue area). But if with the AVAL1D simulation also a release zone in flat range of the slope is assumed, the run-out perfectly fits to the one determined by ELBA. It is interesting that also the topographic regression model derived for the Paznaun valley estimates the same run-out.

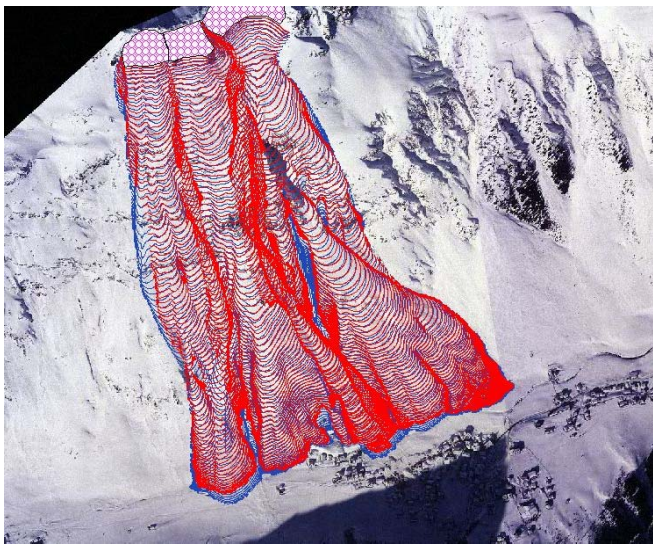

Fig. 4.11: ELBA simulation without entrainment

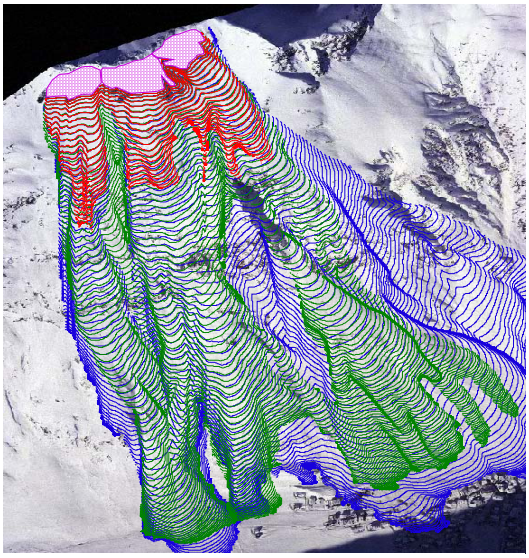

Fig. 412: ELBA simulation with increasing entrainment from 0-0,4m

5 MODIFICATION OF HAZARD MAPS BY PROTECTIVE MEASURES

5.1 Legislation and today's practice

5.1.1 French legislation

MN
In France, the hazard map cannot be modified by the protective measures. The defence structures are only used to protect the existing vulnerability and do not allow new constructions.

5.1.2 Icelandic legislation

TJ
According to the Icelandic hazard zoning regulation, the effect of protective structures shall be assessed and/or calculated as a part of the hazard zoning. The hazard maps should show both the situation in the absence of such measures and risk that is estimated when the structures are taken into consideration. Estimation of the risk below protective structures is highly uncertain. Therefore, the Icelandic zoning regulation states that protective measures against snow avalanches and other slides shall only be built to increase the safety of people in already populated areas. In addition, local authorities are required to take the danger of snow- or landslides into consideration in planning and development of the communities so that the safety of the settlements is improved over time.

5.1.3 Italian legislation

MB

5.1.3.1 Introduction

Although the attention for avalanche problems has grown sharply in the last decades, at present in Italy there is neither a common legislation nor well defined technical criteria concerning hazard zoning in avalanche–prone areas. For this reason, In January 2001 a collaboration project between *AINEVA* (*Italian Interregional Association for Snow and Avalanches*) and the *Hydraulic and Environmental Engineering Department of the University of Pavia* has started, with the aim of defining general guidelines for the management of avalanche problems in mountain areas; these guidelines should serve as a reference common base to set up the specific legislation of the different Italian Alpine Regions. The collaboration is presently in progress; however, the first results of this joint research project have been synthesised in the report "New Italian Zoning Tools", approved by *AINEVA* in March 2002, which basically contains the new Italian criteria for avalanche hazard mapping and the related land-use restrictions. A detailed description of these new criteria is provided in the Cadzie WP5 Final Report; here the attention is only focused on the indications concerning the modification of hazard maps by protective measures.

5.1.3.2 Update of hazard mapping: general criteria

According to the increase of the available information, avalanche hazard maps have to be periodically verified and eventually modified. In particular the updating of hazard maps has to be done if:

1. new historical data comes out (not considered in the previous map preparation and giving rise to an extension of the area affected by past avalanches);
2. new avalanche events occur (in area previously not documented as endangered, as well as in known avalanche area but with intensity and/or extension larger than what was previously known);
3. modifications (natural or artificial) of the territorial and environmental context that give rise to an increase of the degree of exposure to the avalanche danger occur (such as for instance the deforestation of release zones).

The periodic updating of the hazard maps should also consider the longer series of data recording, and the availability of more recent and sophisticated computational models.

The maps update could also consider the decrease of the degree of exposure to the avalanche danger associated to naturally-induced (such as the forestation of the release zone) or artificially-induced (such as the realisation of defence works) modifications of the environment. In any case the construction of structural defence work is allowed only to protect already existing goods exposed to the avalanche danger (and if their relocation is not advantageous in a cost-benefit and/or social perspective).

When admissible in relation to the features of the avalanche site and of the (natural or artificial) modification introduced, the modification of the hazard maps has to be done according to the following general criteria:

(a) In order to maintain a control on the areas potentially exposed to the avalanche danger, especially with respect to the extreme events, the modification of the hazard maps associated to the realisation of structural defence works or to the forestation of the release zones, should not result in a reduction of the overall exposed area but only in a "reclassification" of the degree of exposure of the different areas (this means that no new white areas should arise, but only modification of the boundary between red/blue and blue/yellow zones).

(b) The modification of hazard maps resulting from the forestation of the release zones should be done on the base of specific technical studies in which a proper evaluation of the effects of the new forest on the release and motion of the snow masses is given (with respect to the tree types and density); also the potential exposure of the new forest to processes that can reduce its efficiency in long term perspective, such as landslides or fire, should be accounted for within such evaluations.

(c) The modification of hazard maps resulting from the realisation of structural defence works (active or passive works) should be done on the base of specific technical studies in which a proper evaluation of their effects with respect to the release and motion of the avalanches is given. The maps modification should also properly take into account of the "technical life" of the defence works; with this respect modification are allowed only if maintenance plan for the defence works are operative.

5.1.4 Swiss legislation

SM and UG

In Switzerland the debate about how to consider constructive protection measures in the land use planning is ongoing. Today, no official guidelines about this topic exist and consequently the local authorities – often confronted with economic pressure to reduce the hazard zones after protection measures were completed – have some freedom in their assessment of the new situation.

5.2 Examples and critical evaluation

5.2.1 Icelandic example

TJ
An example of hazard zoning below recently constructed protection measures below Drangagil in Neskaupstaður in eastern Iceland is given in the "Case studies" section of Appendix A.

5.2.2 Italian example

MB
In this Section are shown two different examples of updating of avalanche hazard maps after the realisation of defence works; in particular, in one case (the "Costaccia" avalanche, see below) the map has been modified, whereas in the other case (the "Foppolo" avalanche, see below) the map has been kept unmodified. The two cases are briefly presented, with attention paid to the reasons that have supported the different decision taken concerning the modification of the maps and, with respect to the "Costaccia" case, also to the criteria adopted for the map modification.

5.2.2.1 The "Costaccia" study case

The Costaccia avalanche site is located above the village of Livigno in the Central Italian Alps, within the Lombardia Region. In Figure 5.1 is shown the avalanche hazard map for this site, which is made according to the Swiss Criteria. The blue and red continuos lines indicate the new limits for the hazard zones, whereas the red dashed line represent the old location of the red zone, drawn in the assumption of absence of structural defence work. In actual fact the release zone is presently protected by snow bridges and snow nets to a great extent (see Figures 5.2 and 5.3). Furthermore new rows of snow nets are planned to be built to further increase the safety this site (Figure 5.2). The following considerations have supported the modification of the hazard map in this specific case:

(i) the release zone, which is well defined and circumscribed, will be almost completely secured by retaining works;
(ii) the release zone is easily accessible (is within a sky resort, see Figure 5.2), so that control and maintenance of the defence works is quite easy and relatively cheap;
(iii) the technical life of the bridges/net could be considered to be quite long, given that the slope in not subjected to soilslip or rockfall.

It should be pointed out also that the map modification has considered only the red zone (Figure 5.1), whereas the area potentially interested by the extreme

avalanche has not been modified at all, according of the criteria stated in Section 5.1.3.2.

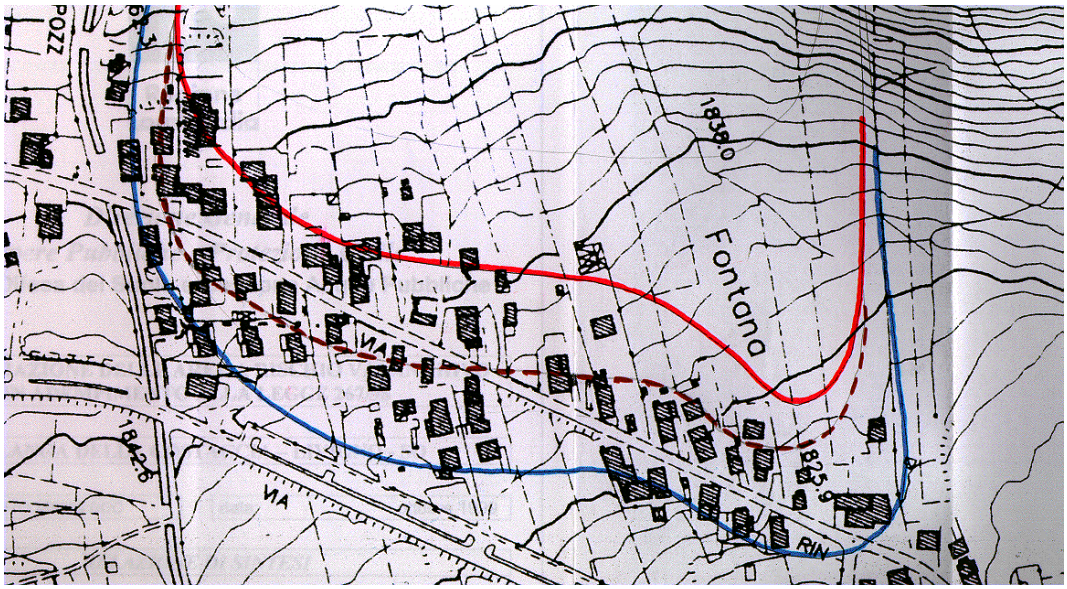

Figure 5.1: Hazard map for the "Costaccia" avalanche. The limit of the high hazard zone before and after the realisation of the defence works are indicated with the dashed and continuous red lines respectively, whereas the limit of the moderate hazard zone is indicated with the blue line and has been kept unmodified even in the presence of protective measures.

Figure 5.2: Aerial view of the release zone of the Costraccia avalanche. The existing snow bridge/nets are clearly visible; the area where the new defence works will be located (in Summer 2002) is also indicated (with the red circle).

Figure 5.3: Side view of the release zone of the "Costraccia" avalanche, with the already existing rows of retaining defence works.

5.2.2.2 The "Foppolo" study case

The "Foppolo" avalanche site is located above the village of Foppolo in the Central Italian Alps, within the Lombardia Region. In Figure 5.4 is shown the avalanche hazard map for this site, made according to the Swiss Criteria. The blue and red continuos lines indicate the limits for the moderate and high hazard zones, respectively. In this site in the late seventies, after a big avalanche event damaging the village, two dams have been built in the run-out zone (black lines in Figure 5.4); furthermore the realisation of snow bridges in the release zone is planned for the Summer 2002 (the area that will be secured by the nets is indicated in Figure 5.4). Even if in this site are present different types of structural defence works (some of them will be built before the next winter season) the hazard maps has not been modified at all, with respect to the case assuming no defence work in place. The reasons for this are the following:

(i) some avalanches have flown over the dams after their realisation, because the height of the dams is quite low (4-5 meters) and their uphill slope not enough steep; therefore the efficiency of these dams should be considered low, also considered that the avalanche release area is extensive (Figure 5.4) and many avalanche could trigger from different basins in a short time interval filling the dams and further reducing its efficiency;

(ii) the new defence works planned in the release zone will secure only a small part of the overall potential release zone, and the avalanches could still release from different sectors and affect the village.

Therefore in this case the modification of the hazard map could be taken into account only when the realisation of retaining works will be extended to a more relevant part of the release zone.

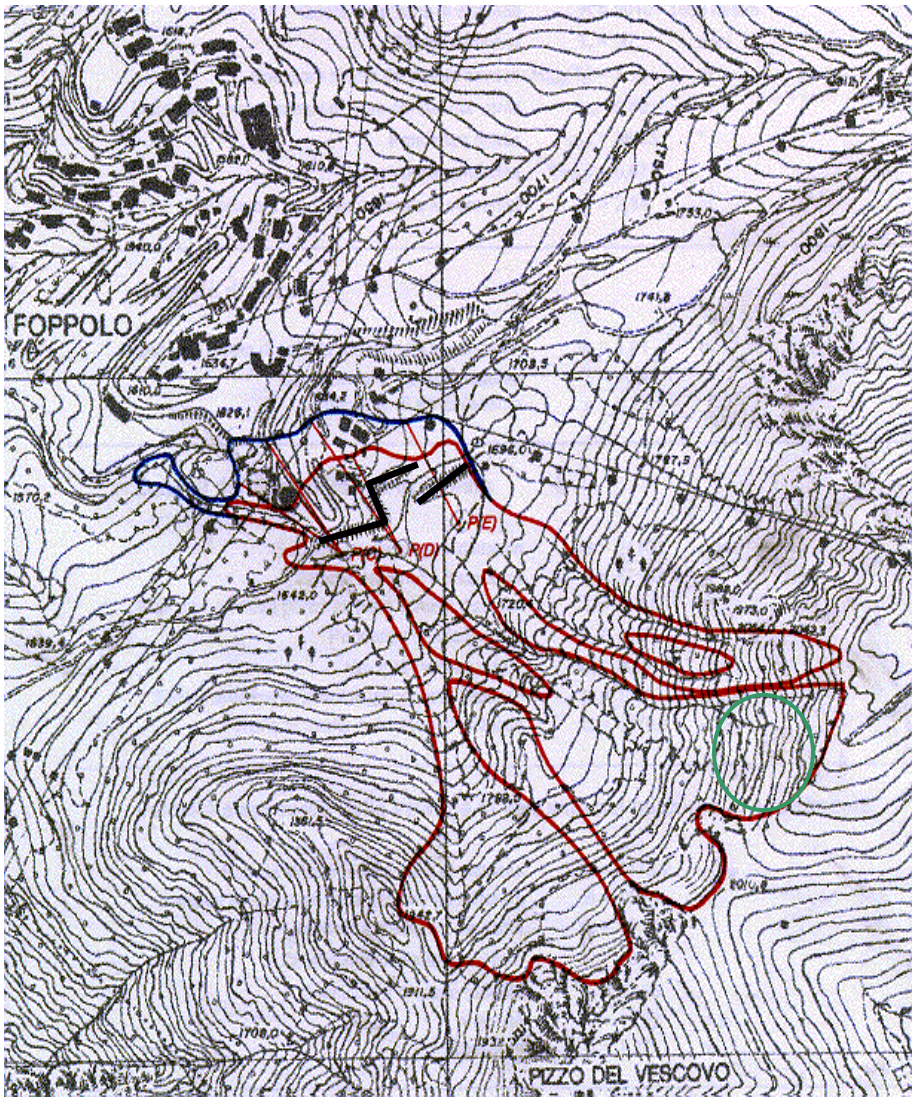

Figure 5.4: Hazard map for the Foppolo avalanche. The green circle indicate the part of the release area that will be secured by snow nets during summer 2002, whereas the black lines indicate the already existing retaining dams. In spite of the presence of these defence works, the hazard maps has not been modified.

5.2.3 Swiss example

SM and UG

In the following, two well documented examples are shown in order to illustrate the variety of approaches in practice. In the conclusions the most important questions to be resolved by guidelines are summarized.

5.2.3.1 Palüda Avalanche, Davos (GR)

5.2.3.1.1 Avalanche situation

The open, slightly convex, clearly definable release area of the Palüda avalanche is located at the south easterly flank of the Schiahorn mountain (Figure 5.5). The entire release area covers 9.5 ha. Beneath of the release area the avalanche track flattens in the area of the upper Büschalp (inclination approx. 19°, length approx. 150-200 m). Small avalanches stop already on this spot. However, further downhill, the slope angle is becoming steeper again. Larger avalanches are flowing mostly unconfined towards the settled area of Davos. In some cases, the avalanche was reported to have been concentrated on little distinctive gullies. A first run-out area exists on the area terrace of Palüda (inclination approx. 11.5°, length approx. 150 m). Below Palüda the track becomes again steeper, until the flat area in the valley bottom is reached.

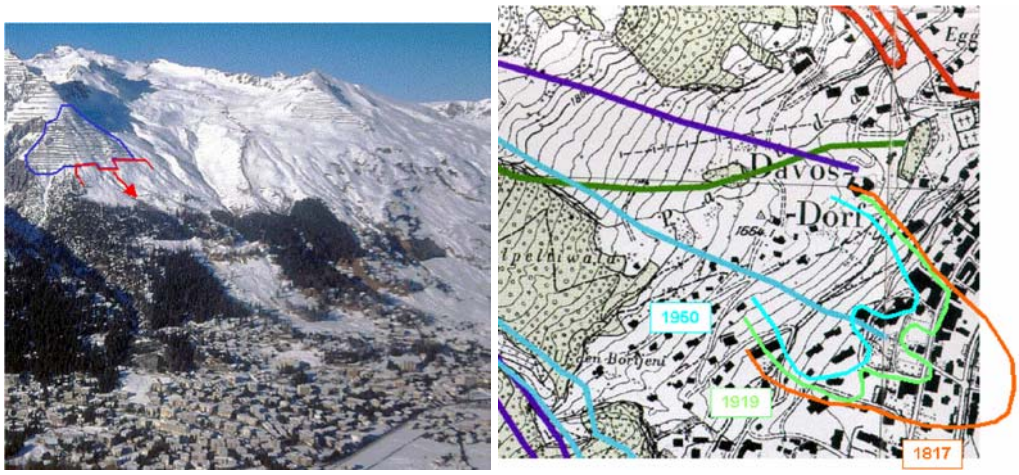

Figure 5.5: Left: Overview Schiahorn – Palüda area, Right: Avalanche register of the Palüda avalanche.

5.2.3.1.2 Avalanche cadastre

Since 1802 7 larger avalanche events were documented in this avalanche track. The largest event in the last 2 centuries took place in 1817. Then, the avalanche crossed the flat valley bottom on a length of approximately 300m before coming to rest. Today, this area in the valley bottom is completely covered by buildings. On 23 December 1919, again a very large avalanche broke loose. Although the run out distance was about 150 shorter than the one of the 1817 avalanche, it caused two fatalities and large damages. As a consequence of this event, the construction of retaining structures in the release area at the Schiahorn mountain started. Further large events took place in 1950, 1951, 1954 and 1968, however, their extents were significantly smaller (Figure 5.5).

5.2.3.1.3. Constructive protection measures

The protection measures at the Schiahorn started in 1919 with the construction of stonewalls in order to form flat terraces. Starting from 1940 steel racks made of railway rails and Larch wood were built. In the 1960's the protection measure were complemented by modern steel retaining bridges. Table 1 gives an overview about the existing constructive measures in the release area:

Table 5.1: Constructive protection measures Schiahorn

Type of work	Year of construction	Length
Wall terraces	1921-1931	3638m
Snow rack	starting from 1945	856m
Snow fences	starting from 1945	360m
Voest Alpine snow bridges (Height 3.0m and 3.5m)	1963-1970	3482m
Fromm Snow bridges (Height 3.0m and 3.5m)	1983-1987	826m

In 1987 an inventory of all protection measures was made and the state of the existing structures was assessed. The only serious problems that appeared were foundations that were not anymore covered by soil. During the last years old constructions were replaced by modern steel snow retaining structures. In the year 2002 it is planed to replace about 700m of 50-year old relatively small structures with new 3.5m high snow retaining bridges, in particular because in the winters 1999 and 2000 some of the defence structures were completely covered by snow.

5.2.3.1.4 Avalanche hazard map of 1985 and 1991, respectively

For the Palüda area an avalanche hazard map was elaborated in the year 1985. In 1991 this map was officially approved and legalized by the government. A substantial basis for the elaboration of this hazard map was an expertise by the Swiss Federal Institute for Snow and Avalanche Research SLF provided in 1977. This expert report stated that although the protection measures were reinforced during the years 1963 – 1970, avalanches with a fracture depth of approximately 70cm (instead of 1.6m without of any protection measures) could potentially broke loose out of the middle part of the protected area. The run-out distance of such an avalanche was calculated to be able to cross the Upper Büschalp with a small velocity and to gain speed again in the steeper track below. The hazard zones in the map of 1985 were delineated based on these calculations (Figure 5.6).

5.2.3.1.5 Avalanche danger map of 1999

The avalanche hazard map of Davos was revised in 1999 (Figure 5.6). The result of the recent hazard evaluation is that in protected area at the east flank

of the Schiahorn no substantial avalanches can break loose due to the additional constructions between 1983 and 1987 and the ongoing replacement of old elements. Small avalanches out of the protected areas as well as small avalanches in the steep track below the Upper Büschalp were assumed as worst-case scenario. Because of its small sizes these avalanches were assumed to stop within the steeper parts of the slopes. No avalanche calculations were performed for these estimates.

Both, the red and the blue hazard zone were reduced remarkably. In the populated area the red and blue zones were replaced by a white zone (no hazard). In the technical report about the avalanche hazard zone the option to delineate the previously red and blue area as yellow zone as a reminder of the previous hazard assessment was mentioned. However, this option was dismissed in the final avalanche hazard map.

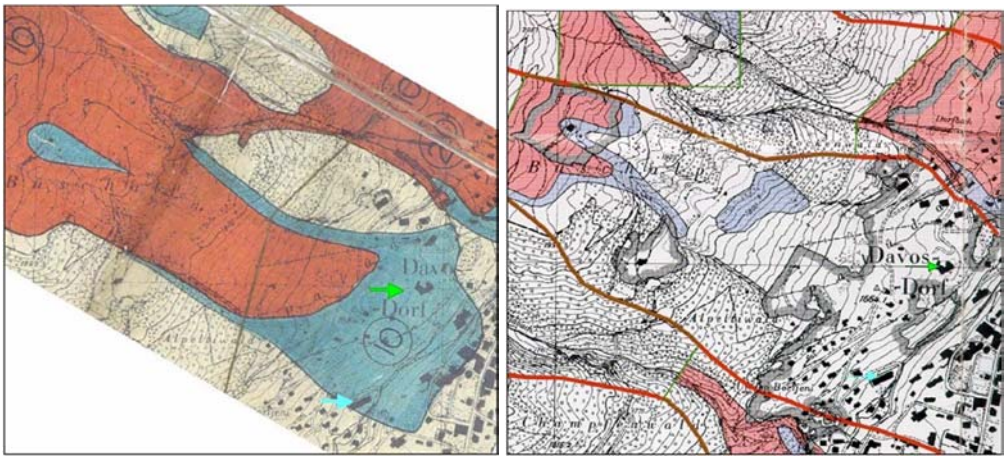

Figure 5.6: Avalanche hazard maps of 1985 and 1999, Palüda, Davos

5.2.3.1.6 Local zoning plan

In the local zoning plan of 1977 the whole red avalanche hazard area was excluded from any residential zone, i.e. the construction of any new building was prohibited. Most of the blue hazard zone became a residential zone “W2” with a small utilisation number of 0.25 which is appropriate to the hazard degree.

The local zoning plan was revised in 2001. The former red zone that was changed into white is still excluded. However, in the former blue zone – today likewise white – the utilisation number was increased remarkably by assigning from uphill to downhill the following zones: Village Boundary Zone II (utilisation number 0.35), Village Boundary Zone I (utilisation number 0.45), Residential Zone (utilisation number 0.85) and Centre Zone (utilisation number 1.25) (see Figure 5.7). In comparison to the previous plan of 1977 the utilisation has more than doubled. Estimates show that due to this increase of the utilisation also the price for one square meter doubled nearly.

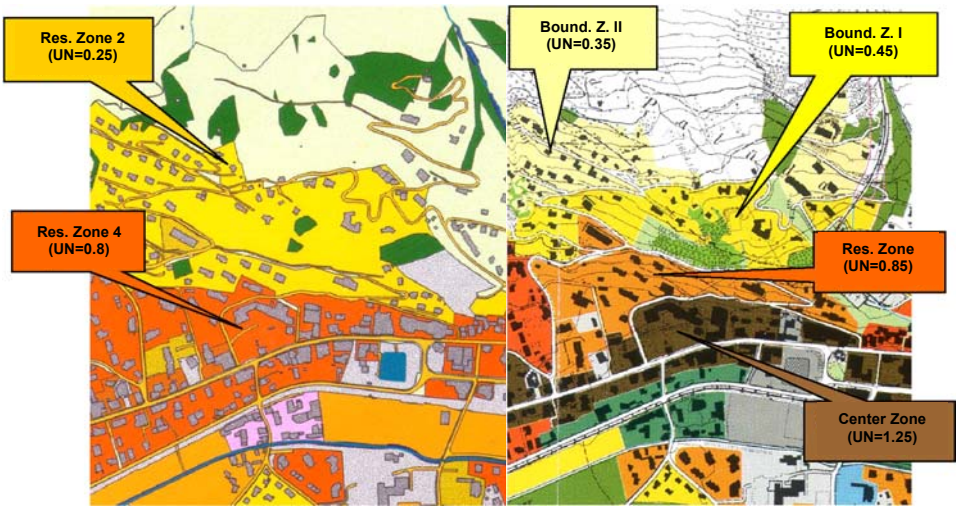

Figure 5.7: Local zoning plan Davos in the area of Palüda (1977 left and 2000 right)

5.2.3.1.7 Summarizing remarks

In the new hazard map as well as in the revised local zoning plan no references to the old hazard situation are present. Only in the technical report about the avalanche hazard map of 1999 the option is mentioned to consider the previously red and blue zone not as white but as yellow hazard zone.

The initial hazard situation without any protection measure is not present at all in the avalanche hazard map and also in the previous hazard map of 1985/91 considered already some effects of the protection structures.

In the technical report of the avalanche hazard map 1999 no specifications were made concerning that the hazard zones are only valid as long as the maintenance of the protection measures is granted.

The avalanche hazard map of 1999 basically assumes that the protection measures are preventing larger avalanches completely, i.e. that no large avalanche can start from above or within the protected area. In the winters 1999 and 2000 the protection measures were at some places completely filled but no large avalanche event took place.

Previously red area was not included in the local zoning plan. However, due to the fact that this former red zone is now white, there might be a possibility that in a future revision the former red zone will be completely forgotten and also included in the local zoning plan.

5.2.3.2 Eggigraben Avalanche, Wengen (BE)

5.2.3.2.1 Avalanche situation

The 39° steep and 1km broad release area of the Eggigraben avalanche is located at the western flank of the Männlichen mountain on an altitude between 2200m and 2000 m a.s.l. (Figure 5.8). In total the size of the release area is more than 40ha, but it is divided by remarkable ridges into 4 major subareas. Some of these subareas have also separated avalanche tracks. Thus, a simultaneous avalanche release out of the whole area can be considered as not frequent.
Below 1450 ma.s.l. the separated avalanche tracks were united before they reach the flat run-out area of Wengen. Wengen is situated on a flat terrain terrace (Wengiboden), high above the valley bottom of the Lauterbrunnen valley. The extreme snow depth in the release area is statistically determined to be about 300 cm.

5.2.3.2.2 Avalanche cadastre

Due to the fact that the Eggigraben avalanche is so close to the village of Wengen, the avalanche activity is very well documented. In 1770, an avalanche crossed the whole terrain terrace of Wengen causing 8 fatalities. In 1885, the avalanche reached the train station of Wengen. Further large avalanches were reported in 1895, 1914, 1931, 1944, 1954, 1968 and 1978. The return frequency of an avalanche that reaches the populated area is about 25 years.

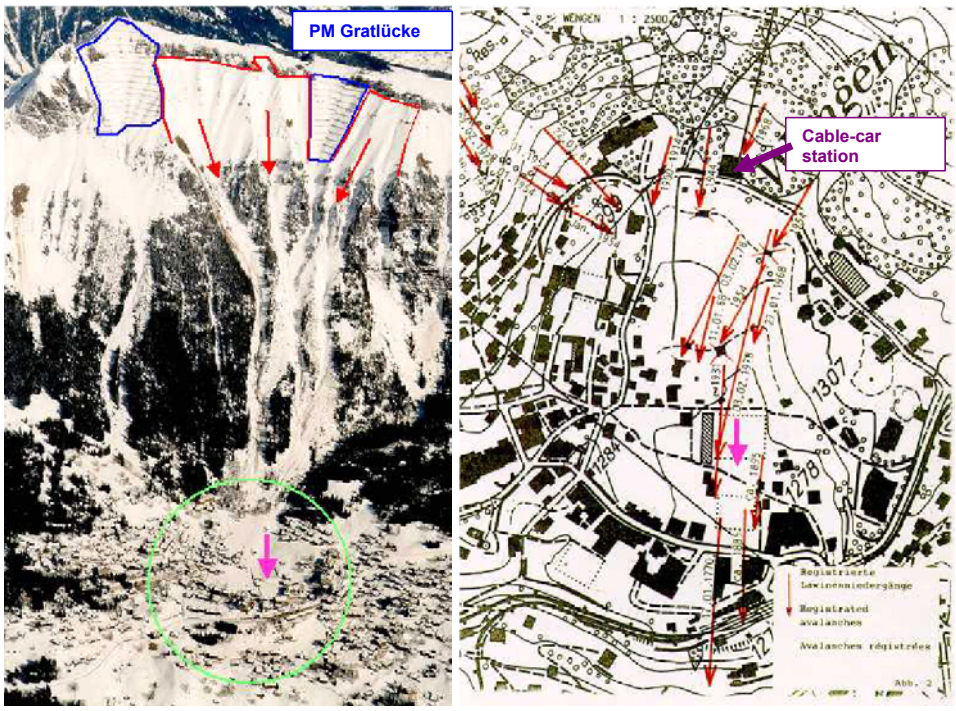

Figure 5.8: Left: Overview of the Eggigraben avalanche with the protection measure (PM) Gratlücke and the village centre of Wengen. Right: Avalanche cadastre of the Eggigraben avalanche.

5.2.3.2.3 Constructive protection measures

To cover the whole release area of the Eggigraben avalanche about 16 km of retaining structures would be necessary and the time of construction was estimated to about 30 years. To avoid this very high expenditures it was decided to protect only one subarea, named Gratlücke, that covers an area of 4 ha with 1870m of steel retaining bridges (construction period: 1979 – 1986, expenditures: 3.75 Mio CHF). The main goal of this protection structure was to ensure that the Eggigraben avalanche can not be released on the whole area simultaneously. In addition to the constructive protection measures forest was replanted in some locations.

The construction was built according to the official guidelines and proved to prevent larger snow movements. Even in the extreme winter of 1999 the snow retaining bridges were not filled to the top.

However, out of the remaining non protected subareas, larger avalanches were released in 1995 (stopped shortly before the cable-car station Wengen – Männlichen) and in 1999 an avalanche strongly damaged this cable-car station located in the red avalanche area. As consequence of the snow rich winters 1995 and 1999 some small damages were reported that did not at all influence the security provided by the measures.

5.2.3.2.4 Avalanche hazard map of 1974

The avalanche hazard map was elaborated based on the avalanche cadastre, field investigations and avalanche run-out calculations. The avalanche cadastre was considered as the most valuable basis. Avalanche calculations showed that it was not possible that an avalanche that is released only of one or two subareas is able to cross the whole terrain terrace of Wengen. It was assumed that the 1770 avalanche broke loose on the whole potential release area.

For the hazard map of 1974 it was assumed that a 300 year avalanche event can release simultaneously from 3 of 4 subareas on a width of approximately 550m and an area of 18ha. The existing buildings were considered as resisting forces in the avalanche calculations, leading to a reduction of the run-out distance of about 20%. The red zone reached the main street and the blue zone ended at the train station. Additionally the yellow zone was assigned to the whole area that was covered by the 1770 avalanche as a reminder that can result of an extreme large avalanche event. 20 buildings were situated in the red and 19 buildings in the blue zone.

5.2.3.2.5 Avalanche hazard map of 1991

Five years after the completion of the defence structure Gratlücke, the avalanche hazard map of Wengen was revised. Avalanche calculations were used in order to delineate the reduced avalanche hazard zones. The basic assumption was that the new protection measure will prevent an avalanche release out of more than two sub areas simultaneously. Therefore, the release area was reduced from 18ha to 10.5ha. The run-out distances were calculated to be approximately 130m shorter than in the hazard map of 1974. In Wengen, the previously red and blue areas were not converted directly into a white zone but into a yellow zone. In the technical report to the revised hazard map it was explicitly mentioned that the hazard zones are only valid if the protection measures are in good conditions. The authorities of Wengen agreed to maintain them sufficiently.

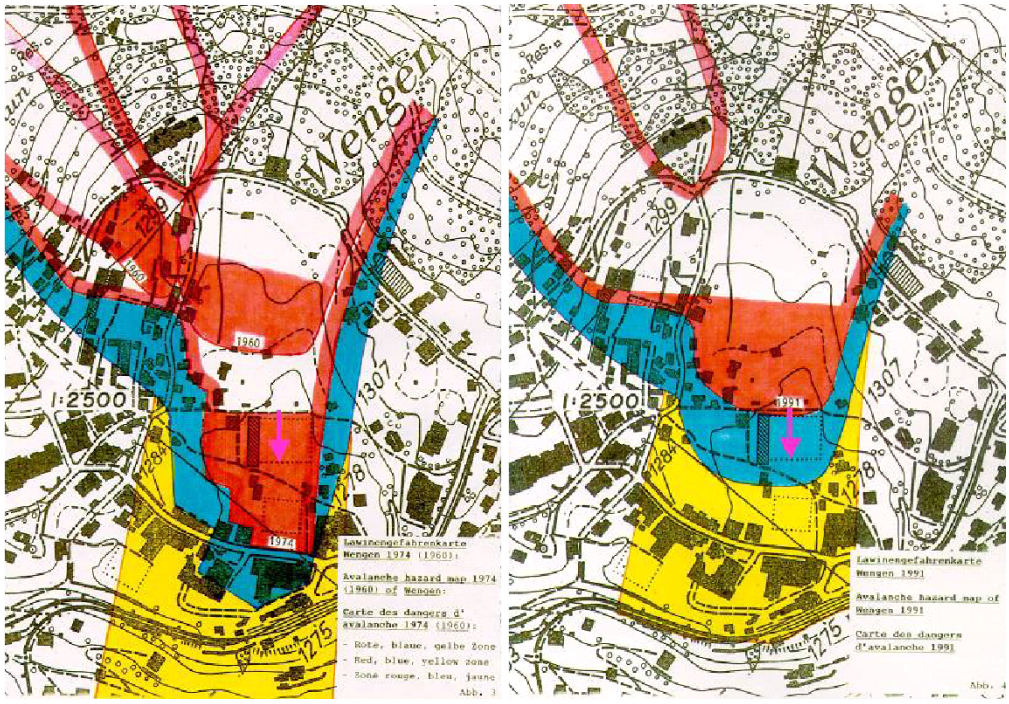

Figure 5.9: Avalanche hazard maps of Wengen of 1974 and 1991

5.2.3.2.6 Local plan/zone planning

In 1974 the red hazard zone was excluded, i.e. new buildings were prohibited. In the blue zone, for renovations and new buildings special reinforcement regulations applied. In the revision of the local zoning plan in 1996 the area covered by the red zone in the avalanche hazard map of 1974 remains unchanged, although the red and blue hazard zones were reduced in the revised avalanche hazard map.

5.2.3.2.7 Summarizing remarks

In the revised avalanche hazard map the former extents of the hazard areas are not shown.

Former red and blue zones were not turned directly into white zones but assigned as yellow hazard zones.

It was assumed that the protection measure is completely effective. Partly failures of the protection measures were studied but it turned out that they do not matter in comparison to the hazard of the remaining unprotected areas.
In the previously existing red area, no residential zone was assigned in the local zoning plan.

5.2.3.3 Conclusions

The two case studies reveal that guidelines should be focused on the following main questions:

- How should the effectiveness of a measure be evaluated?
- How to define reasonable scenarios for the remaining hazard situation?
- How to deal with the uncertainties involved with the avalanche calculation procedures?
- How to represent previous hazard situation before the protection measures took effect?
- How to ensure the permanent maintenance of the defence structures?
- What should be allowed as utilisation in the areas that were protected by the constructive measures?

6 RISK MANAGEMENT IN AVALANCHE HAZARD MAPPING

UG and SM

6.1 Introduction

Entering an endangered area bears risks but provides also opportunities. Risks can be damages or fatalities. Opportunities may be a fast traffic connection or a residential house on a place with a beautiful view or even the survival of a mountain community. This effect can be illustrated with the example of the village Andermatt, Canton Uri, Switzerland. In the beginning a small settlement was protected by a natural forest. The people liked to live and make business in Andermatt and therefore the village grew also into endangered areas. These areas had to be protected by expensive constructive protection measures in order that the people can live safely in the extended areas. In the past, it was obviously the political decision that these protection measures had to be built. The benefit of entering into the new areas was considered to be higher than the costs that were caused by the construction of these measures. Today, another expansion of the protection measures is discussed as shown in the Fig. 1. The question is again, whether or not it is still reasonable to extend the defence structures to gain new residential areas.

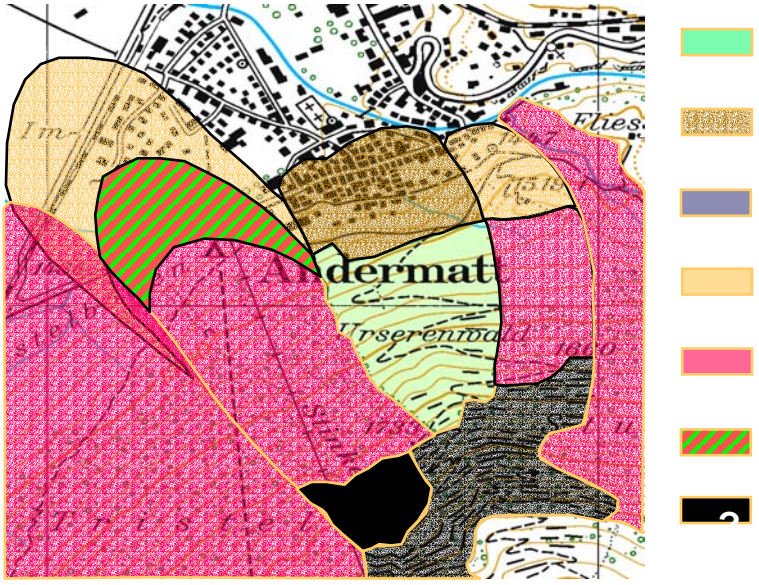

Figure 6.1: Example Andermatt, Canton Uri, Switzerland: Existing protection measures and their contribution to protect settled areas as well as projected defence structures.

It is the main goal of this Section to provide tools to answer these kind of questions. In order to better understand the structure of this section it is useful

to take a look at the general risk management process circle in Figure 6.2. In adoption of this general risk management circle the four main sections are: risk analysis, risk assessment, study of measure possibilities and the cost-effectiveness assessment. At the end of the section a case study is presented.

6.2 Risk management

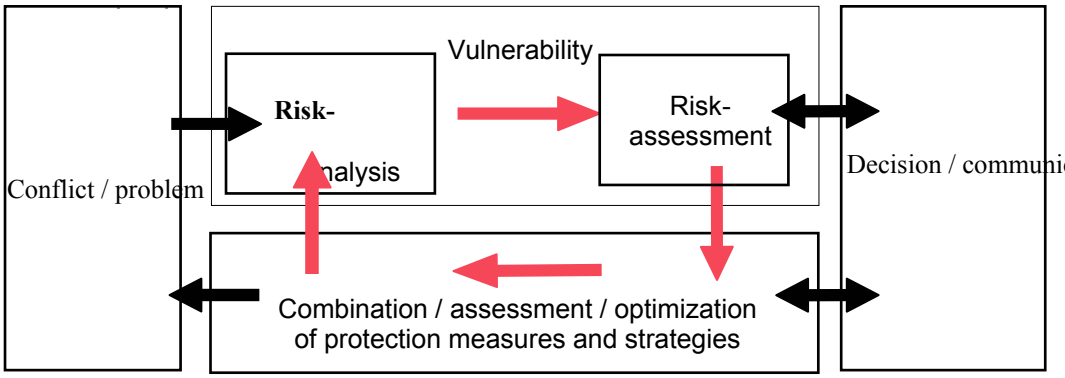

Figure 6.2: General risk management circle.

At the beginning of every risk management process, the *conflict or the problem* has to be identified and clearly defined. In the second step, the *risk analysis*, the following basic questions have to be answered with respect to an avalanche hazard problem have to be answered: What is the frequency and intensity of a hazardous process? How many persons might be killed? What is expected to be destroyed/damaged?

The *risk assessment* is focussed on the following questions: How does the worst case scenario look like? Are individual persons or the public willing or able to accept the damages or even fatalities?

The *study of measure possibilities* tries to the questions: What possibilities do we have to reduce the risk? How does a measure exactly reduce the risk? What are the costs of these measures?

Finally, the *cost-effectiveness assessment* is focused on the key-question what measure or what combination of measures are the most cost-effective one. The cost-effectiveness assessment provides the tool to make a decision and to communicate and explain the reasons for this decision.

6.2.1 Risk analysis

With the risk analysis the interaction of the natural hazards with the land use of human beings are investigated and quantified using scientific based methods. First of all the term “risk” needs to be defined. Several definitions of risk exist.

For the purpose of this section the definition R = P(i) * D(i) is used, where P(i) is the probability of an incident and D(i) is the damage amount caused by that incident.

The risk analysis can be divided into the following steps:

(1) The hazard analysis is used to determine the frequency, intensity of the hazardous process. The intensity includes both, the impact that a process can have as well as the delineation of the area that is affected by the hazard.
(2) Within the damage potential evaluation the severity of an incident is determined by summarising all the values and people that might be present within the endangered area. In addition to the counting of values in the endangered area, the sensitivity of objects to the hazard is also important to estimate the overall damage of an event appropriately.
(3) Finally, risk calculation methods are used to express the relation between the hazard and damage potential in numbers.

Most of the preceding sections of workpackage 1 are dealing with the hazard analysis, i.e. how to estimate impact and frequency of an avalanche hazard and how to delineate hazard maps. Therefore the hazard analysis will not be discussed here.

The damage that can be caused by a hazardous event depends mainly on the presence of an object in the endangered area and its vulnerability against the event.
The probability of presence of stationary objects like buildings is given. For individual persons living in endangered areas, average values of presence time for external working (60%) and not external working persons (90%) can be roughly estimated.

The risk calculation combines the hazard analysis and the damage potential evaluation in order to complete the risk analysis. The risk can be calculated for individuals as well as collectively using equations 1-4 for settlement areas. Note, that in some of the equations 1-4 also elements of the risk assessment are already implemented. These elements will be explained in more detail in the next section.

Basic risk equation: $R = P(H) * P(O) * P(D) * V_O$ [*] (6.1)
Objects in general: $R = P(H) * P(O) * f(D_H, S_O) * V_O$ [*] (6.2)
Individual objects: $r_{ij} = P(H_j) * P(O_i) * f(D_{Hj}, S_{Oi}) * P(D_i) * V_{oi}$ [**](6.3)

Collective risk: $$R_{tot} = \sum_{i=1}^{n} \sum_{j=1}^{m} r_{ij}$$ [*] (6.4)

Parameter and unit descriptions:

R = risk
P(H) = probability of hazard [1/year]
P(O) = probability of object presence
P(D) = probability of damage
VO = risk assessment value or damage potential [e.g. CHF]
DH = hazard intensity [kN/m^2]
SO = sensitivity of object to damage
r_{ij} = individual risk of an object
i = 1,2,3……n object
j = 1,2,3,…..m hazard events
R_{tot} = collective risk
[*] = unit: e.g. CHF/year
[**] = unit: 1/year

Based on these equations, tables for different purposes can be calculated as shown in Table 1 of the individual risk of death for persons in buildings. The start of the red zone corresponds to the frequency of a 5 year avalanche. In Table 6.1 the class "Not enforced" summarize every category (incl. concrete constr.) that has no specific avalanche enforcement. In the red zone, f(DHj ,SOk) is considered to be 1. The average presence of people P(Oi) is estimated to 0.75. The average value for fatalities P(Di) is assumed to be 0.46. In the blue zone, the P(Di) of objects is assumed as following: Light constr. = 1; Chalets = 0.3; Brikwork = 0.03 and concrete constructions = 0.

Table 6.1: Individual risk of death for persons in buildings

Description of position		Ind. risk of being killed	
Hazard Area	Building type	T = 1 year	T = 70 years
Start of red	Not enforced	0.055	0.98
Center of red	Not enforced	0.028	0.86
End of red	Not enforced	0.0091	0.47
Start of blue	Chalet	0.0017	0.11
Center of blue	Light const.	0.0022	0.14
Center of blue	Chalet	0.00067	0.046
Center of blue	Concret const.	0	0
End of blue	Chalet	0.00016	0.011

Since risk calculations have to be made for various scenarios , the risk is not one single value, but a function of the probability of every scenario. Therefore, an illustrative way to express the risk is the probability-damage amount diagram, that can be used for settled areas as well as for traffic roads (Figure 6.3).

Note that for the probability of the damage not only the run-out distance of the scenario has to be considered but also the area that is covered by the hazard.

The statistical damage expectation value per year is corresponding to the area below the connecting lines of the scenarios. This line can also be approximated by a function Pi = f(Di). With this function, the area can be integrated as

$$R = \frac{1}{n}\sum_{i=1}^{n} P_i \cdot D_i$$

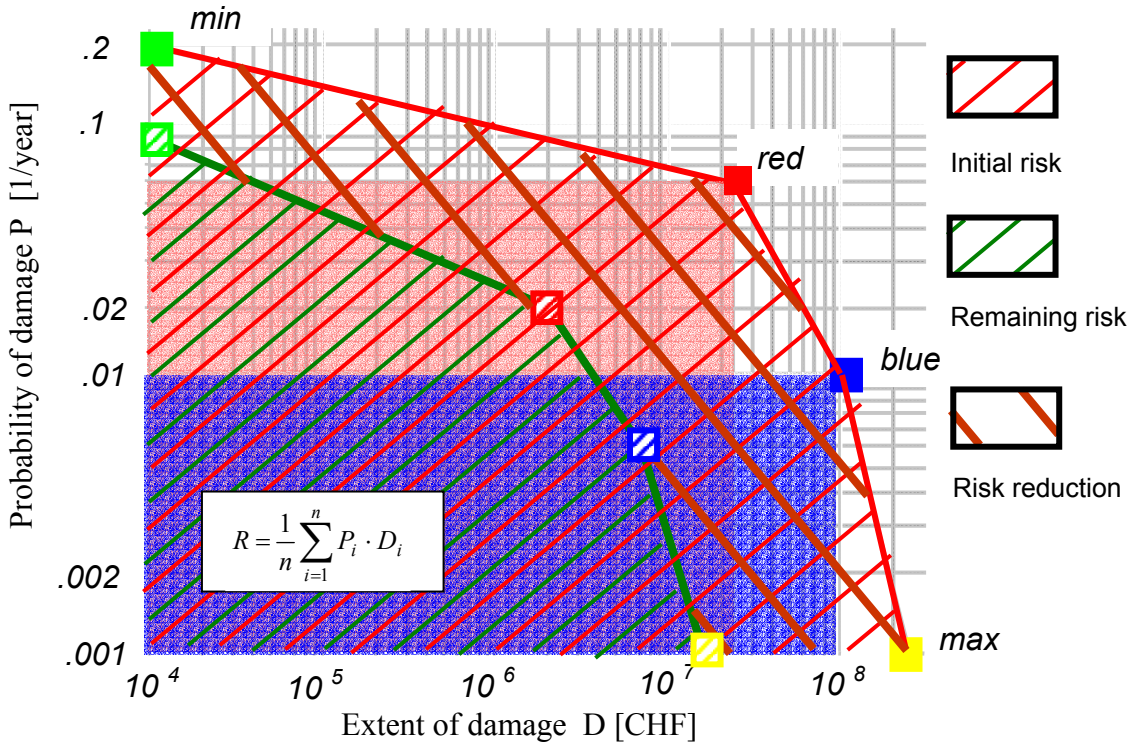

Figure 6.3: Probability-damage amount diagram (modified after(Wilhelm 1997))

6.2.2 Risk assessment

The risk assessment is focused on values and objectives of the society. Therefore, the results of the risk analysis step have to be put into relation with aspects of chances and benefits as well as with the individual and collective risk perception / behaviour of the society.

For this purpose, the spatial and temporal specification of a system size is mandatory in order to assess a worst-case scenario. The assessment of the risk can be performed either hazard- or economy-oriented. The difference between these two perspectives can be illustrated using an example about an initiative to hold open the road crossing the Lukmanier Pass during winter time. This road used to be closed during the winter season. However, since the tourism in the ski resort of Disentis is in hard competition to ski resort of Andermatt (with direct connections to the south via the Gotthard tunnel as well as to the central part of Switzerland) and Flims (more close to Zurich than Disentis) there is a strong demand to open the road also during winter time in order to enable a short access to Disentis from the south. The hazard oriented avalanche system definition focuses on the avalanche risk (92 avalanche paths, 25km road, 1000 vehicles per day), the costs for measures (construction work, cost of closure days) and the effectiveness of the measures (risk reduction). However, the related assessment of cost-effectiveness in this system might be too narrow, since the political decision will also include the economy-oriented system point of view. With this perspective, the mobility and cash flow objectives in order to increase the competitiveness may lead to a completely different cost-effectiveness and consequently to different worst case scenario. Therefore, it is very important to define a system boundary that reflects the situation appropriately.

The risk assessment has to take also into consideration psychological effects like aversion i.e. the over proportional weight of risks with a big damage potential. Human behaviour reveals that the perception of risk is not linearly. One event with 7 fatalities is considered to be a higher risk than 7 incidents with only 1 fatality although the naked risk numbers are the same. In general, risks with a big damage potential and a low damage probability are less accepted than risks with a low damage potential and a frequent damage probability – even when the naked numbers of the risk are equal. Wilhelm (1997) analysed the aversion for settlement areas as well as for traffic roads using all historical data of the avalanche accidents in Switzerland that happened between 1946 and 1993 in the respective areas. He found the aversion factors δ that are listed in Table 6.2.

Table 6.2: Aversion factors δ for settlement areas and for railways and traffic roads (λ=lethality, β= average number of persons in a car).

Area	Description	DC1	DC2	DC3	DC4
Railways Traffic roads	$D = \lambda * \beta$	$D_i \leq 3$	$3 < D_i \leq 8$	$9 < D_i \leq 16$	$D > 16$
	Aversion δ	1	3	7	15
Settlement areas	Fatalities F	$F_i \leq 3$	$3 < F_i \leq 9$	$10 < F_i \leq 19$	$F > 20$
	Aversion δ	1	2	4	8

However, a sensitivity analysis of the contribution of these factors reveals that it should be applied only very carefully within the risk assessment, since this factor has a tremendous influence with respect to the cost-effectiveness. Until new research results confirm these aversion factors, they should not be applied for the assessment of measure project in settlement areas. This could result in an overestimation of the initial risk and consequently in a too high risk reduction and a too high benefit of the measure.

The question of what risk is acceptable on an individual scale is another important topic of the risk assessment, that influences political decisions. On a pure individual level, to be killed by a hazard is not acceptable, i.e. a person would pay "unlimited" costs to avoid this event. However, the acceptance of risk can be estimated indirectly by reviewing the decisions that have been taken historically in order to reduce individual risks. The risk of dying at the age of 10 to 15 (lowest risk age) is about 10-4. Postulating that the risk of natural hazard should be not more than 1% of this general individual risk, the acceptable rate would be about 10-6. This value corresponds very well with findings on other topics, where the acceptable risk for people that are not voluntarily in a risky situation is considered to be 10-5 to 10-6. For situations where people are well aware of the increased risk and exposed themselves completely voluntarily to the risk (like for example climbing an active volcano or backcountry skiing), individual risks acceptance levels of up to 10-2 were found based on observed risk situations.

6.2.3 Measure analysis

The protection measures can be structured principally according to the duration of their effect into permanent or temporary measures and to the type of intervention into active (i.e. influence actively the occurrence / non-occurrence of avalanches) or passive (i.e. avoid to be present in the endangered area) measures. To evaluate the most appropriate measure for a particular situation, an analysis of the effects for every measure has to be performed. Taking measures in a risk situation will have effects, but in most cases not all the risk can be reduced. Therefore, it is necessary to study carefully these effects. Figure 6.4 shows a general scheme for the effect analysis, which clearly reveals that not only the avalanche related effects has to be considered, but also the socio-economic and cultural consequences of the measures. The protective effect of a retaining structure in a release area is for example related to material and immaterial goods. Houses can remain at their place, a new street can be built (material reasons), people remain in a village because they feel save (immaterial). Also negative effects of retaining structures, i.e. the impact on the landscape aesthetic, have to be considered. The value of these effects has to be assessed in relation to economic value of this land use improvement.

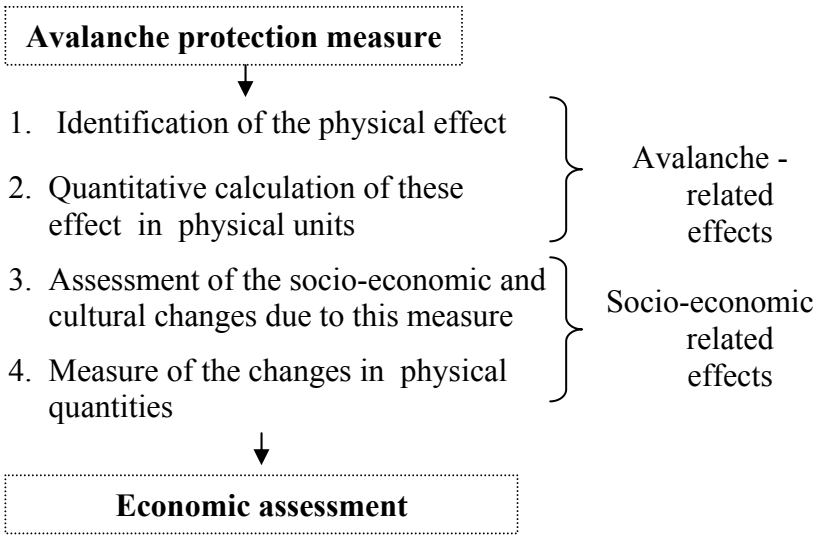

Figure 6.4: A general scheme for the effect analysis

Every measure has positive (benefit) and negative effects (costs). The benefit corresponds to the risk reduction. We will see later how this can be related to the costs. The most important figures to calculate the *costs* are:

I_0 Investment costs: Either the overall total at the time t0 (cost estimate) or considered as construction costs Cc during the construction period. [€]
C_c Construction costs: Operating costs during the construction period [€/year]
C_m Maintenance costs, regularly – not varying much [€/year]
C_r costs of repair, irregularly – varying quite much [€/year]
V_n Value at the end of the life period of the construction. This value might be positive (benefit for a replacement construction) or negative (costs of disposal) [€]
P Interest rate [%]

The annual costs are calculated using the equation:

$$C_a = C_c + C_m + C_r + \frac{(I_0 - V_n)}{n} + \frac{(I_0 - V_n)}{2}\frac{p}{100}$$

Not all the effects of avalanche protection measures can be calculated using monetary costs. Ecological costs as for example the change of the landscape by technical measures (retaining structures etc.) can not be calculated reasonably with money.

Usually, the most successful strategy is not one single measure alone, but a *combination of measures*. However, often some measures are redundant. For the estimation of the redundancy, it is useful to distinguish between measures

that affect only a small part of the system (selective measures) and others that influence the whole system (general measures). An avalanche gallery is an example for a selective measure, since it is able to protect the road only on the length where it is constructed. Instead a road closure is protecting the whole road and therefore will also protect the area of the gallery during the time period of the closure. For the cost-effectiveness calculations, this redundancy has to be taken into account. For a more detailed procedure to consider the effects of redundancy refer to (Wilhelm 1999 p. 90ff.).

The final goal of this analysis of the measure possibilities is to gather all the necessary information in order to be able to decide afterwards which measures should be chosen from a cost-effectiveness point of view.

6.2.4 Project evaluation

All the previously described steps are the basis for the decision whether or not a measure or a combination of measures is reasonable to implement. From an economic perspective, a protection measure can be seen as an investment. Staehlin (cited in Wilhelm 1997) provided the following definition of investment: “Under investment all the measures are understood that spend money to provide a tool in order to be able to either increase profit or reduce expenditures in future”. Protection measures are exactly fitting to this definition, since their initial expenditures are aimed to reduce either the damages to human lives and goods or to enable to raise more profit than it would have been possible without measures. Note that investments can be made into goods but also into human resources (avalanche education, bulletin) as well as research (avalanche bulletin improvement).

Generally, every project evaluation method should provide a tool to help to make a decision. Therefore, an effect analysis and a clearly defined decision criteria (e.g. cost-benefit ration, maximum benefit value, minimum effectiveness) are mandatory for every method. The differences between the methods are laying within the assessment criteria, i.e. how the transformation of project effects are assessed (monetarily or not).

For the understanding of these differences, it is necessary to be aware of the differences between effectiveness and efficiency. Efficiency is defined as the best ratio between input and output. This ratio can be maximized following the principle of the lowest input (safe-money principle) or if a certain input is provided to maximize the output. Effectiveness on the other hand is describing, whether or not measures are suited to their goal. Effectiveness is usually measured in percentage of the goal fulfilling of the measure. Effective measures need not to be also efficient and vice versa. A protective forest in a release area is for example very effective but due to the fact of the high costs of maintenance it is not necessarily efficient.

Based on this considerations, we present in the following paragraphs two different approaches for the project evaluation:
the cost-benefit analysis (CBA) and the cost-effectiveness analysis (CEA).

The cost-benefit analysis (CBA) aims to convert the effects of measures into money in order to have a purely economic cost-benefit decision criteria. In economy a project evaluation among different competing projects is based on the ratio between the expected benefits and costs, both expressed in terms of money. The project with the best ratio will be implemented pretending the benefit to be higher than the costs (see cost-benefit diagram below). In other words, the CBA is primarily based on efficiency.
The CBA provides a flexible tool to assess the whole spectrum of the effects of protection measures in the context of the overall economic system. In Switzerland this is useful, since the costs for avalanche protection measures are mostly paid by other authorities (cantons, federation) than the ones that profit from the benefits (regions, communities).
The crucial point of this analysis is the monetarily assessment of the benefits. It is very important to disclose all the assumptions and procedures involved in this process, because it is quite easy to influence the related transfer functions and the choice of indicators consciously or unconsciously. However, since the predominate objective of the measures is to avoid damages, it is possible to use partly (except for fatalities) approximated market prices.
Another deficiency of the CBA is related to its focus on efficiency. Based on the CBA, it is possible that a measure that is most efficient, but only of second priority, is chosen instead of a less efficient but first priority measure (sub optimal).

The cost-effectiveness analysis (CEA) establish a system based on clearly defined rules to compare the monetarily measured costs directly to the non-monetarily expressed effectiveness of a measures. The costs are estimated identically to the CBA on a monetarily basis. However, the benefits are analysed with respect to the objectives of the measure. Often the scale of percentages is used to express the achieved benefits by a method. It is also possible to introduce weights in order to support more relevant parts of the effects of a measure. The results can be presented in form of x-y-diagrams. The different units on both axis do not permit a direct comparison between costs and benefits but only a relative comparison among competing projects. In a simplified version of the CEA, it is also possible to compare only the costs to the effects, i.e. costs on one axis and the risk reduction on the other. However, this diagram (Fig. 5) gives no judgement about whether or not the effect is to be considered as sufficient in comparison to the objectives of a measure. The CEA has proofed to be a valuable tool in practice. The results are especially valid with respect to the technical productivity of a measure. But as within the CBA, the assessment criteria have to be disclosed to be as objective as possible.

In both approaches it is necessary to make the benefit of the risk reduction of measures somehow comparable to their costs. Therefore, special methods to quantify the benefits of measures are mandatory. The most suited method for the assessment of the benefits for avalanche protection measures with respect to a cost-benefit analysis is the damage cost method. This method is very valuable for all possibly damaged goods or services that can be related to a monetarily value, but it is less easy to apply when the damage concerns non-material values like “fear” or “image of a tourism resort”. Since the principle of the damage method is to calculate the costs to repair a damage, it is also not well suited to assess an irreversible damage. The damage cost method postulates the benefit of a good or of a service to be at least in minimum as high as the costs for the reparation of the damages. The underlying assumption is that the status-quo was optimal. The benefits were calculated based on either the effectively happened damages (ex post) or the probability that a damage might happen. For the damage cost method a risk analysis is mandatory in order to provide the probability of a damage. In addition, a definition of a time period is necessary. With this two elements it is possible to monetarily assess the “saved” damage costs in comparison to a situation without protection measures. Insurance values are well suited to assess buildings. Costs for household effects and infrastructure can be estimated to a percentage of the building value.

The other well suited method, which is especially useful to assess the cost of one reduced fatality within the cost-effectiveness method, is the marginal cost method. Under marginal costs, the cost associated with one additional unit of production are understood. In a cost function graph, the marginal costs can be displayed as the tangent of the cost function.

In the context of protection measures this means that the additional costs have to be paid to increase the risk reduction through an additional protection measure (=unit of production). If an additional measure is very expensive and contributes only to a small increase of risk reduction, the marginal costs of this measure is high and vice versa.
The marginal cost method is based on the willingness of the society in the past to pay for a risk reduction. The idea of this approach is to assess the marginal costs (MC) for a risk reduction that the society was willing to pay based on a review of already established projects. Most often the risk reduction unit is expressed in terms of the number of “saved” statistical fatalities. The marginal costs that were paid in the past is used to assess the benefit of new projects.

The cost functions for about 100 established and not established projects in the Figure 6.5 shows that in the past the average costs (AC) for the reduction of one fatality per year is about 10 Mio CHF. The marginal costs of existing projects are increasing from a minimum of less than 10’000 CHF up to a maximum of 140 Mio CHF. The latter seems to be far beyond a reasonable value. Based on the analysis of such kind of marginal cost assessments, several assessment strategies for future projects are possible, i.e.

Strategy A: In future, only projects with MC less than 5 Mio CHF should be granted. This strategy is useful for a first rough evaluation of projects that are really necessary.

Strategy B: Only projects should be granted that have AC of less than 5 Mio CHF, which is half of the value for the past established projects.

Strategy C: Only projects should be granted that have MC of less than 10 Mio CHF. With this strategy, in the past only about half of the projects would have been granted.

Strategy D: Only projects should be granted that have MC of less than 20 Mio CHF.

Strategy E: The AC of the projects should not exceed the AC of the established projects of 10 Mio CHF. With this strategy, no improvements would be achieved in comparison to the past.

Which strategy should be chosen is a political decision.

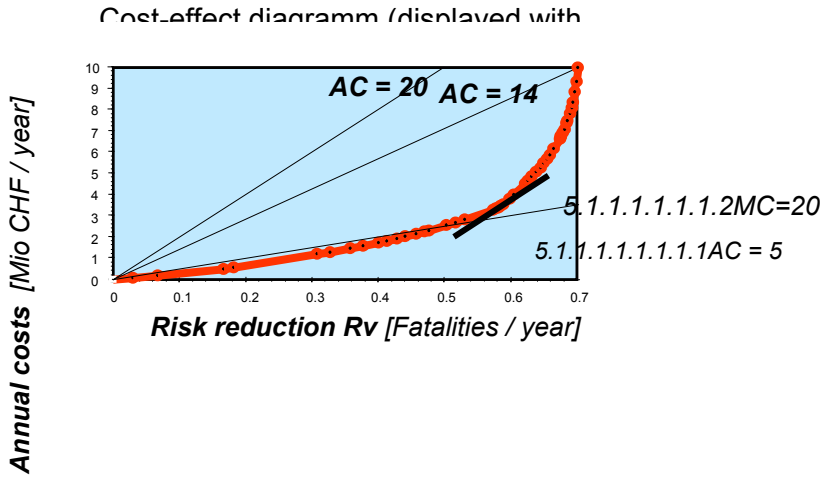

Figure 6.5: Cost-effect diagram (MC: Marginal Costs, AC: Average Costs)

Another approach to assess the value of one fatality would be the human capital approach. This approach aims to calculate the damage as the loss of income that the person who died would have been able to earn during the remaining time of his life. For this calculation an average age and salary of all fatalities were used. In Switzerland such calculations result in an amount of 1'164'000 Mio SFr., which is about a factor 9 less than the marginal cost approach. This value seems to be too small with respect to the historical willingness to pay for a fatality.

There are a lot of other methods available, but either they are too time consuming for a practical application or the necessary data for the method is usually not available. Wilhelm (1997) gives a good introduction over many more approaches and place them into a larger context of assessment methods.

Since the financial resources are usually limited, it is not possible to implement all measures that are contributing to a risk reduction. Hence, normally an optimisation of costs and benefits under the conditions of limited financial resources is required.

6.3 Case study: Damage cost method to assess the benefits of the retaining structure measures at the Schiahorn, Davos

6.3.1 Introduction

In order to illustrate some aspects of the theory outlined in the previous section, a case study in the area of Davos is given. The damage cost method can be illustrated using the well documented case of the defence structure measures at the Schiahorn. Based on the knowledge of the avalanche history, of the amount of defence structures and of the property value in the settlement, it is possible to assess the cost-benefit analysis for this protection measure and to show the critical points of such an assessment.

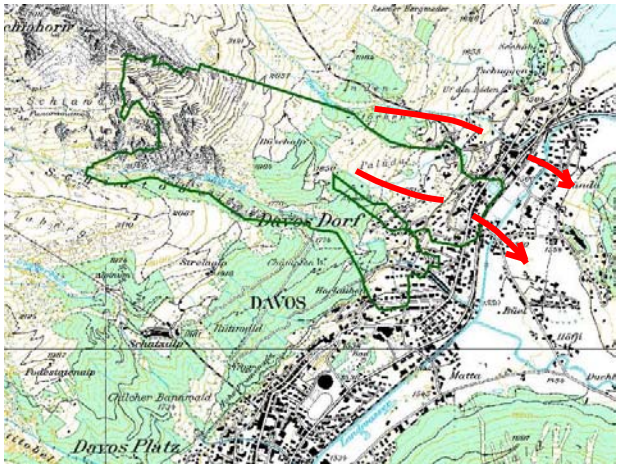

Figure 6.6: Overview over the two main avalanche paths in the case study Schiahorn, Davos

6.3.2 Avalanche history

Since 1802 larger avalanche events were documented in this avalanche track. The largest event in the last two centuries took place 1817. Then, the avalanche crossed the flat valley bottom on a length of approximately 300m before coming to rest. Then, almost no building was existent in the run-out area of the avalanche. Today, this area in the valley bottom is completely covered by buildings. On 23 December 1919, again a very large avalanche broke loose.

Although the run-out distance was 150m shorter than the one of the 1817 avalanche, it caused two fatalities and large damages. As a consequence of this event, the construction of retaining structures in the release area at the Schiahorn mountain started. Further large events took place in 1935 (only Schiatobel) 1950, 1951, 1954, 1962 (only Schiatobel) and 1968, however, their extents were significantly smaller.

6.3.3 Protection measures

The protection measures at the Schiahorn started in 1919 with the construction of stonewalls in order to form flat terraces. Starting from 1940 steel racks made of railway rails and Larch wood were built. In the 1960's the protection measure were complemented by modern steel retaining bridges. Table 6.3 gives an overview about the existing constructive measures in the release area:

Table 6.3: Constructive protection measures Schiahorn

Type of work	Year of construction	Length
Wall terraces	1921-1931	3638m
Snow rack	starting from 1945	856m
Snow fences	starting from 1945	360m
Voest Alpine snow bridges (Height 3.0m and 3.5m)	1963-1970	3482m
Fromm Snow bridges (Height 3.0m and 3.5m)	1983-1987	826m

The defence structures, built between 1963 – 1970 and 1983 – 1987 are the core element of this construction. They cover an area of approximately 16ha. The costs of this construction can be estimated as following, using typical cost estimates for Switzerland:

Investment costs: typical number for Switzerland: 1 Mio Sfr per ha → 16 Mio Sfr.
Maintenance costs per year: 0.5% of Investment costs: 80’000 Sfr/year
Repair costs per year: 0.5% of Investment costs: 80’000 Sfr/year

Assuming a life-time for the constructions of about 50 years, this results in yearly costs of about half a million Sfr per year (320’000 + 80’000 + 80’000 Sfr = 480’000 Sfr.).

6.3.4 Worst case scenario definition

For the purpose of this example, we assume a strictly hazard-oriented approach and neglect for example the fact that frequent avalanche accidents in Davos would also erode the tourism significantly and would also influence the decision whether or not to build defence structures.

The event in 1919 was used as basis for the worst case scenario, since then already houses were available that influenced the avalanche. Using the two-dimensional numerical simulation model AVAL-2D for dense snow avalanches (Gruber, 1998), this event has been back-calculated in order to obtain an equivalent avalanche run-out distance scenario not only at the Palüda site where the avalanche happened, but also in the Schiatobel. Today's scenario is reflected by the new avalanche hazard map that was elaborated in 1999. In Figure 6.7 the two scenarios used in this case study are shown.

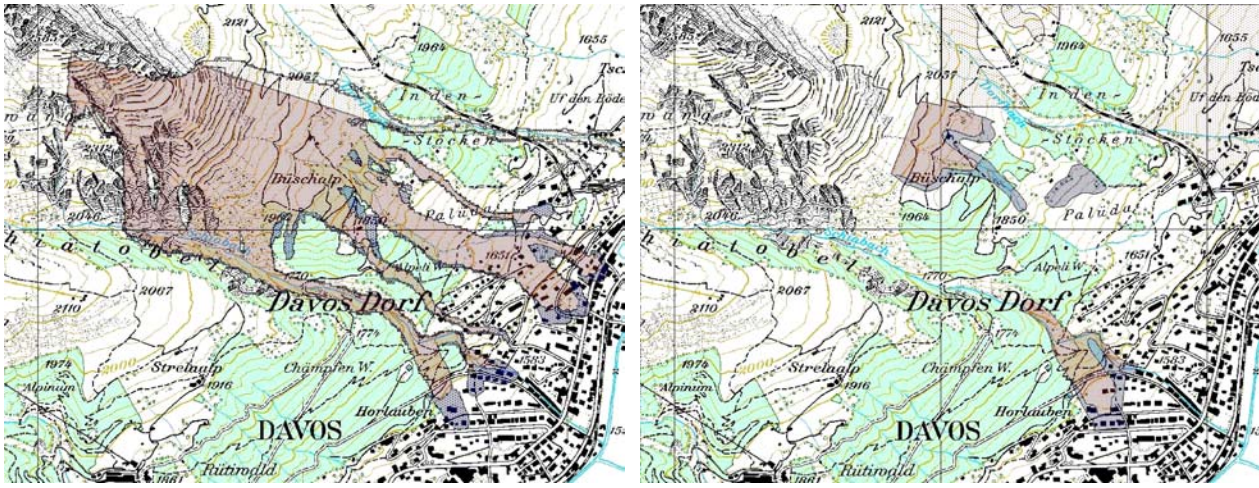

Figure 6.7: Left side: Worst-case scenario without avalanche defence structures, similar to the 1919-avalanche event. Right side: Avalanche hazard map 1999: Worst-case scenario with avalanche defence structures.

6.3.5 Collecting the damage potential in the endangered area

For the identification of the objects, the Geographic Information System (GIS) of the community of Davos was used. In this system all objects are stored digitally. In addition to the data of this Information System data was gathered by in loco investigations. In table 4 the attributes of the objects that were used for the calculation of the damage costs are listed. The building type is necessary to calculate the individual risk (see Table 6.1) as well as to estimate the value of the house.

6.3.5.1.1.1.1Adress	Street, number
Building class/type	BC 1 = Light construction BC 2 = Chalet-type BC 3 = Brickwork BC 4 = Concrete construction BC 5 = Concrete construction, reinforced
Size of the house Size of hotel, pension	Number of apartments Number of beds
Existence of avalanche side windows (a.s.w.)	Yes/no
Remarks and Specialities	

Table 6.4: Collected attributes of the objects. BC = Building Class.

For these categories average insurance values are available (Table 6.5). Using these values it is possible to calculate the number of persons living in the endangered area (Figure 6.8, Table 6.6) and the damage potential of all objects and persons. In Table 6 the value of one person is assumed according to the marginal cost approach for the past willingness to pay: 10 Mio. Sfr.. This value leads to a very high total damage potential of several milliards (US: billions) of SFr. Using the human capital approach of 1.165 Mio SFr. the total damage amount would be significantly smaller.

Table 5: Value assessment for objects and people per measurement unit (MU) and probability of presence.

Object	Measurement Unit (MU)	Value per MU	Number of persons per MU	Probability of presence of a person
One-Family-House	House	SFr. 590'000	2.4	68%
Several-Family-House	Appartement	SFr. 330'000	2.4	68%
Hotel	Bed	Depends on class*	0.6	68%
Business house small	Business	SFr. 1'400'000	3	31%
Business house big	Business	SFr. 2'800'000	6	31%
Restaurant	Restaurant	SFr. 830'000	20	43%
Barn small	Barn	SFr. 20'000	Negligible	-
Barn big	Barn	SFr. 80'000	Negligible	-
Garage	Garage	SFr. 20'000	Negligible	-
Household inventory	House	0.24 * val. of house	-	-
Infrastructure	House	0.15 * val. of house	-	-
Economics	House	0.10 * val. of house	-	-
Agriculture	Area [a]	SFr. 0	Negligible	-
Forest, Prot. Forest	Area [a]	SFr. 370	Negligible	-

*) The value of the hotel depends on the hotel class (usually given by stars)

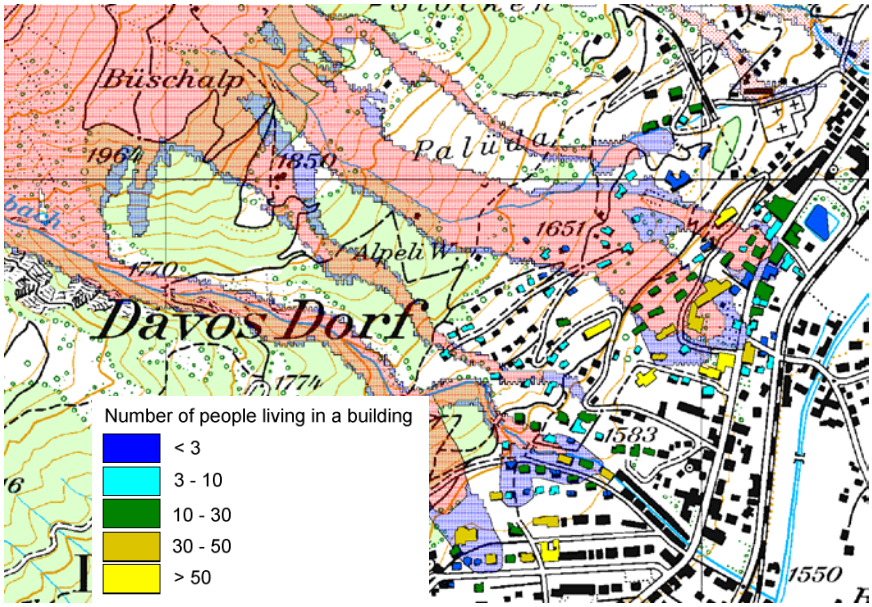

Figure 6.8: Number of persons living in the endangered areas (modified after Staub and John 2001)

Table 6.6: Damage potential V_0 differentiated according to the hazard zones.

	Number of people		Damage potential of objects [Mio. SFr.]		Total damage potential [Mio. SFr.] (1 fatality = 10 Mio. SFr.)	
	Red Zone	**Blue Zone**	**Red Zone**	**Blue Zone**	**Red Zone**	**Blue Zone**
Scenario without Constr.	549	369	163	116	5660	3817
Scenario with Constr.	56	188	6	56	570	1937

In Figure 6.9 the damage potential per avalanche track is visualised. In the area of Palüda, the damage potential is completely reduced, whereas in the area of Schiatobel and Horlauben, the damage potential is only reduced by approximately one third.

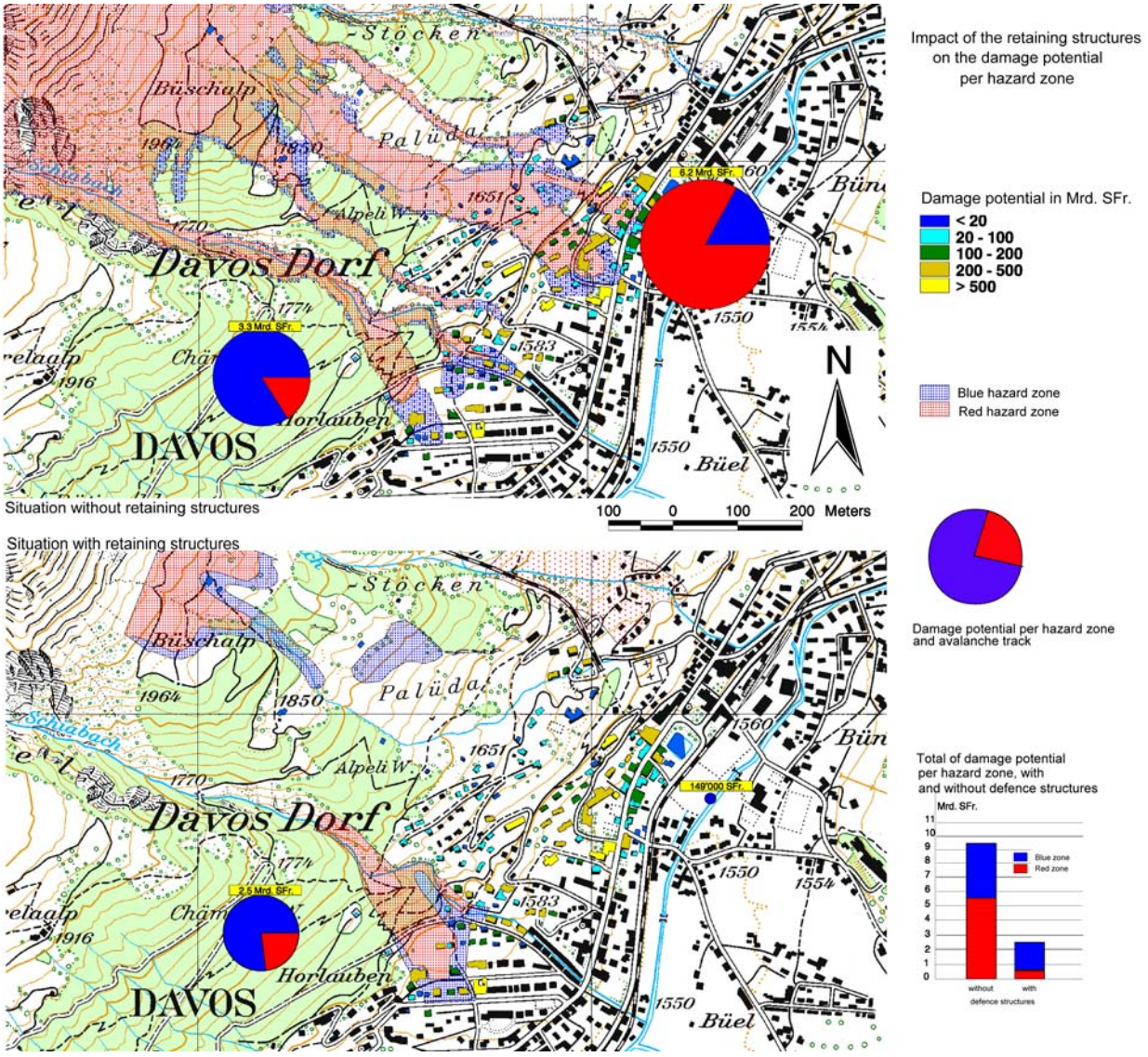

Figure 6.9: Impact of the retaining structures on the damage potential per hazard zone and avalanche track (modified after Staub and John 2001).

6.3.6 Risk calculations

For the assessment of the risk the damages sensitivity, the probability of presence and the probability of an event has to be assessed according to the general equations 6.1-6.4.

The risk Ri is calculated using the damage probability P(D) and the damage amount DA:

$$Ri = DA * P(D) \quad (6.5)$$

Calculation of the damage amount DA:

The damage amount DA [SFr] is calculated using the damage potential VO [SFr], the sensitivity of object to damage SO [-], the lethality L and a reduction factor RF [-]:

$$DA = VO * SO * L * RF \quad (6.6)$$

The *sensitivity of an object* to damage depends on the expected impact force of an avalanche, i.e. the position within the hazard zone and the ability of the house to withstand the avalanche. Latter is a function of the construction class of the house. In addition, windows on the avalanche side of the house decrease the resistance force and increase the SO value. The scale of SO is between 0 (no damage) and 1 (total loss of value). 10 kN/m2 is considered the impact force of an avalanche with a return period of 300 years in the blue zone and 30 kN/ m2 is considered as the impact force of a similar avalanche in the red zone. Table 6.7 provides the assumptions that were done for the Davos example. In the red zone, all constructions, except for reinforced concrete constructions, will be destroyed in a way that it will be cheaper to completely rebuild the houses instead of make any repair work (total damage). In the blue hazard zone, the damages are considered less grave.

Table 6.7: Value assessment for objects and people per measurement unit (MU) and probability of presence. BC: Building Class (see table 6.4 for definitions). a.s.w.: avalanche side windows.

Object	Damage sensitivity S_0	
	Impact pressure of 10 kN/m^2	Impact pressure of 30 kN/m^2
Building		
BC 1, with/no a.s.w.	1	1
BC 2, with/no a.s.w.	0.3	1
BC 3 and 4, with a.s.w	0.03	1
BC 3 and 4, no a.s.w.	0	1
BC 5 with a.s.w.	0	0.03
BC 5 no a.s.w.	0	0
Forest	0.5	1

Agricultural Areas	0	0

The problematic of the *lethality* is only valid for people. Therefore, for objects the value 1 is used. The following values were used for the assessment of the lethality, i.e. the probability of the consequences of a burial by an avalanche. These values are based on historical events (Wilhelm 1997). Approximately in 46% of the cases fatalities occurred, 19% have been injured and all that did not survived (54%) needed support.

Table 6.8: Values of lethality of an event in dependence of the red and blue hazard zone. For objects the Lethality is considered to be one.

Consequences of avalanche	Lethality L
Persons	
Fatality	0.46
Injury	0.19
Need for support	0.54
Others	1

In open slope or even convex slope terrain the avalanche travels one time more to the one side and the other time more to the other side. Therefore the avalanche hazard maps are often designed/mapped too wide for one single event. Therefore it is reasonable to make risk calculations for a single avalanche event with a *reduction factor* that take this precaution measure into account. In this example a reduction factor of 0.8 and 0.5 is applied respectively for the red and the blue zones, i.e. it is assumed, that one single event will cover in average 80% of the red and 50% of the blue zone.

Calculation of the damage probability P(D):

The yearly damage probability is assessed by assessing the probabilities for avalanche event occurrences of a specific extent as shown in Figure 6.10.

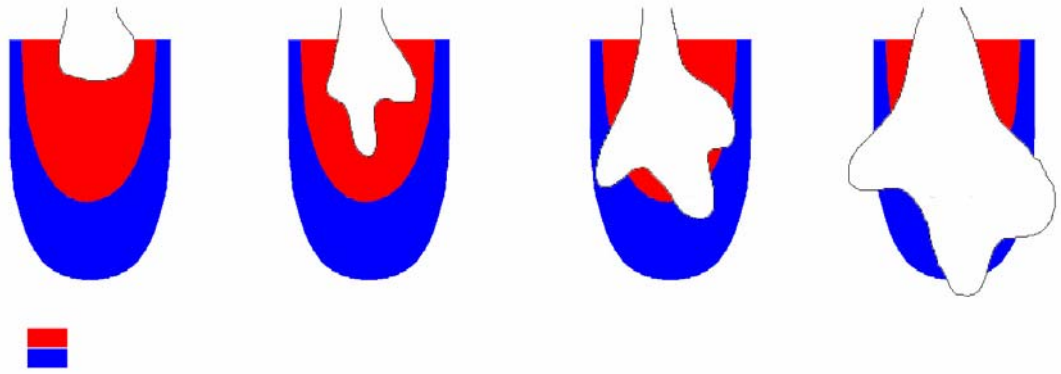

Figure 6.10: Concept for the assessment of the damage probabilities.

Using probabilities of avalanches within Monte Carlo Simulations, instead of red and blue hazard zones, results in similar scenarios with similar occurrence probabilities.

The *minimum event* is assumed to be the beginning of the red zone. This event occurs frequently (every fifth year). The damage amount of this scenario can be estimated to be about 10'000.- Sfr, since normally no building is constructed in this area. The overall contribution of such kind of events to the risk is minimal.

The following values are based on average occurrence probabilities of events within the red and blue zone (for details see Wilhelm 1997).

The *red event* has an average probability of 0.019. The avalanche enters the red zone but does not touch the blue zone. In this case an average impact pressure of 10kN/m^2 is relevant within the red zone.

The *blue event* has an average probability 0.009. The avalanche enters the blue hazard zone but does not reach its limits. In the red zone an impact pressure of 30kN/m^2 is applied and in the blue zone one of 10kN/m^2.

The maximum event will destroy the whole damage potential, but has only a very small probability of 0.001. In the red zone an impact pressure of 30kN/m^2 is applied and in the blue zone one of 10kN/m^2.

Table 6.9 shows an example of a calculation of the yearly risk value for the two objects 1915 and 1920 for the red event (0.0019). In the same way, the other events can be calculated using the specific parameters.

Table 6.9: Simplified example of the calculation of the risk value for two objects in the red hazard zone.

6.3.6.1.1Object category	Object Number	Number of measurement units	Value of measurement unit (Vo) [SFr]	Damage Sensitivity (So)	Letality L	Damage Potential D_P [Fr]	Damage Amount D_A [SFr.]	Total risk [SFr./a]	Risk for fatality [Number of fatalities per year]	Risk for objects [SFr./a]
People										
Dead	-	56,3	10.000.000	0,03	0,46	563.000.000	6.215.520	-	-	-
injured	-	56,3	14.100	0,03	0,19	793.830	3.620	-	-	-
Need help	-	56,3	5.000	0,03	0,54	281.500	3.648	-		-
Building										
BC3(with a.s.w.)	*1915*	1	2.870.000	0,03	1	2.870.000	68.880	2.408.348	0,24	31.812
BC3(with a.s.w.)	*1920*	1	983.000	0,03	1	983.000	23.592	365.172	0,04	10.896
Houshold										
24% of building	-	1	924.720	1	1	924.720	22.193			
Agriculture										
forest [a]	-	314,8	370	0,5	1	116.476	46.590	1.744	0,00	1.744
Infrastructure										
15% of building	-	1	577.950	1	1	577.950	13.871	-	-	-
Economics.										
10% of building	-	1	385.300	1	1	385.300	9.247	-	-	-
Total						569.932.776	6.407.162	**2.775.264**	**0,27**	**44.452**

Damage probability P(D) = 0,019
Reduction factor RF = 0,8

The annual damage expectation value (risk) is calculated using the integral of the area below the risk curve of the probability-damage-diagram (see Figure 6.3). The integration is done for each object. It is based on the areas in between the events min, red, blue and max using equations 6.7 and 6.8.

$$R_i = \int_{P(s)2}^{P(s)1} P(D)^a \cdot dP(D) \qquad (6.7)$$

$$R_i = -a\left(D_{A_2}\right)\left(P(D)_1^{a+1} - P(D)_2^{a+1}\right)/\left(P(D)_2^a \cdot (a+1)\right) \qquad (6.8)$$

with:

$$a = (\log D_{A_2} - \log D_{A_1})/(\log P(D)_2 - \log P(D)_1)$$

The resulting overall risk for the area is shown in Table 6.10. The protection measures prevent in average 3 fatalities per year and a annual damage of about

1.4 Mio. SFr. In comparison to the annual costs of approximately 0.5 Mio SFr, the efficiency of the protection measures is very high, even if one completely neglects the most important factor, the fatalities.

Table 6.10: Collective risk of all scenarios for the whole area.

Scenario with defence measures	Risk of fatalities [Number of fatalities per year] Risk of damages to objects [Mio. SFr. per year] Total risk [Mio. SFr. per year]	0.7 0.18 7.1
Scenario without defence measures	Risk of fatalities [Number of fatalities per year] Risk of damages to objects [Mio. SFr. per year] Total risk [Mio. SFr. per year]	3.7 1.6 38.5

7 CONCLUDING REMARKS AND NEEDS FOR FUTURE MODEL DEVELOPMENT

KK

The main goal of the CADZIE workpackage 1 is to improve the hazard assessment process by integrating uncertainty and to develop "best-fit" models. This goal can only be achieved if both the stochastic characteristics of the avalanche system as well as the physically describable behaviour are modelled adequately. Although there exist numerous empirical and dynamical models in theory and computational form, till now only few attempts have been carried out to combine these different concepts. No attempt is made in this report of synthesizing the contributions or combining those into a proposed "best practice". However, this latter step is planned as part of forthcoming work.

For both the occurrence probability as well as the run-out probability the possibilities, the power, but also the problems of existing and new methods has been discussed. Especially the integration of stochastic variables into mechanical-physical models raises the hope of possible improvement of the process description including empirical probability.

Suggestions for future model development

CH, CK, and DI
In order to account for the extraordinary variability of avalanche motion in response to initial and boundary conditions, flow-regime transitions and snow mass balance should be properly described. The vast majority of models in use today completely neglect these phenomena.

In simple models, flow-regime transitions may be captured "manually" by choosing different sets of parameter values in different sections of the path. It is obvious that only very few experts will be able to correct for model deficiencies in this way, and a high degree of subjectivity is thereby

introduced. What appears to be missing at present is a dynamical determination of the effective constitutive law of avalanching snow in response to the local flow parameters.

Simulations of powder snow avalanches have already illustrated that the mass may grow enormously if sufficient erodible snow is available in the track. While the avalanche without entrainment already begins to decelerate in the track, in the presence of entrainment, maximum speed is reached only at the beginning of the run-out zone. It is highly probable that such a result is also valid for dense snow avalanches. On long avalanche paths, initial snow avalanche mass appears to be much less important than snow entrainment for a wide range of initial conditions.

Furthermore, density variations are represented in very few models, and then simply, while the resultant effects on other physical parameter values such as viscosity, are not represented in any of the dynamics models. Other aspects of the moving media (e.g. particle size distributions, particle concentration and rotation, temperature changes, and energy dissipation) are not adequately described in any of the dynamics models.

Hence, significant improvements in the quality of avalanche hazard mapping require parallel progress along three complementary paths:

- *Improved knowledge of initial conditions:* Combining an extensive survey of the parameter space with detailed simulations of selected scenarios for each practical problem should contribute towards a more comprehensive assessment of avalanche hazard, taking into account the uncertainty of our estimates and computations. Beyond this, research into the quasi-stochastic (climate, probability distribution of key weather elements) as well as causal factors (topography) determining release areas and volumes in function of avalanche frequency needs to be intensified.
- *Modelling of the basic physical processes of avalanche dynamics:* Higher accuracy and reliability of the dynamics models can only be achieved if snow entrainment or deposition and changes in the flow regime are correctly captured. Particle-dynamics models hold promise as a tool for studying the basic processes, interpreting measurements, and for developing practically useful continuum approximations. Detailed analysis of theoretical approaches successful in other gravitational mass movements should stimulate future development in avalanche dynamics.
- *Comprehensive measurements on real avalanches:* For guiding model development and allowing full verification of sophisticated models, a new generation of experiments is required in which the processes in the interior of avalanches are studied in detail.

All points listed above underline the substantial benefits, and even necessity, of international collaboration in the field of avalanche dynamics. The need is felt most urgently for experimentation due to the high costs of the required

equipment. But if progress in modelling is to keep pace with experiment, parallel development of nearly identical models should be abandoned in favour of co-ordinated investigations at different levels, from basic studies of granular dynamics to the elaboration of practical procedures for hazard mapping. Within Europe, the EU programs act as a catalyst in this integrative process.

8 REFERENCES

Arnalds, T, Jónasson, K., and Sigurðsson, S. Þ. In press?. Avalanche hazard zoning in Iceland based on individual risk. *A. Glaciol., **38**.*

Barbolini, M. 1998. VARA one- and two-dimensional models. In Harbitz, C.B., ed. EU Programme SAME. A Survey of computational models for snow avalanche motion. Oslo, Norwegian Geotechnical Institute, 59-63. (NGI Report 581220-1.)

Barbolini, M. 1999. Dense snow avalanches: computational models, hazard mapping and related uncertainties. (Ph.D. thesis, University of Pavia.)

Barbolini, M., Ceriani, E., Dal Monte, G., Segor, V. and Savi, F., 2000b. The Lavanchers avalanche of February 23rd 1999, Aosta Valley, Italy. Proceedings of ISSW 2000, October 1st 2000, Big Sky, Montana, 519-527.

Barbolini, M., U. Gruber, C.J. Keylock, M. Naaim, and F. Savi. 2000a. Application of statistical and hydraulic-continuum dense snow avalanche models to 5 real European sites. Cold Reg. Sci. Technol. 31(2), 133-149.

Barbolini, M. and Keyloch, C.J., A new method for avalanche hazard mapping using a combination of statistical and deterministic models*, Natural Hazards and Earth System Sciences*, n.2, pp 1-7, 2002.

Barbolini, M., Keyloch, C.J. and Savi, F. *Statistical methods for the evaluation of friction coefficients in avalanche hazard mapping.* Presented at the II International Conference on Avalanche and Related Subjects, Kirovsk, Russia, September 3-7 2001. Submitted for publication to Data of Glaciological Studies

Barbolini M., Natale L. and Savi F. 2002: "*Effect of Release Condition uncertainty in avalanche hazard mapping*" Natural Hazard 25(3), 225-244.

Barbolini M., Savi F. 2001. Estimate of uncertainties in avalanche hazard mapping. *Annals of Glaciology,* **32**, 299-305.

Barbolini, M. Savi, F., Gruber, U., Keylock, C., and Naaim, M. 1998. Application and evaluation of different avalamche models at five real sites in Europe. (Deliverable D3 of the EU project SAME), http://same.grenoble.cemagref.fr/.

Bartelt, P. and Christen, M. 1998. A computational procedure for instationary temperature-dependent snow creep. Springer. 368 –385.

Bartelt, P., Salm, B. and Gruber, U., Calculating dense-snow avalanche run-out using a Voellmy-fluid model with active/passive longitudinal straining, Journal of Glaciology, 45(150), 242-254, 1999.

BFF/SLF, Richtlinien zur Berücksichtigung der Lawinengefahr bei raumwirksamen Tätigkeiten, Bundesamt für Forstwesen and Eidgen. Institut für Schnee- und Lawinenforschung, EDMZ, CH-3000 Bern, 1984.

Beghin, P. and X. Olagne. 1991. Experimental and theoretical study of the dynamics of powder snow avalanches. Cold Regions Sci. Technol. 19, 317–326.

Bozhinskiy, A.N. and A.N. Nazarov. 1998. Dynamics of two-layer slushflows. NGI Publications **203**. *(25 Years of Snow Avalanche Research at NGI, Anniversary Conference, Voss, Norway, 12–16 May, 1998, Proceedings)*. Norwegian Geotechnical Institute, Oslo.

Bozhinskiy, A.N., A.N. Nazarov, V.N. Sapunov, and P. Chernouss. 1996. The mathematical model of slushflow dynamics. *Proc. of the Int. Conf., Apatit JSC, Kirovsk, 1996,* 44–49.

Brandstätter, W., G. Hagen, H. Hufnagel, and H. Schaffhauser. 1996. Ein gasdynamisches Lawinensimulationsmodell. *Proceedings INTERPRAEVENT 96, Garmisch Partenkirchen.*

Burnet, R. and Marti, G. 1998. Avalanche maps and databases in Europe. (Deliverable D1 of the EU project SAME), http://same.grenoble.cemagref.fr/.

Casti, J. L. 1992. Reality Rules, Wiley.

Dewarrat, X., 2001: Les avalanche Salezertobel et Dorfberg: Gestion des risks. Travail de diplome. Département de genie civil. Ecole polytechnique fédérale de Lausanne EPFL et Eidg. Institut für Schnee- und Lawinenforschung SLF, Lausanne/Davos.

Eglit, M.E. 1983. Some mathematical models of snow avalanches. In: *Advances in the Mechanics and the Flow of Granular Materials* Vol. **2,** 577–588 (Shahinpoor, M., ed.), Trans Tech Publ., Clausthal - Zellerfeld, and Gulf Publ. Co., Houston, Texas.

Eglit, M.E. and N.N Vel'tishchev. 1985. Issledovanije matematicheskih modelei snezhno-pilevoi lavini (Investigation of mathematical models of powder-snow avalanche*). Materialy Glyatsiologicheskikh Issledovaniy (Data of Glaciological Studies)* **53**, 116–120 (In Russian with English summary).

Fukushima, Y. and G. Parker. 1990. Numerical simulation of powder snow avalanches. *J. Glaciol.* **36** (123), 229–237.

Gruber, U. 1998: Der Einsatz numerischer Simulationsmodellen in der Lawinengefahrenkartierung. Möglichkeiten und Grenzen. Dissertation Universität Zürich. Zürich.

Gruber, U. and Bartelt, P. 2000. Study of the 1999 avalanches in the Obergoms valley, Switzerland, with respect to avalanche hazard mapping. Proceedings of ISSW 2000, October 1st 2000, Big Sky, Montana, 495-501.

Harbitz, C. (ed.) 1998. A survey of computational models for snow avalanche motion. (Deliverable D4 of the EU project SAME), http://same.grenoble.cemagref.fr/. Also in *Norwegian Geotechnical Institute*, report **581220-1**.

Harbitz, C.B., Harbitz, A. and Nadim, F. 2001. On probability analysis in snow avalanche hazard zoning. *Annals of Glaciology,* **32**.

Harbitz, C.B., D. Issler, and C.J. Keylock. 1998. Conclusions from a recent survey of avalanche computational models. *NGI Publications* **203**. *(25 Years of Snow Avalanche Research at NGI, Anniversary Conference, Voss,*

Norway, 12–16 May, 1998, Proceedings). Norwegian Geotechnical Institute, Oslo.

Hermann, F., D. Issler, and S. Keller. 1994. Towards a numerical model of powder snow avalanches. *In:* S. Wagner *et al.* (eds.), *Proc. 2nd Europ. Comp. Fluid Dynamics Conf., Stuttgart, 1994,* 948–955. J. Wiley & Sons, Ltd., Chichester, UK.

Hestnes, E. 1990. Norwegian Demands on Avalanche Safety — Legislation, Quality Policy and Judicial Practice. *Norwegian Geotechnical Institute*, report **581000-4**.

Hestnes, E. and Lied, K. 1980. Natural-Hazard maps for land-use planning in Norway. *Journal of Glaciology*, Vol. **26**, No. **94**.

Holler, P. and Schaffhauser, H., 2000. The avalanches of Galtur and Valzur in February 1999. Proceedings of ISSW 2000, October 1st 2000, Big Sky, Montana, 514-519.

Hopf, J.: 1998, An Overview of Natural Hazard Zoning with Special Reference to Avalanches, In Proceedings of the Anniversary Conference for the 25 Years of Snow Avalanche Research at NGI, Voss, Norway, 12–16 May 1998, NGI Publications No. 203, 28-35.

Issler, D. 1998. Modelling of snow entrainment and deposition in powder snow avalanches. *Annals of Glaciol.* Vol. **26** (Proc. Intl. Symposium on Snow and Avalanches, Chamonix, France, 1997), 253-258.

Jóhannesson, T. 1998. Icelandic avalanche run-out models compared with topographical models used in other countries. In *Proceedings of the Anniversary Conference for the 25 Years of Snow Avalanche Research at NGI,* Voss, Norway, 12–16 May 1998, NGI Publications No. 203, 43-52.

Jóhannesson, T. and Arnalds, T. 2001. Accidents and economic damage due to snow avalanches and landslides in Iceland. *Jökull*, **50**, 81-94.

Johnson, D.E. 1998. Applied Multivariate Methods for Data Analysis. Duxbury Press, 567 pp.

Jónasson, K., Sigurðsson, S. Þ., and Arnalds, T. 1999. *Estimation of Avalanche Risk.* Icelandic Meteorological Office, Rep. R99001.

Keylock, C.J. and Barbolini, M., Snow avalanche impact pressure/vulnerability relations for use in risk assessment, *Canadian Geotechnical Journal*, 38(2), 227-238, 2001.

Keylock, C.J., McClung, D.M., and Magnusson, M.M. 1999. Avalanche risk mapping by simulation. *Journal of Glaciology* **45** (**150**), 303-314.

Kleemayr, K., Tartarotti,T., Kreuzer, St., Botthof, M., Janu, St., Fieger, St., Jäger, G., 2002. NAFT 2000. Internal report. Institute of forest and mountain risk engineering, University of Bodenkultur, Vienna.

Koel, T.M. 2001. Classification of upper Mississippi River pools based on contiguous aquatic/geomorphic habitats. Journal of Freshwater Ecology, 16, 159-170.

Kuhn, M. 1983: Physikalische Grundlagen des Energie- und Massenhaushaltes der Schneedecke, Innsbruck 1983.

Kulikovskiy, A.G and E.I. Sveshnikova. 1977. Model dlja rascheta¨dvizhenija pilevoi snezhnoi lavini (A model for calculation of motion of powder snow

avalanche). *Materialy Glyatsiologicheskikh Issledovaniy (Data of Glaciological Studies)* **31**, 74–80 (In Russian with English summary).

Lied, K. and Bakkehøi, S., Empirical calculation of snow-avalanche run-out distance based on topographic parameters, *Journal of Glaciology*, 26(94), 165-177, 1980.

McClung, D.M. 2000. Extreme avalanche run-out in time and space. *Canadian Geotechnical Journal*, **37**, 161-170.

McClung, D.M. and Lied, K., Statistical and geometrical definition of snow avalanche run-out, *Cold Regions Science and Technology*, 13(2), 107-119, 1987.

McClung, D.M. and Schaerer, P.A., *The avalanche handbook*, Seattle, WA, The Mountaineers, 1993.

Mendenhall, W. and Sincich, T. 1996. *A Second Course in Statistics: Regression Analysis*. 5th edition, Prentice-Hall, New Jersey, 899 pp.

Meunier, M. and Ancey, C. 2003. Towards a conceptual approach to predetermining high-return-period avalanche run-out distances. 35 pages. Submitted for publication in Journal of Glaciology.

Milligan, G.W. 1980. An examination of the effects of six types of error perturbation on fifteen clustering algorithms. Psychometrika, 45, 325-342.

The Ministry for the Environment. 2000. *Regulation on hazard zoning due to snow- and landslides classification and utilisation of hazard zones and preparation of provisional hazard zoning.* (Regulation, the Ministry for the Environment, Reykjavík, Iceland).

Munter, W. 1991. Neue Lawinenkunde. 76 pp. SAC-Schweizer Alpenklub

Naaim, M. 1995. Modélisation numérique des avalanches aérosols. *La Houille Blanche* Nr. 5/6–1995, 56–62.

Naaim, M. and Gruber, U. 1998. Integration of different avalanche models in a single, GIS based user interface. (Deliverable D2 of the EU project SAME), http://same.grenoble.cemagref.fr/.

Nairz, P. 1996. Overview and comparison of avalanche prediction methods. Diploma thesis. Institut of Forest and mountain risk engineering. University of Bodenkultur Vienna.

Natale, L., L. Nettuno and F. Savi. 1994. Numerical simulation of dense snow avalanche: an hydraulic approach. In Hamza, M.H., ed. Proceedings of 24th International Conference on Modelling and Simulations, MS'94, 2-4 May, Pittsburgh, Pennsylvania. Anaheim, International Association of Science and Technology Development (IASTED) ACTA PRESS, 233-236.

Nazarov, A.N. 1991. Matematicheskoe modelirovanie snezhno-pilevoi lavini v ramkah uravnenii dvuhsloinoi melkoi vodi (Mathematical modeling of a snow-powder avalanche in the framework of the equations of two-layer shallow water. *Izv. Akad. Nauk SSSR Mekh. Zhidk. Gaza* **1**, 84–90. English transl. in *Fluid Dynamics* **12** (1991), 70–75.

Nazarov, A.N. 1992. Opit primenenija dvuhsloinoi modeli dlja rascheta dvizhenija pilevih lavin (Use of two-layer model for calculating of motion of powder snow avalanches). *Materialy Glyatsiologicheskikh Issledovaniy*

(Data of Glaciological Studies) **73**, 73–79 (In Russian with English summary).

Nazarov, A.N. 1993. Matematicheskoe modelirovanie nestacionarnogo dvizhenija snezhno-pilevyh lavin (Mathematical modelling of non-stationary motion of powder-snow avalanches). *Thesis, Moscow,* 170pp. (In Russian).

NGI 1997. Hazard zoning methods of snow avalanches, debris flows and rock falls. *Norwegian Geotechnical Institute*, report **589210-3**.

NGI 2001. EU Program CADZIE WP5 — Norwegian Zoning Tools. *Norwegian Geotechnical Institute*, report **20011001-02**.

Norem, H. 1995. Shear stresses and boundary layers in snow avalanches. *Norwegian Geotechnical Institute*, report **581240–3**.

Pasqualotto, M. 1998. Esposizione al rischio di valanghe e pianificazione territoriale. *Neve e Valanghe*, 37, 28-33. (In Italian)

Perla, R., Cheng, T.T., and McClung, D.M. 1980. A two-parameter model of snow-avalanche motion. *J. Glaciol.,* **26**(94), 197-207.

Rapin, F. 1995. French theory for the snow avalanches with aerosol. *In:* G. Brugnot (ed.), *Université européenne sur les risques naturels. Session 1992: Neige et avalanches.* Pages 163–172. Editions du CEMAGREF.

Rapin, F. and Ancey, C. 2000. Condition of two major avalanches in 1999 at Chamonix, France. Proceedings of ISSW 2000, October 1st 2000, Big Sky, Montana, 509-514.

Rohrer, M.B. 1992. Die Schneedecke im Schweizer Alpenraum und ihre Modellierung, Züricher Geographischen Schriften 49, Geographische Institut, E Züricher Geographischen Schriften 49: TH Zürich.

Salm, B., A. Burkard and H. Gubler. 1990. Berechnung von Fliesslawinen: eine Anleitung für Praktiker mit Beispielen. Eidg. Inst. Schnee- und Lawinenforsch. Mitt., 47, 41 pp.

Scheiwiller, T. 1986. Dynamics of Powder Snow Avalanches. *Ph.D. thesis.* Available as: *Mittlg. Versuchsanstalt für Wasserbau, Hydrologie und Glaziologie, Swiss Federal Institute of Technology Zurich*, Nr. **81**, 115 p.

Schuhmacher, S., 1999: Kartierung von Gefahrenzonen und die damit verbundenen gesamtgesellschaftlichen Kosten. Diplomarbeit, Assistenzprofessur Forstliche Ressourcenökonomie. Departement Wald- und Holzforschung, ETH Zürich. Zürich.

Sigurðsson, S., Jónasson, K., and Arnalds, T. 1997. Transferring Avalanches Between Paths. In Hestnes, E., ed. *25 years of snow avalanche research.* Oslo, Norwegian Geotechnical Institute, 259-263 (Publication no. 203).

Staub, M. und John, D., 2001: Visualisierung von Lawinenrisiken. Entwicklung eines GIS-basierten Konzepts anhand des Fallbeispiels Schiahornlawine in Davos. Diplomarbeit, Institut für Orts-, Regional- und Landesplanung ORL und Eidg. Institut für Schnee- und Lawinenforschung SLF, Zürich/Davos.

Tesche, T.W. 1986. A three dimensional dynamic model of turbulent avalanche flow. *Proc. Int. Snow Science Workshop, Lake Tahoe California*, 1–27.

Toppe, R. 1987. Terrain models — a tool for natural hazard mapping. International Association of Hydrological Sciences Publ. **162** (Symp. at Davos 1986 — Avalanche formation, Movement and Effects).

Voellmy, A. 1955. Über die Zerstörungskraft von Lawinen. Schweiz. Bauztg., 73(12/15/17/19), 159-165, 212-217, 246-249, 280-285.

Wilhelm, C., 1997: Wirtschaftlichkeit im Lawinenschutz. Methodik und Erhebungen zur Bewertung von Schutzassnahmen mittels quantitativer Risikoanalyse und ökonomischer Bewertung. Eidg. Institut für Schnee- und Lawinenforschung (SLF), Daos, Mitteilung Nr. 54, 309 S.

Wilhelm, C. 1997. Wirtschaftlichkeit im Lavinenschutz - Methodik und Erhebungen zur Beurteilung von Schutzmassnahmen mittels quantitativer Risikoanalyse und ökonomischer Bewertung. *Mitt. Eidgenöss. Inst. für Schnee- und Lawinenforsch.*, Davos no. 54, 309 pp. (In German).

Wilhelm, C., 1999: Kosten-Wirksamkeit von Lawinenschutzmassnahmen an Verkehrsachsen. Praxishilfe BUWAL, Bern.

WMO. 1999. Comprehensive risk assessment for natural hazards. *World Met. Org./TD* no. 955.

Zwinger, T., Kluwick, A., and Sampl, P. 2003. Simulation of Dry-Snow Avalanche Flow over Natural Terrain. In Hutter, K., N. Kirchner, ed. *Dynamic Response of Granular and Porous Materials under Large and Catastrophic Deformations, Lecture Notes in Applied and Computational Mechanics.* Springer, Heidelberg, **11**, 161-194.

Appendix A - Hazard zoning methods in Iceland

CONTENTS

A1 HAZARD ZONING METHODS IN ICELAND

The Icelandic Meteorological Office does not directly participate in the hazard zoning work package of Cadzie (WP1). It was nevertheless considered appropriate to describe Icelandic hazard zoning methods briefly in this report for completeness. The following description is mainly based on the report by Jónasson et al. (1999) and a paper by Arnalds et al. (in press?).

Avalanche hazard is a threat to many residential areas in Iceland. In 1995 two avalanche accidents in the villages Súðavík and Flateyri causing a total of 34 fatalities in areas thought to be safe prompted research on avalanche hazard assessment. A new method was developed in a collaboration between IMO and the University of Iceland (Jónasson et al., 1999), and in 2000 a new regulation on avalanche hazard zoning was issued (The Ministry for the Environment, 2000). The method and regulation are based on individual risk, or annual probability of death due to avalanches. The major components of the method are the estimation of avalanche frequency, run-out distribution, and vulnerability. The frequency is estimated locally for each path under consideration but the run-out distribution is based on data from many locations, employing the concept of transferring avalanches between slopes (Sigurðsson et al., 1997). Finally, the vulnerability is estimated using data from the 1995 avalanches. Under the new regulation, new hazard maps have been prepared for 6 of the most vulnerable villages in Iceland. Hazard zones are delineated using risk levels of 0.2·10-4, 0.7·10-4, and 2·10-4 per year, with risk less than 0.2·10-4 per year considered acceptable. When explaining the new zoning to the public, a measure of annual individual risk that allows comparison with other risks in society has proven advantageous.

A1.1 Hazard zoning based on individual risk

In Switzerland and Austria the delineation of hazard zones is based on the estimated frequency of snow accumulation in starting areas of avalanches. A physical model is applied to calculate a corresponding run-out of avalanches. In Switzerland the limit of the hazard zones is located at the calculated run-out of an avalanche corresponding to snow accumulation in the starting area with a frequency 1/300 yr-1. In Norway the limit of the hazard zones is delineated where the frequency of avalanches is estimated to be 1/1000 yr-1.

Risk is the probability of a loss or injury. The loss can take several forms, such as economic loss, environmental damage or loss of lives. Models to evaluate risk usually deal with the risk as a product of factors. The World Meteorological Organization has proposed a risk model for weather related hazards (WMO, 1999). The WMO model splits the risk in a hazard prone area into hazard potential (hazard frequency and intensity) and vulnerability. If individual risk is to be estimated the exposure of the individual to the hazard prone area should be incorporated.

Although the economic loss due to avalanches in Iceland has been significant (Jóhannesson and Arnalds, 2001), the loss of lives is a dominant factor when considering the acceptability of the risk for the society. Furthermore, the avalanche risk is typically quite concentrated. It has been estimated that about 5000 people are living in densely populated areas of Iceland where there is a considerable avalanche hazard. This figure has been corroborated by the hazard zoning work. In the past few decades the average number of deaths due to avalanches in these areas has been about 2 persons per year. This indicates an average annual individual risk of about 4·10-4 per year for people living in these areas. This is about 5 times the average annual individual risk due to traffic accidents in Iceland. The risk within the most endangered areas is of course much higher and thus unacceptable by any measure. After some deliberation, it was decided to base the Icelandic hazard zoning regulation on individual risk. By reducing the individual risk, the aggregated risk to the society would also be reduced. Since there is only a small proportion of the population exposed to the risk, an acceptable risk for the individuals will most likely also lead to acceptable risk for the society.

The Icelandic risk model can be split into four modules. The first two are the estimated frequency of avalanches in the slope above the area where the risk is to be estimated, and the run-out distribution of avalanches. These two components together encompass the hazard frequency part of the general risk model. The vulnerability is represented by the probability of being killed if staying in a house that is hit by an avalanche and the exposure is the proportion of the time that a person is expected to be staying within the hazard prone area.

Although the Icelandic risk model is the first method of this kind to be put into operation for avalanche hazard zoning it should be noted that Keylock et al. (1999) proposed a method for the estimation of individual avalanche risk based on run-out ratios, and Wilhelm (1997) analysed the economic risk to traffic due to avalanches.

A1.1.1 Transferring avalanches

In order to estimate the run-out distribution of avalanches in a particular avalanche path it is usually necessary to include, implicitly or explicitly, information about run-out lengths in other avalanche paths. This is necessary since the observed avalanches in each path are usually few and a reliable statistical estimate cannot be obtained from the limited local observations alone. In order to facilitate an estimation of the run-out distribution it is useful to transfer avalanches between slopes. It is possible to use both physical and topographical models for the transfer of avalanches between paths and different statistical approaches can be used. Sigurðsson et al. (1997) attempt to classify the different types of transfer methods.

The transfer method used in the Icelandic risk model is built around the PCM-model of avalanche flow. The model is a physical model with two free parameters, the Coulomb friction parameter μ and the mass-to-drag parameter M/D (Perla et al., 1980). However, the curvature term, κ, is separated from the M/D-term in our version of the model, i.e. the differential equation of the model is

$$\frac{1}{2}\frac{\mathrm{d}}{\mathrm{ds}}(\mathrm{u}^2) = g(\sin\theta - \mu\cos\theta) - (\mu\kappa + \frac{1}{M/D})u^2 \qquad \text{(A1)}$$

where u denotes the speed of the avalanche, s the distance along the path, θ its slope, and g the gravitational acceleration. In the numerical solution, a smoothing procedure is applied, so that the path has a continuous curvature rather than being composed of straight line segments.

There is an infinite number of parameter pairs (M/D, μ) that will simulate the run-out length of a given avalanche in a given avalanche path. We refer to this set of pairs in the (M/D, μ)-space as an isorunline. In order to find a single pair to simulate each avalanche, the choice of possible parameters is restricted to a line in the parameter space, called the parameter axis. The chosen axis has the equation

$$\mu = 0.6 - 0.0006\, M/D \,. \qquad \text{(A2)}$$

This, of course, is a simplification, but the resulting parameter values are within a range suggested by studies of the PCM-model in other countries, and it has furthermore been shown that the final risk estimate is not very sensitive to the location of this axis (Jónasson et al., 1999). Figure A1 shows the isorunlines of several Icelandic avalanches together with the parameter axis. In order to transfer an avalanche from one path to another, i.e. to find a likely run-out distance in the second path, we find the parameter pair which is the interception between the axis and the isorunline of the avalanche for the first path. A simulation with the PCM-model and this parameter pair is then run in the second path.

A1.1.2 Run-out distribution

The transfer of avalanches makes it possible to transfer avalanches in a data set collected in many avalanche paths to a single path and subsequently estimate the distribution of run-out lengths. The data set used for the Icelandic risk model consists of 196 avalanches that were recorded in 81 different paths. To estimate the run-out distribution in a given path, one could transfer all these avalanches to the path. To simplify the procedure and to avoid problems caused by unevenness in the run-out area the approach has been adopted to estimate the distribution in a single artificial path and then transfer this globally

estimated distribution to the path under consideration. The path used for the estimation is chosen to be typical for Icelandic avalanche slopes. It is parabola shaped, 700 m high and 1600 m long. This slope is referred to as the standard path.

The probability density of the run-out lengths is estimated using a so-called kernel estimation (cf. Jónasson et al., 1999). It should be noted that special consideration must be given to the data set. There is a reason to believe that in the data set of 196 avalanches there are much too few small avalanches compared to longer ones. This bias is estimated using data from avalanche paths where records are more complete and the probability distribution is corrected accordingly. The probability density of the run-out length, r, is referred to as f(r).

The run-out length of avalanches in the standard path also gives a numerical measure for the run-out length. We call the run-out length in the standard path run-out index. The unit of the run-out index is hectometres, so that an avalanche that reaches 1540 m in the standard path has a run-out index of 15.4. The run-out index is also a useful concept in the absence of avalanches, we can e.g. say that a location where an avalanche with run-out index 13 would stop has run-out index 13. The run-out index concept can be extended to other types of transfer methods (Sigurðsson and others, 1997).

A1.1.3 Frequency

If we estimate the frequency of avalanches at one location in an avalanche path, the run-out distribution will provide us with frequency estimates for other parts of the slope. Let us assume that the frequency is estimated at run-out index r0. For confined paths with complete records of avalanches for T years and a total of Nr0 avalanches with run-out greater than r0 , the estimated frequency at r0 is simply

$$F_{r_0} = \frac{N_{r_0}}{T} \quad . \qquad \text{(A3)}$$

The frequency at another location in the path, r, may then be estimated as

$$F_r = F_{r_0} \int_r^\infty f(s)ds \Big/ \int_{r_0}^\infty f(s)ds \quad . \qquad \text{(A4)}$$

The lower the value of r0 (i.e. the shorter the run-out), the more statistically reliable the estimate of the frequency becomes because Nr0 will then be higher. However, avalanche records are more likely to be incomplete for low values of r0 . The completeness of the recordings also differs with time, the further back

we go the more incomplete the records become. It can therefore be of advantage to estimate the frequency at several points in the path using different observation periods and compare the estimates.

The estimation of avalanche frequency can be adapted to unconfined slopes, taking into account the average width of avalanches and the total width of the slope. The statistical reliability of the frequency estimate for confined slopes can also be improved if it can be assumed that adjacent paths have similar characteristics and therefore the same frequency. The frequency is then estimated jointly for all the paths (Jónasson et al., 1999).

A1.1.4 Vulnerability

The vulnerability of persons to avalanches will depend on several factors, such as whether they are inside a building, the strength of the building, and the size and speed of the avalanche. For the avalanches in Súðavík and Flateyri, information is available about how many people were staying in each of the houses that were hit and how many were killed. The speed of the avalanches when they hit the houses was estimated using the PCM model. Figure A2 shows the fraction of people that were killed as a function of the calculated speed. As expected, the probability of being killed increases sharply as the speed increases. It is plausible to assume that this probability is approximately proportional to the kinetic energy of the avalanche. However, even at high speeds there seems to be some chance of surviving and therefore a non-zero probability of survival is assumed in the limit of very high speeds. A continuously differentiable function has been fitted to the data using maximum likelihood estimation with the assumption that the probability of being killed is

$$d(v) = \begin{cases} kv^2 & \text{if} \quad v < v_1 \\ c - \dfrac{a}{v-b} & \text{if} \quad v > v_1 \end{cases} \qquad \text{(A5)}$$

The value of the terminal death probability is chosen to be 0.05. This gives the estimates v1 = 23.0, k = 0.00130 and a = 1.151, b = 18.61. The fitted function is shown in Figure A2. The data from Súðavík and Flateyri are considered to be representative for the consequences of avalanche impact on non-reinforced single family houses in Icelandic hazard areas.

A1.1.5 Exposure

The exposure of persons to the avalanche hazard depends on their age and the type of building. For homes the exposure can be as high as 75% but in industrial buildings it will rarely be more than 30%. The Icelandic hazard zoning regulation, described below, adopts the concept local risk, which is

defined as the annual probability of being killed for a person that stays all the time in a non-reinforced building. The local risk therefore omits the exposure. The actual risk may in each case be found given an appropriate assumption regarding the exposure.

A1.1.6 Risk model

Given an estimate, Fr0, of the avalanche frequency at a particular location, r0 , in an avalanche path, the individual risk at any location in the path may be readily obtained. The risk contribution of avalanches that exceed the given location, r, where the risk is to be estimated can be represented as an integral

$$\text{Risk at } r = F_{r_0} \int_r^\infty f(s) d(v_r(s)) ds \Big/ \int_{r_0}^\infty f(s) ds \quad . \qquad \text{(A6)}$$

where vr(s) is the speed of an avalanche with run-out s at location r. The purpose of the second integral is to normalise the run-out density function in the interval [r0 ,∞).

A1.1.7 Acceptable risk

When individual involuntary risk is less than 10-6 per year there is usually no reason for mitigation. When the annual risk is as high as 10-4 per year (approximately the risk of fatal traffic accidents in Iceland) there are, on the other hand, grounds for taking costly actions to reduce it. Thus an acceptable individual risk level will usually lie somewhere between these values. During formulation of the hazard zoning regulation the acceptable risk level was considered from several viewpoints, with the safety of children being the most important factor. The total annual mortality rate of children in Iceland is about 2·10-4 per year. It is clearly unacceptable that children living in areas threatened by avalanches have a much higher mortality rate than other children. It was considered acceptable that avalanche risk would contribute about 10% to the total risk of children, keeping in mind that other factors in the environment might be favourable, such as lower risk of traffic accidents. The acceptable risk for homes was thus set at 0.2·10-4 per year. Taking the exposure of 75% this gives an acceptable local risk of about 0.3·10-4 per year if the person is not exposed to significant avalanche risk when not at home.

A1.2 Application of the risk model

Parallel to the development of the risk model it was applied to practical hazard zoning projects and the results were compared to the results of other zoning

methods. After the regulation on avalanche hazard zoning was issued in 2000, hazard maps have been finalised for seven villages.

A1.2.1 Regulation

The Icelandic regulation on hazard zoning is based on the local risk described above. The local risk of 0.3·10-4 per year is defined to be acceptable for residential areas and three types of hazard zones are defined where the risk is progressively higher, see Table A1. The guidelines for the zoning and utilisation of the hazard zones are tailored to attain the acceptable risk level in residences when the exposure and increased safety provided by reinforcements have been taken into account. For industrial buildings the guidelines probably correspond to a somewhat higher risk, but this may be justified by the absence of children.

Table A1: Icelandic hazard zone definitions

Zone	Lower level of local risk	Upper level of local risk	Building restrictions
C	3·10-4 yr-1	—	No new buildings, except for summer houses*, and buildings where people are seldom present.
B	1·10-4 yr-1	3·10-4 yr-1	Industrial buildings may be built without reinforcements. Homes have to be reinforced and hospitals, schools etc. can only be enlarged and have to be reinforced. The planning of new housing areas is prohibited.
A	0.3·10-4 yr-1	1·10-4 yr-1	Houses where large gatherings are expected, such as schools, hospitals etc., have to be reinforced

*If the risk is less than 5·10-4 per year

The Icelandic zoning regulation states that effect of protective structures built in order to reduce the risk due to snow avalanches and other slides shall be assessed and/or calculated. This applies in particular to catching and deflecting dams in avalanche run-out areas and to supporting structures in starting zones. In areas that are protected by protective structures, both local risk in the absence of such measures and local risk taking the structures into consideration shall be shown on the hazard map.

A1.2.2 Completed hazard zoning projects

The first hazard map according to the regulation, was finalised in May 2001, for the village of Neskaupstaður in eastern Iceland. Since then five other maps have been completed, for Siglufjörður, Seyðisfjörður, Eskifjörður, Ísafjörður and Bolungarvík, in that order. The majority of houses in urban areas of Iceland that are threatened by avalanches are located in these communities. Other types of rapid mass movements in steep slopes, such as slush flows,

landslides and rock-fall also threaten some of the areas. The Icelandic hazard zoning regulation requires that these hazards should also be accounted for in the risk estimates. A comprehensive risk model has not been developed for these types of hazards and a more subjective approach has therefore been necessary. The avalanche risk estimation methods described above have been applied to some paths in all the areas where hazard maps have been finalised. It should, however, be noted that the data set which forms the basis for the risk model consists mostly of avalanches from relative high slopes (by Icelandic standard), i.e. between 500 and 800 m high. In lower slopes it has been necessary to adapt the results of the risk model subjectively. Since the model is based on a one-dimensional avalanche model it does not give an indication of the lateral extent of the hazard zones. For that purpose the Austrian avalanche model SAMOS (Zwinger et al., 2003) has been run for most of the investigated avalanche paths. The results of the risk model have then been adjusted according to the results of the SAMOS simulations.

The hazard zoning regulation defines a framework for the hazard zoning process. The communities which are endangered by avalanches request a risk assessment from the Ministry for the Environment. The ministry appoints a hazard zoning committee with two representatives from the ministry and two representatives from the community. The hazard zoning committee then requests a risk assessment from the IMO. The committee reviews the results of the IMO and presents them to the public in the community. It has proved useful, to have representatives of the community involved in most of the hazard zoning process and to take responsibility for the final result. As a part of the procedure of introducing the hazard maps, reports relevant to the hazard zoning are published on a web page (www.vedur.is/snjoflod/haettumat).

A1.2.3 Case studies

Figure A3 shows a hazard map for the eastern part of Neskaupstaður. The mountain above the settlement rises to 700 to 900 m a.s.l. The mountainside is cut by many large gullies, which accumulate snow during northerly winds. Two avalanches, to the west of the area shown on the map, resulted in a tragic accident in 1974. The lower parts of four of the main avalanche paths (which total about seven) in the eastern part of Neskaupstaður are located in the area. The frequency of avalanches from the seven main gullies was considered to be comparable, except for Urðarbotn where the frequency is lower. The frequency was, therefore, estimated jointly for all the gullies except Urðarbotn, yielding an estimate of F13 = 0.05, i.e. 5 avalanches per century from each gully with run-out beyond run-out index 13. The frequency from Urðarbotn was considered to be 5 times lower, due to the size, shape and location of the starting areas. The hazard lines directly below the gullies represent risk calculations with the Icelandic risk model using the frequency estimates. The

shape of the hazard lines is otherwise based on the results of SAMOS-simulations and on subjective judgment.

Figure A4 shows a hazard map for the Drangagil area in Neskaupstaður where protection measures consisting of supporting structures, braking mounds and a catching dam have been constructed. The map shows the estimated isorisklines in the absence of protection measures (shown in Figure A3) and the estimated local risk after the structures have been fully completed.
Estimation of the risk below protection measures is notoriously difficult and is inevitably associated with a substantial uncertainty. The Icelandic hazard zoning regulation states that defences against snow avalanches and other slides shall only be built to increase the safety of people in areas already populated. In spite of the fact that protective structures are designed and built with the aim of making the safety of people below them acceptable, local authorities are to take the danger of snow- or landslides into consideration in planning and development of the communities.

A1.3 Conclusion

The results of the risk calculations indicate that the average probability of being killed if staying in a house in the Icelandic hazard zones that is hit by an avalanche is about 0.1-0.25. Given the acceptable local risk of $0.3 \cdot 10\text{-}4$ per year this indicates an acceptable annual exceedance probability of avalanches in the range from 1/7500 to 1/3000. These are very low probabilities and can be difficult to communicate to the public. The use of individual risk has proved to be useful in this situation, since it makes it possible to compare the avalanche risk to other risks that people are more familiar with. This has in some cases changed the risk perception of the public and increased their risk awareness.

One approach to check the validity of the risk estimate of the hazard maps is to aggregate the total risk in all seven villages, take the age of the villages into account, and compare the result with the actual number of fatalities in past avalanche accidents. A rough calculation of this type indicates that the risk has been somewhat overestimated on average. A possible explanation is that in an uncertain situation where the hazard zoning relies heavily on subjective judgment the experts have a tendency to be conservative. However, we believe that where the risk model is directly applicable, i.e. in typical avalanche paths with recorded avalanches, the risk estimates are less biased.

Although the risk model leaves many gaps for the experts to fill in with their personal judgment, based on experience, it provides a framework for that judgment. It enables them to structure their decisions and provides them with a useful tool to formulate the final result.

A1.4 Figures

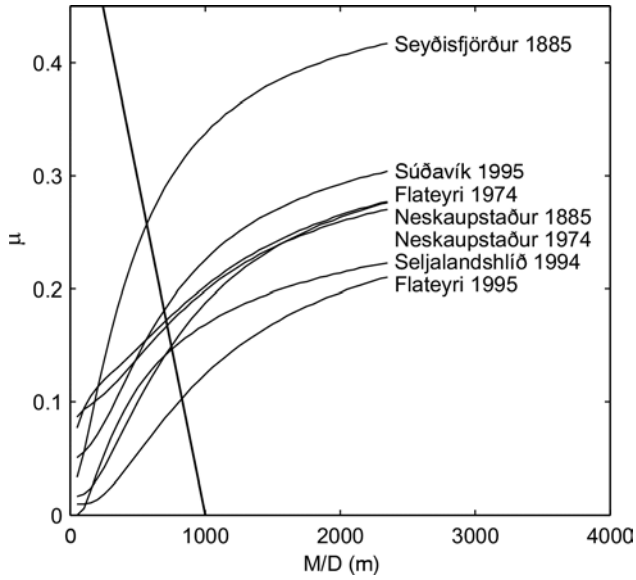

Figure A1: Isorunlines of a few well known Icelandic avalanches and the parameter axis.

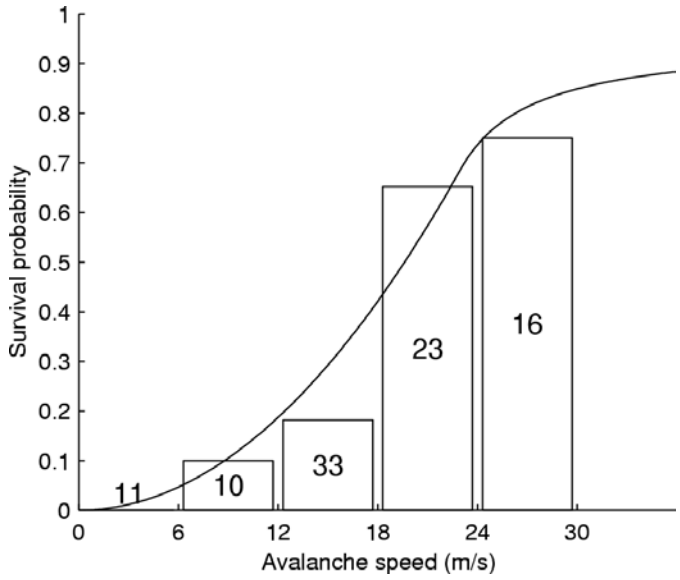

Figure A2: The death rate in the avalanches at Flateyri and Súðavík as a function of avalanche speed. The numbers within the bars indicate the number of people that were at home for each speed interval. The curve is the fitted death probability (cf. eq. A5).

Figure A3: A hazard map for the eastern part of Neskaupstaður in eastern Iceland. The solid line (—) indicates the boundary of the category A hazard zone, the dashed line (– –) the boundary of the B zone and the dashed-dotted line (– · –) the boundary of the C zone (cf. Table A1). The hazard map applies to the situation before the construction of protection measures. Also shown are several of the longer recorded avalanches and their dates. The avalanches were released from the starting areas Urðarbotn, Drangagil, Nesgil and Bakkagil, counting from west to east. The lines along the slope are longitudinal sections used for the model computations. The numbers adjacent to the lines indicate run-out indices.

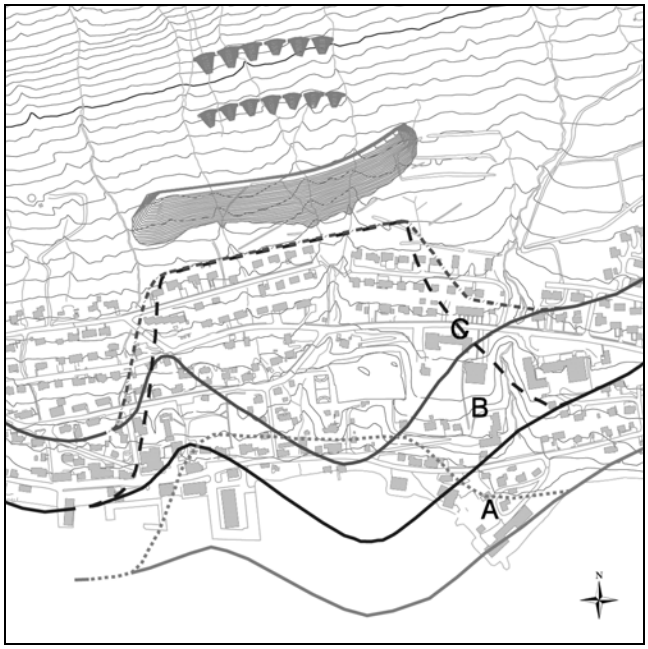

Figure A4: A hazard map for the area below Drangagil in Neskaupstaður showing the estimated local risk both in the absence of protection measures

(solid lines, same as shown in Figure A3) and the estimated local risk after the structures have been fully completed (dashed lines, the B and the C lines coincide below the dam). The protection measures consist of supporting structures (not shown in the figure), 10 m high braking mounds and a 17 m high catching dam.

Kontroll- og referanseside/
Review and reference page

Oppdragsgiver/*Client* EU/NFR SIP6 **Kontraktsreferanse/ *Contract reference*** EVG1-CT-1999-0009	**Dokument nr/*Document No.*** 20001018-2 **Dato/*Date*** 2003-06-16
Dokumenttittel/*Document title* EU Programme CADZIE New concepts in avalanche hazard mapping **Prosjektleder/*Project Manager*** Ulrik Domaas **Utarbeidet av/*Prepared by*** Carl B. Harbitz	**Distribusjon/*Distribution*** ☐ **Fri/*Unlimited*** ☒ **Begrenset/*Limited*** ☐ **Ingen/*None***
Emneord/*Keywords* Snow avalanche, hazard	
Land, fylke/*Country, County* **Kommune/*Municipality*** **Sted/*Location*** **Kartblad/*Map*** **UTM-koordinater/*UTM-coordinates***	**Havområde/*Offshore area*** **Feltnavn/*Field name*** **Sted/*Location*** **Felt, blokknr./*Field, Block No.***

Kvalitetssikring i henhold til/*Quality assurance according to* NS-EN ISO9001

Kontrollert av/ *Reviewed by*	Kontrolltype/ *Type of review*		Dokument/*Document* Kontrollert/*Reviewed* Dato/*Date*	Sign.	Revisjon 1/*Revision 1* Kontrollert/*Reviewed* Dato/*Date*	Sign.	Revisjon 2/*Revision 2* Kontrollert/*Reviewed* Dato/*Date*	Sign.
UD	**Helhetsvurdering/ *General Evaluation* ***		2003-06-16					
UD	**Språk/*Style***		2003-06-16					
UD	**Teknisk/Technical** **- Skjønn/*Intelligence*** **- Total/*Extensive*** **- Tverrfaglig/ *Interdisciplinary***		2003-06-16					
KHE	**Utforming/*Layout***		2003-06-16					
CH	**Slutt/*Final***		2003-06-16					
JGS	**Kopiering/*Copy quality***							

*** Gjennomlesning av hele rapporten og skjønnsmessig vurdering av innhold og presentasjonsform/**
On the basis of an overall evaluation of the report, its technical content and form of presentation

Dokument godkjent for utsendelse/ *Document approved for release*	Dato/*Date* 2003-06-16	Sign.